Development of an impermeant photolabel for studying the structure, function and regulation of glucose transporters

Clark, Avril Elizabeth

Award date:
1994

Awarding institution:
University of Bath

DEVELOPMENT OF AN IMPERMEANT PHOTOLABEL FOR STUDYING THE STRUCTURE, FUNCTION AND REGULATION OF GLUCOSE TRANSPORTERS

Submitted by **Avril Elizabeth Clark**

For the degree of PhD at the University of Bath 1994

ProQuest LLC
789 East Eisenhower Parkway
P.O. Box 1346
Ann Arbor, MI 48106-1346

CONTENTS

ABSTRACT

A new exofacial photoaffinity label for studying glucose transporters has been developed. This compound is 2-N-[4-(1-azi-2,2,2-trifluoroethyl)benzoyl]-1,3-bis-(D-mannos-4-yloxy)-2-propylamine (ATB-BMPA). Binding of ATB-BMPA to the erythrocyte glucose transporter (GLUT1) renders the protein less susceptible to proteolysis by trypsin and thermolysin than both unlabelled GLUT1 and cytochalasin B-labelled GLUT1. The GLUT1 18 kDa tryptic fragment has a lower affinity for ATB-BMPA and a higher affinity for D-glucose than untreated, native GLUT1.

The ability of GLUT1 mutants expressed in CHO cells to transport 2-deoxy-D-glucose and to bind the external and internal ligands, ATB-BMPA and cytochalasin B has been investigated. Mutation of glutamine 282 to leucine in transmembrane segment (TM) 7 of GLUT1 selectively perturbs binding of the external ligand, ATB-BMPA to the mutant GLUT1. The mutation of tyrosine 293, at the top of TM7, to isoleucine renders the mutant GLUT1 unable to transport 2-deoxy-D-glucose or to bind the internal ligand, cytochalasin B. A GLUT1 mutant in which proline 385, in TM10, is substituted with isoleucine loses the ability to transport 2-deoxy-D-glucose and to bind ATB-BMPA. The ability of GLUT1 to bind the external ligand, ATB-BMPA, is lost upon deletion of 25 residues from the C-terminal of GLUT1. The results obtained are interpreted in terms of the possibility of a close association of transmembrane segments 7 and 12 in the 3-dimensional structure of GLUT1. The six transmembrane segments of the C-terminal half of GLUT1 may be arranged concentrically, with TM7 next to TM12, to form a channel. The outside site would be occupied by an upward movement of TM7 and TM12 which may move a

proteolytic cleavage site into an inaccessible location. Tyrosine 293 may form part of a hydrophobic region at the external binding site. Mutation of tyrosine 293 may prevent the conformational change that is required to transport a substrate and to subsequently expose the internal binding site. The proline-rich region of TM10, particularly proline 385, may play an important role in the conformational changes of the glucose transporter protein.

The impermeant photolabel ATB-BMPA has been used in conjunction with specific antibodies to GLUT1 and to the insulin-responsive isoform (GLUT4) to investigate the insulin-stimulation of glucose transport activity in rat adipocytes. GLUT4 is found to be the major isoform in rat adipocytes and accounts for ≈ 90 % of the cell-surface glucose transporters in insulin-stimulated cells. Insulin is found to increase cell-surface GLUT4 by ≈ 15-20-fold and cell-surface GLUT1 by ≈ 4-fold. These levels of stimulation are contrasted with the increase in glucose transport activity which is ≈ 30-fold. The appearance of both GLUT1 and GLUT4 at the cell-surface precedes the transport stimulation which shows a lag period of ≈ 47 sec. The discrepancies between transport stimulation and transporter translocation may be due to an ≈ 2-fold intrinsic activation of the transporters.

ACKNOWLEDGEMENTS

I would particularly like to thank my supervisor Dr G D Holman for all his help and encouragement. Many thanks also to all the members of lab 3.33, past and present, for all their help and for making life in the lab so enjoyable.

Thankyou to all my friends and special thanks to my parents and to Jon Allman for their support and encouragement.

The work in this thesis was supported by the SERC and the MRC. Thankyou also to Dr S A Baldwin and Dr M Hashiramoto and colleagues for collaborating on portions of this thesis

ABBREVIATIONS

ASA-BMPA	2-N-(4-azidosalicoyl)-1,3-bis-(D-mannos-4-yloxy)-2-propylamine
ATB-BMPA	2-N-(1-azi-2,2,2-trifluoroethyl)benzoyl-1,3-bis-(D-mannos-4-yloxy)-2-propylamine
ATP	Adenosine triphosphate
BB-BMPA	2-N-(4-benzoyl)-benzoyl-1,3-bis-(D-mannos-4-yloxy)-2-propylamine
BCA	Bicinchoninic acid
BMPA	1,3-bis-(D-mannos-4-yloxy)-2-propylamine
BSA	Bovine serum albumin
cAMP	Adenosine 3',5'-cyclic monophosphate
CD	C-terminal deletion mutant
cDNA	Complementary deoxyribonucleic acid
CHO cells	Chinese hampster ovary cells
COS-7 cells	Monkey kidney cells
DMF	Dimethylformamide
DMSO	Dimethylsulphoxide
DPM	Disintegrations per minute
DTNB	5,5'dithiobis-(2-nitrobenzoic acid) : Ellmans reagent
DTT	Dithiothreitol
E. Coli	*Escherichia coli*
EDTA	Ethylenediaminetetraacetic acid
ELISA	Enzyme-linked immunosorbent assay
GLUT	Glucose transporter isoform
GTP	Guanosine triphosphate
GTV	GLUT4-containing vesicles
HDM	High density microsomes
Hepes	N-2-hydroxyethylpiperazine-N'-2-ethane sulphonic acid
HepG2	Hepatoma G2
IAPS	Iodo-4-azidophenylamido-7-O-succinyldeacetyl
IBMX	Isobutylmethylxanthine
IRS-1	Insulin receptor substrate-1
K_D	Dissociation constant
kDa	kilodalton
K_i	Affinity constant
KLH	Keyhole limpet haemocyanin
K_m	Michaelis constant
KRH	Krebs-Ringer Hepes buffer
LDM	Low density microsomes
MBS	N-maleimidobenzoic acid-N-hydroxysuccinimide ester

Mega 10	Decanoyl-N-methyl-glucamid
M_r	Molecular mass
mRNA	Messenger ribonucleic acid
NEM	N-ethyl maleimide
NSF	NEM-sensitive factor
NTCB	2-Nitro-5-thiocyanobenzoic acid
PAGE	Polyacrylamide gel electrophoresis
PAO	Phenylarsineoxide
PBS	Phosphate-buffered saline
PDM	Protein depleted membranes
PEG	Polyethylene glycol
PI	Phosphatidylinositol
PKC	Protein kinase C
PM	Plasma membrane
PMA	Phorbol 12-myristate 13-acetate
PMSF	Phenylmethanesulfonyl fluoride
RT	Room temperature
SCAMPS	Secretory component-associated membrane proteins
S.E.M.	Standard error of the mean
SDS	Sodium dodecylsulphate
SH	Src homology domain
SNAPS	Soluble NSF accessory proteins
TBS	Tris-buffered saline
TCA	Trichloroacetic acid
TEMED	N,N,N',N'-tetramethylethylene diamine
TES	Tris/EDTA/sucrose buffer
Thesit	Nonaethylene glycol dodecyl ether, $C_{12}E_9$
TK	Turnover/K_m
TM	Transmembrane segment
Tris	Tris-(hydroxymethyl)-methylamine
Tween-20	Polyoxyethylenesorbitan monolaurate
UV	Ultraviolet
VAMP	Vesicle-associated membrane protein
V_{max}	Maximal velocity

AMINO ACID ABBREVIATIONS

3 letter code	Amino acid	1 letter code
Ala	Alanine	A
Arg	Arginine	R
Asn	Asparagine	N
Asp	Aspartate	D
Cys	Cysteine	C
Gln	Glutamine	Q
Glu	Glutamate	E
Gly	Glycine	G
His	Histidine	H
Ile	Isoleucine	I
Leu	Leucine	L
Lys	Lysine	K
Met	Methionine	M
Phe	Phenylalanine	F
Pro	Proline	P
Ser	Serine	S
Thr	Threonine	T
Trp	Tryptophan	W
Tyr	Tyrosine	Y
Val	Valine	V

CHAPTER 1 : INTRODUCTION

1.1. The Glucose Transporter Family

The uptake of glucose into cells is a very important process and is achieved by a protein present in the cell membrane. The hexose transporter in most mammalian cells is the passive, facilitative diffusion type in which net transport always occurs in the direction of high to low sugar concentration. However, a number of cell types such as kidney, small intestine and bacterial cells contain an active transporter protein that can transport sugars against their concentration gradient by co-transporting ions such as H^+ or Na^+. The transporters display a strong specificity for D-stereoisomers of pentose and hexose monosaccharides adopting the chair configuration of the pyranose ring such as D-glucose, D-galactose or D-mannose. A family of glucose transporters have now been identified (Table 1) which display a high degree of sequence homology and are all predicted to have a similar structure within the membrane, consisting of 12 membrane spanning domains. However, they vary greatly in their tissue distribution, specificity and regulation. In order to have a better understanding of the way that the protein transports sugars, the conformational changes of the glucose transporter upon binding of external and internal ligands have been investigated in the native erythrocyte glucose transporter and in a number of mutant glucose transporter proteins. The regulation of glucose transport in the adipose cell, where two different glucose transporter isoforms are both differentially regulated by insulin has also been investigated

Designation (alternative)	M_r (residues)	Major sites of expression	Chromosomal location
GLUT1 (erythrocyte/ HepG2)	54117 (492)	erythrocyte, blood-brain barrier, placenta, fetal tissues	1
GLUT2 (liver)	57000 (524)	liver, pancreatic ß-cell, kidney, small intestine	3
GLUT3 (brain)	53933 (496)	brain (neurones)	12
GLUT4 (insulin-responsive)	54797 (509)	brown and white adipocytes, heart and skeletal muscle	17
GLUT5 (small intestine)	54983 (501)	small intestine	1
GLUT7 (microsomal)	53000 (528)	endoplasmic reticulum of hepatocytes	not determined

Table 1 Properties of the Mammalian Facilitative Diffusion Glucose Transporter Family

1.1.1. The Erythrocyte, HepG2-type Glucose Transporter (GLUT1)

The erythrocyte glucose transporter is known to be an integral membrane protein with an approximate molecular weight of 55 kDa, as shown by SDS-PAGE. An antibody generated against this protein was used by Mueckler *et al*, (1985), to screen a cDNA library prepared from the human HepG2 hepatoma cell line. A cDNA encoding a 492 amino acid glucose transporter protein was isolated. The predicted amino acid sequence corresponded with partial amino acid data obtained for the erythrocyte transporter.

Birnbaum *et al*, (1986), cloned and sequenced glucose transporter cDNA from adult rat brain and found 97.6 % identity to the HepG2 glucose transporter. GLUT1 mRNA has been identified in most tissues, the highest levels being in fetal tissues and placenta. The highest levels in adults are found in brain, kidney and colon, with only low levels in liver and skeletal muscle, two important sites of glucose uptake. GLUT1 is also expressed in most cultured cell lines, generally at much higher levels than in the original cell type. Elevated levels of GLUT1 have also been observed in a range of tumours (Yamamoto *et al*, 1990).

1.1.2. The Liver-Type Glucose Transporter (GLUT2)

Birnbaum *et al*, (1986) noted that very little mRNA was detected in rat liver when screened for rat brain glucose transporter mRNA compared with the large levels of glucose transport observed and so concluded that a different glucose transporter must be present in rat liver. In 1988, two groups cloned a unique glucose transporter

from human and rat liver. Thorens *et al*, (1988), screened a rat liver cDNA library with rat brain glucose transporter cDNA and found a protein of 522 amino acids with 55 % identity with GLUT1. They expressed the protein in an E. Coli mutant deficient in glucose transport activity and showed that the protein transported glucose.

Fukumoto *et al*, (1988), obtained a human GLUT2 cDNA from kidney and liver cDNA libraries and found a protein of 524 amino acids with a 55.5 % identity with GLUT1. There is 82 % identity between human and rat GLUT2. GLUT2 is expressed at highest levels in liver and pancreatic ß-cells, and at lower levels in kidney and small intestine.

GLUT2 differs from GLUT1 in that it transports fructose, with an apparent K_m of 100 mM (Gould *et al*, 1991). It is also unable to bind the internal ligand forskolin (Hellwig & Joost, 1991) and binds cytochalasin B only weakly (Ciaraldi *et al*, 1986, Hellwig & Joost, 1991).

Insulinoma cells express GLUT1 rather than the GLUT2 which is normally present in the pancreatic ß-cell (Thorens *et al*, 1988). Thorens *et al*, (1988) suggest that this abnormal expression of GLUT1 may be related to an inability of the insulinoma cells to secrete insulin in response to elevated glucose levels.

1.1.3. The Brain-Type Glucose Transporter (GLUT3)

The GLUT3 glucose transporter isoform was first identified by probing a human fetal skeletal muscle library with GLUT1 cDNA (Kayano *et al*, 1988). The GLUT3 cDNA was found to encode a protein of 496 amino acids having 64 % and 52 % identity with GLUT1 and GLUT2 respectively. GLUT3 mRNA is present in

all tissues but is most abundant in adult brain, kidney, gall bladder and placenta. GLUT3 has been expressed in CHO cells (Asano *et al*, 1992), where it was found to be localized mainly to the plasma membrane. GLUT3 has similar characteristics to GLUT1, but has a lower K_m and V_{max} for 3-O-methyl-D-glucose transport (Asano *et al*, 1992c). GLUT3, like GLUT1, has been found to be overexpressed in cancer tissue (Yamamoto *et al*, 1990).

1.1.4. The Insulin-Responsive Glucose Transporter (GLUT4)

GLUT4 was first identified using a monoclonal antibody (mAb IF8) prepared against a low-density microsomal fraction of rat adipocytes (James *et al*, 1988). The antibody was used to immunodetect a 43 kDa protein in the plasma-membrane of rat adipocytes, whose concentration was increased 5-fold after cellular insulin exposure. James *et al*, (1989), obtained GLUT4 cDNA from both rat adipocyte and heart libraries. Birnbaum (1989) cloned GLUT4 cDNA from a skeletal muscle library. GLUT4 was found to be a 509 amino acid protein with 65 % identity with GLUT1.

The highest levels of GLUT4 mRNA are in insulin-responsive tissues such as cardiac and skeletal muscle, heart and brown and white adipose tissue (James *et al*, 1989). GLUT4 mRNA is also expressed in 3T3-L1 adipocytes but only after differentiation of the fibroblastic cell line into adipocytes (James *et al*, 1989).

1.1.5. The Small Intestine Glucose Transporter (GLUT5)

The GLUT5 cDNA was isolated from a human small intestine cDNA library by Kayano *et al*, (1990). GLUT5 encodes a protein of 501 amino acids and has 41.7 %, 40 %, 38.7 % and 41.6 % identity with GLUT's 1, 2, 3 and 4, respectively. The mRNA is found at high levels in small intestine and at much lower levels in kidney, skeletal muscle and adipocytes. Burant *et al*, (1992), have expressed GLUT5 in *Xenopus* oocytes and have shown that it is a high affinity fructose transporter that is not inhibited by cytochalasin B or D-glucose.

Although both GLUT2 and GLUT5 are in small intestine, GLUT2 is located on the basolateral membranes of the absorptive cells and GLUT5 is located on the apical membranes of the absorptive cells. Therefore Burant *et al*, (1992), suggest that GLUT5 is the most important transporter for fructose uptake from the lumen of the small intestine.

1.1.6. The Glucose Transporter Pseudogene (GLUT6)

A glucose transporter pseudogene was identified by Kayano *et al*, (1990), and is part of an 11 kilobase transcript that is expressed in all tissues examined. A portion of this pseudogene (1.5 kilobase pairs) has 79.6 % identity with GLUT3. Because of the presence of multiple stop codons and frame shifts the sequence can not encode a functional glucose transporter protein. However, this pseudogene was termed GLUT6.

1.1.7. The Microsomal Glucose Transporter (GLUT7)

GLUT7 was identified when Waddell *et al*, (1992) used antibodies raised against a 52 kDa rat liver microsomal glucose transport protein (a component of the glucose-6-phosphatase system) to screen a rat liver cDNA library. Two of the positive clones were found to be GLUT2 but the other 4 clones encoded a unique microsomal glucose transporter protein. The largest GLUT7 clone encoded a protein of 528 amino acids with 68 % identity to GLUT2. GLUT7 has an additional 6 amino acids at its C-terminal compared with GLUT2 and these amino acids contain a consensus motif for membrane-spanning proteins targeted to the endoplasmic reticulum. When GLUT7 was expressed in COS-7 cells (Waddell *et al*, 1992), it was found in the endoplasmic reticulum and nuclear membrane and was shown to be functionally active in glucose transport.

1.2. The Structure of the Glucose Transporter Protein

1.2.1. The Two-Dimensional Membrane Topology of the Glucose Transporter

Analysis of the hydropathy profile of the GLUT1 amino acid sequence led Mueckler *et al*, (1985) to suggest a model for the glucose transporter in which it has 12 integral membrane spanning segments with both N- and C-termini located in the cytoplasm (Fig. 1). There is a large hydrophilic loop of 65 amino acids between transmembrane segments (TM) 6 and 7 and an extracellular loop of 33 amino acids between TM1 and TM2, containing an asparagine which is glycosylated by a mannose-rich carbohydrate moiety (Mueckler *et al*, 1985).

The two-dimensional structural topology of the glucose transporter protein in the membrane has still not been totally proven. The cytoplasmic location of the C-terminal and the central hydrophilic loop have been confirmed by studies with proteolytic enzymes (Cairns *et al*, 1987) and specific peptide antibodies (Davies *et al*, 1987, 1990). Davies *et al*, (1990) produced anti-peptide antibodies to a number of the predicted intracellular and extracellular extramembranous domains but only those against the large central loop and C-terminal recognized the native transporter. The exofacial location of cysteine 429 (predicted to be in TM12) has been confirmed by studies in which the substitution of cysteine prevented inhibition of glucose transport by sulphydryl-reactive agents (Wellner *et al*, 1992). Also the loop between TM1 and TM2 is known to be extracellular because it contains the single site of N-linked glycosylation of the transporter (Cairns *et al*, 1987).

Analysis of the amino acid sequences of the other members of the glucose transporter family suggest that they all have a similar membrane topology to that of

Fig. 1. Predicted model for the arrangement of the GLUT1/HepG2 glucose transporter in the plasma membrane as proposed by Mueckler *et al* (1985). The glucose transporter is predicted to have 12 membrane spanning segments with the N- and C-termini facing into the cytoplasm. The glucose transporter is glycosylated on asparagine 45 in the extracellular loop between transmembrane segments 1 and 2. Regions of the glucose transporter involved in the binding of the exofacial photolabel ATB-BMPA (Ala 301-Arg 330) and the endofacial photolabel cytochalasin B (Phe 389-Trp 412) are shown (Davies *et al*, 1992).

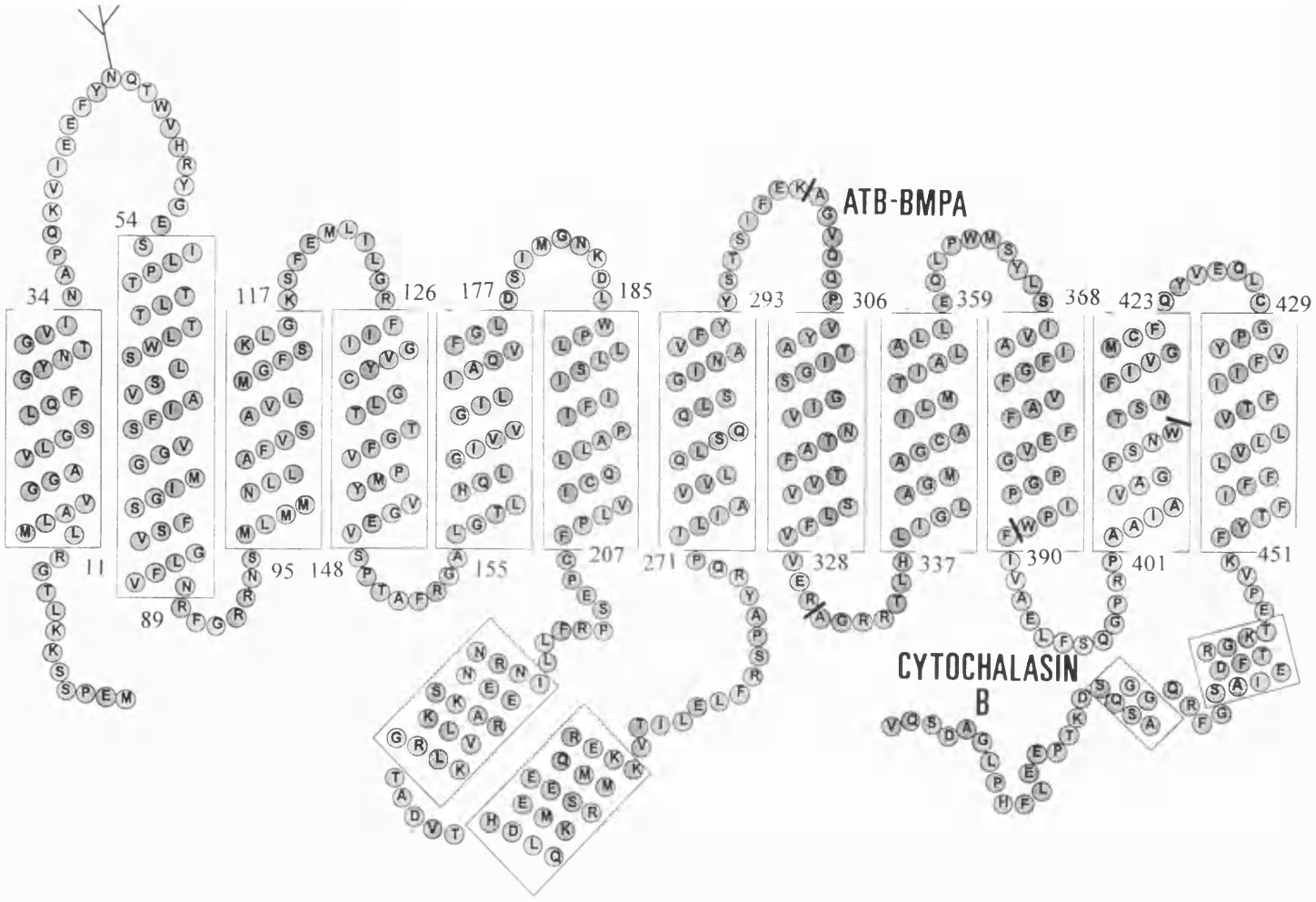
ATB-BMPA
CYTOCHALASIN B
54
34
117
126
177
185
293
306
359
368
423
429
11
89
95
148
155
207
271
328
337
390
401
451

GLUT1. GLUT2 varies greatly from GLUT1 in two domains (Fukumoto *et al*, 1988, Thorens *et al*, 1988). GLUT2 has a larger extracellular loop (between TM1 and TM2) with an extra 32 amino acids. Both transporters are glycosylated in this region. The C-termini of GLUT1 and GLUT2 are not well conserved and GLUT2 has a potential cAMP dependent-protein kinase phosphorylation site in its C-terminal portion (Fukumoto *et al*, 1988).

GLUT4 has a slightly longer N-terminal region before TM1. GLUT1 and GLUT4 sequences vary most in the predicted soluble domains, particularly the large cytoplasmic C- and N-termini and central loop regions and also within the predicted transmembrane segment 3 (James *et al*, 1989).

1.2.2. Glycosylation of the Glucose Transporter

The heterogeneity of the glucose transporter on SDS-PAGE, where it runs as a broad band corresponding to an approximate molecular weight of 45-65 kDa, is due to glycosylation of the transporter on asparagine 45 (Mueckler *et al*, 1985). Removal of the carbohydrate by endoglycosidase F treatment produces a single band on SDS-PAGE of 46 kDa (Gorga *et al*, 1979). Feugeas *et al*, (1990) found that N-glycanase treatment of the human erythrocyte glucose transporter resulted in an inhibition of glucose transport activity and so concluded that glycosylation is essential for glucose transport activity. However, partial removal of the carbohydrate with endo-ß-galactosidase did not reduce glucose transport activity (Wheeler & Hinkle, 1981).

Mutation of asparagine 45 to either aspartate, tyrosine or glutamine resulted in the mutant GLUT1 clones having an increased K_m for 2-deoxyglucose uptake and a

much lower affinity for both the internal ligand, cytochalasin B, and the external ligand, ATB-BMPA, than the wild-type GLUT1 (Asano *et al*, 1991). Subsequent studies by Asano *et al* (1993) have shown that the lack of N-glycosylation causes improper targeting of the protein to the cell surface. The stability of the glycosylation-deficient GLUT1 protein is also decreased (Asano *et al*, 1993).

1.2.3. The Three-Dimensional Structure of the Glucose Transporter

The three-dimensional structure of the glucose transporter is not at present known due to the difficulties in obtaining crystals, and so crystallographic data, for this membrane-associated protein. Chin *et al*, (1987) reported circular dichroism measurements that indicated that the purified erythrocyte glucose transporter protein (GLUT1) contains mainly (> 82 %) α-helical structure with small amounts of ß-turn of ≈ 10 % and of random coil of ≈ 8 % but with no ß-strands. Fourier Transform Infrared Spectroscopy of this glucose transporter (Alvarez *et al*, 1987, Cairns *et al*, 1987) suggested that it is mainly α-helical with a little ß-sheet and random coil conformation. The cytoplasmic C-terminal portion removed by trypsin was also found to contain α-helical structure (Cairns *et al*, 1987).

A speculative model for the 3-dimensional arrangement of the 12 membrane spanning segments is shown in figs. 2 & 3. The duplication of sequences in the N and C-terminal halves of the transporter has led to speculation that a gene duplication event may be responsible for the present structure of the glucose transporter and that the two halves might be arranged in a similar manner (Maiden *et al*, 1987).

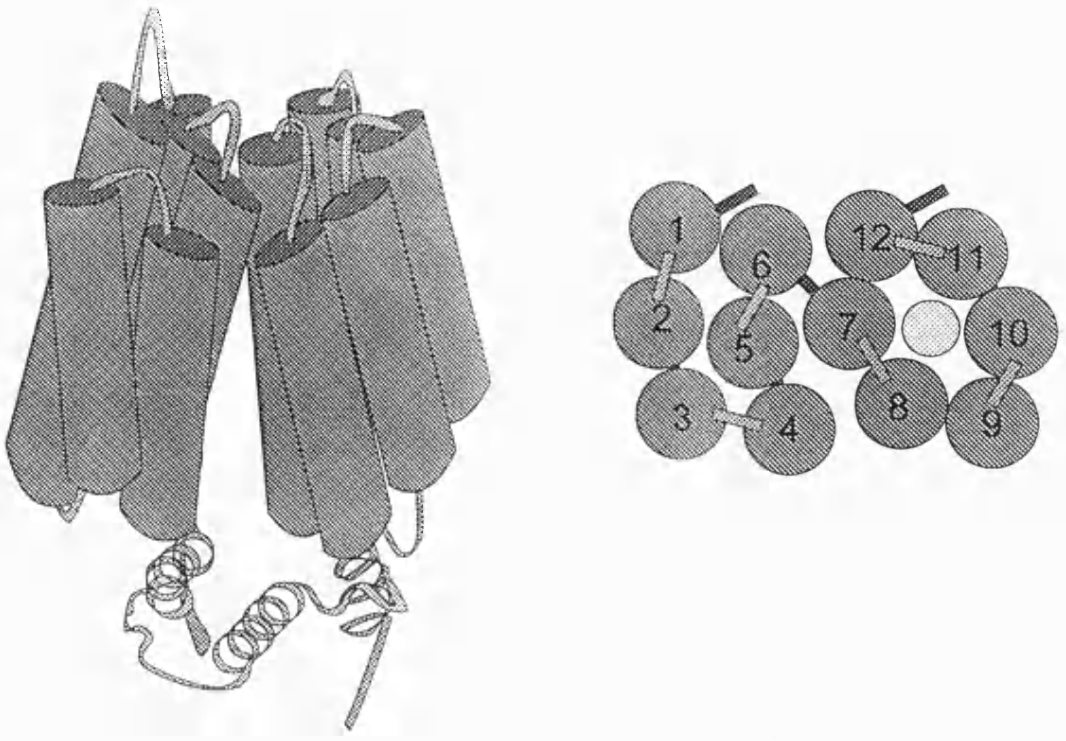

Fig. 2. **A speculative model for the 3-dimensional arrangement of the 12 membrane spanning segments of the** glucose **transporter protein.** The model predicts that the N- and C- terminal halves of the glucose transporter might be arranged in a similar manner. Transmembrane segments 7, 8 and 11 are predicted to be amphipathic and may form part of a hydrophilic channel (Mueckler *et al*, 1985).

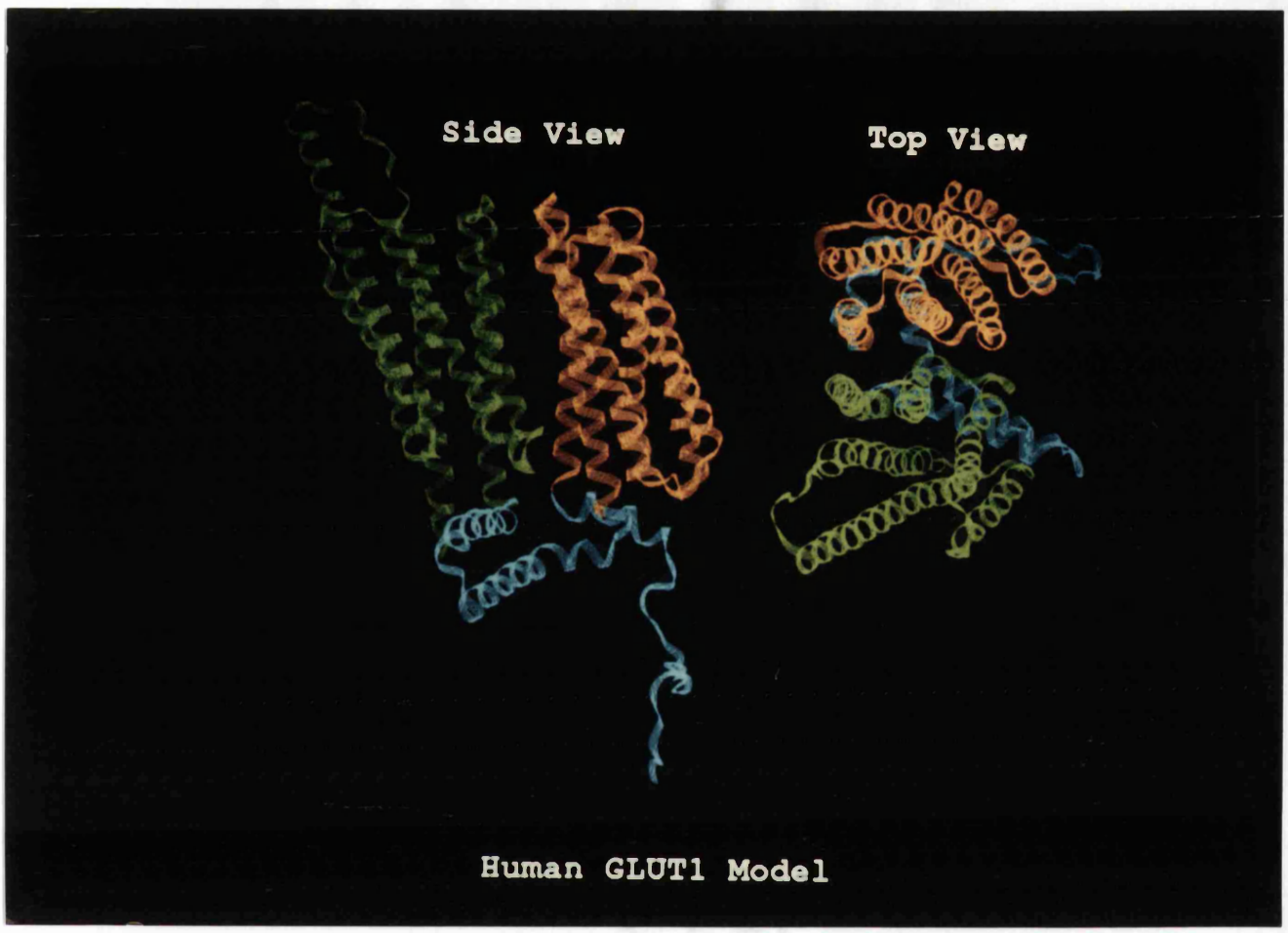

Fig. 3. A putative model of GLUT1 (produced by Dr P. Hodgson, University of Bath). A putative model of GLUT1 based on molecular dynamic simulations. The N- and C-terminal halves are shown in green and orange, respectively. The cytoplasmic central loop and C-terminal are shown in blue.

Transmembrane segments 7, 8 and 11 are predicted to be amphipathic and may form part of a hydrophilic channel (Mueckler *et al*, 1985).

All evidence presently available suggests that glucose is transported through the C-terminal half of the protein only. The photoaffinity ligands, cytochalasin B, ATB-BMPA and IAPS-forskolin all bind, in a glucose displaceable manner, to the C-terminal half only (Karim *et al*, 1987, Clark & Holman, 1990, Wadzinski *et al*, 1990, Hellwig *et al*, 1992). Katagiri *et al* (1992) replaced the intracellular C-terminal domain of GLUT1 with that of GLUT2 and found that the C-terminal domain conferred GLUT2-like properties on the transporter, suggesting that the diversity of the C-terminal domains of the glucose transporter isoforms may contribute to the diversity of the differing characteristics of the glucose transporter isoforms.

Although the N-terminal half does not appear to bind transporter ligands, it is essential for glucose transport activity and is probably involved with transporter regulation. It has been suggested that the N-terminal of GLUT4 is necessary for sequestration of this isoform within the cell (Piper *et al*, 1992, 1993). The external ligand, ATB-BMPA, only binds to the bacillovirus-expressed C-terminal half of GLUT1, when the N-terminal half of GLUT1 is also expressed (Cope, Holman & Wolstenholme, manuscript in preparation). Mutation of asparagine 45, which prevents the normal glycosylation of GLUT1 in the N-terminal half of the protein, has been found to alter GLUT1 targeting and stability (Asano *et al*, 1991, 1993).

1.2.4. The Higher Order Structure of the Glucose Transporter

Whether the glucose transporter protein is present in the membrane as a

monomer or as an oligomeric form is still not known. Radiation inactivation studies have been carried out by a number of groups. Jacobs *et al*, (1987), suggest that the adipocyte glucose transporter (now known to be GLUT4) occurs as a monomer in the plasma membrane, whilst existing as a homodimer, or as a stoichiometric complex with a protein of approximately equal size, in the intracellular membrane pool. Jarvis *et al*, (1986), suggest that the human erythrocyte glucose transporter exists as a dimer in the membrane with an apparent M_r of 124 ± 11 kDa, whereas Cuppoletti *et al*, (1981) obtained a M_r of 185 kDa, suggesting a tetramer. Hebert & Carruthers, (1992) suggest that the native glucose transporter is a homotetramer which is stabilized by intramolecular disulphide bonds and that it can be transformed to dimeric GLUT1 by alkaline reduction.

Pessino *et al*, (1991) expressed chimeric glucose transporters with the C-terminal of GLUT1 replaced with the C-terminal of GLUT4 in CHO cells harbouring endogenous GLUT1. They found that endogenous GLUT1 could be immuno-precipitated with an anti-GLUT4 peptide antibody and therefore suggested that GLUT1 may exist as a dimer or higher order oligomer. Burant & Bell, (1992) coexpressed two different glucose transporter isoforms in *Xenopus* oocytes and found that the oocytes produced kinetic properties that reflected the parental transporters rather than a protein with intermediate properties. Also when varying amounts of a normal and functionally inactive transporter were coexpressed, they found no inhibition of glucose transport. They therefore concluded that a monomer is the functional unit of transport activity (Burant & Bell, 1992).

1.3. Glucose Transporter Kinetics and Substrate Recognition

1.3.1. Glucose Transporter Kinetics

The erythrocyte glucose transporter exhibits asymmetrical kinetics, the K_m and V_{max} values for zero-*trans* efflux being considerably greater than those for influx (Lowe & Walmsley, 1986). The transporter also exhibits *trans*-acceleration, that is, the stimulation of the unidirectional flux of labelled sugar across the membrane by the presence of unlabelled sugar on the opposite side of the membrane. Glucose transport in erythrocytes is highly temperature dependant. Lowe and Walmsley (1986) found that the inequalities in the maximum rates of zero-*trans* efflux and influx and equilibrium exchange, decrease as the temperature rises and almost disappear at physiological temperature. At low temperatures, the marked asymmetry arises mainly from the high proportion of inward-facing transporters and transporter-glucose complexes. At physiological temperatures, the transporter is fairly evenly distributed between outward- and inward-facing conformations and the affinity for glucose is about 2.5 times greater outside than inside (Lowe & Walmsley, 1986).

Whereas transport in erythrocytes is asymmetric, in the rat adipocyte glucose transport properties were found to be symmetrical in both the basal and insulin-stimulated states (Taylor & Holman, 1981).

1.3.2. The Alternating Conformation Model

Glucose transport in the erythrocyte is purely passive and does not require any input of energy, from either a concentration gradient of a second carried substrate or a chemical reaction , such as the hydrolysis of ATP. In 1952, Widdas demonstrated that human erythrocyte and sheep placental glucose transport were characterised by simple Michaelis-Menten saturation kinetics. His studies led to the proposal of the alternating conformation model for sugar transport (Fig. 4).

The glucose transporter is proposed to contain mutually exclusive saturable sugar influx and efflux sites. When sugar binds to one of these sites to form the carrier-sugar complex, a conformational change is promoted that results in sugar translocation, dissociation of the sugar from the carrier at the opposite side of the membrane, and the exposure of the glucose transport site at the opposite side of the membrane. The carrier is now available for transport in the opposite direction or can isomerize back to its original state with the sugar binding site exposed at the original side of the membrane.

Appleman & Lienhard (1989) measured the rates of interconversion of the transporter conformers T_i and T_o in the presence and absence of D-glucose using intrinsic fluorescence. The values of the individual rate constants obtained were consistent with the alternating conformation model (Appleman & Lienhard, 1989).

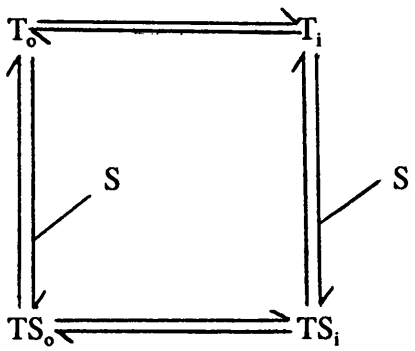

Fig. 4. The alternating Conformation Model for Sugar Transport In the absence of substrate (S), the transporter (T) can exist as only 1 of 2 possible interconverting isomers: T_o where the binding site faces the outside of the cell, and T_i where the binding site faces the inside of the cell. On addition of intracellular or extracellular sugar (S), a transporter-sugar complex is formed which undergoes a conformational change to expose the sugar at the opposite side of the membrane, where it is released.

1.3.3. Multiple-Site Models

A number of more complex models for glucose transport have been proposed in which multiple substrate binding sites are simultaneously present on the transporter (Helgerson & Carruthers, 1987, Hebert & Carruthers, 1992). The glucose carrier is proposed to contain saturable sugar influx and efflux sites that exist simultaneously. In order to explain the *trans*-phenomena in glucose transport, these investigators suggest that the two sites display negative cooperativity.

Hebert & Carruthers (1992) propose that the glucose transporter protein is tetramer and is stabilized by intramolecular disulphide bonds. According to their model, in a multisubunit transporter the transfer of substrate to an inside site is conformationally coupled to the exposure of an external site on another subunit of the transporter. This would allow external and internal ligands to simultaneously occupy the oligomeric transporter.

Hellwig & Joost, (1991) investigated the affinities of various ligands for GLUT1, GLUT2 and GLUT4 glucose transporter isoforms in a number of different tissues. They suggest that the complex differences they found result from the interaction of more than one heterogeneous binding site on the glucose transporter with the ligand.

Nishimura *et al*, (1992a) using monoclonal antibodies directed against erythrocyte GLUT1 found that D-glucose binding inhibited the binding of these monoclonal antibodies by 50 %. A high concentration of cytochalasin B inhibited the binding of one of these monoclonal antibodies to the erythrocyte GLUT1. However, a low concentration of cytochalasin B enhanced the binding of another of the monoclonal antibodies which presumably recognised a different epitope. Nishimura

et al, (1992a) therefore suggest the existence of high and low affinity binding sites for D-glucose and cytochalasin B. They suggest that the binding of these ligands cause different conformational changes within the glucose transporter depending on whether they occupy a low or a high affinity site.

1.3.4. Side Specificity of the Glucose Transporter

Side specificity of the glucose transporter in erythrocytes has been investigated using D-glucose analogues (Barnett *et al*, 1973a, b, 1975). Introduction of bulky groups into the hydroxyls at the C4 and C6 positions of D-glucose produced analogues which were tolerated by the external site of the transporter. However, substitution at C1 of D-glucose resulted in loss of binding. The reverse occurred when glucose derivatives interacted with the internal site of the transporter. Here, C1 alkyl substituted compounds bound well, but C4 and C6 derivatives did not. Barnett *et al* (1973a,b) concluded that there must be a structural link between the inside and outside sites which forces the sugar to enter the transporter from the outside with C1 first and C4/C6 trailing. This polarization of the sugar is maintained throughout the transport channel (Fig. 5). 4,6-O-ethylidene-D-glucose is a good outside specific hexose while propyl ß-D-glucopyranoside is inside specific (Barnett *et al*, 1973b).

Spacial requirements for hexose binding to the outside site of the rat adipocyte glucose transporter have also been investigated (Holman *et al*, 1981). The spacial requirements were found to be similar to those of the erythrocyte glucose transporter with only small differences in the affinity for various analogues. The affinity

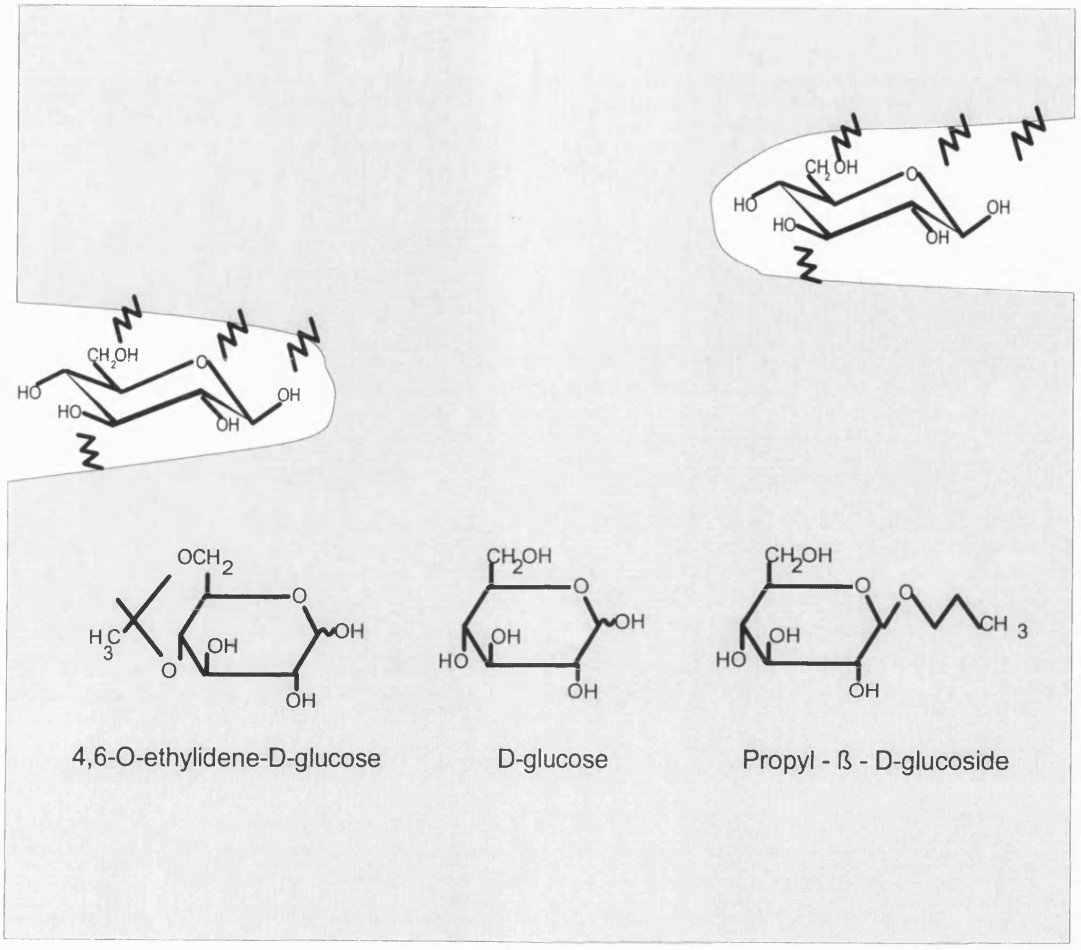

Fig. 5. Possible model for sugar transport in the erythrocyte (Barnett *et al*, 1973a, b). Glucose is proposed to enter the transporter with C1 first and C4/C6 trailing and this polarization is maintained throughout the transport channel. 4,6-O-ethylidene-D-glucose is a good outside-specific hexose while propyl-ß-D-glucoside is inside-specific.

constants for the various analogues were similar in basal and insulin-stimulated cells indicating that insulin does not cause a major structural change in the transporter, but instead increases the availability of sites of identical specificity (Holman *et al*, 1981).

1.3.5. Photoaffinity Labels for the Glucose Transporter

1.3.5.1. Cytochalasin B

Irradiation of ^{3}H-cytochalasin B (Fig. 6) in the presence of purified glucose transporter or erythrocyte membranes results in stereospecific, D-glucose inhibitable, low efficiency (1-5 %), covalent incorporation of labelled ligand into the glucose transporter (Shanahan, 1982). GLUT1 and GLUT4 have a strong affinity for cytochalasin B. The dissociation constants (K_D) for cytochalasin B binding to the glucose transporter in erythrocytes (K_D = 190 nM) and in adipocytes (K_D = 160 nM) are similar (Hellwig & Joost, 1991).

Cytochalasin B is thought to bind at the internal surface of the glucose transporter in the region of TM10 and TM11 between Phe 389 and Trp 412 (Holman & Rees, 1987, Davies *et al*, 1992). Cytochalasin B is permeable to cells. It is not specific for the glucose transporter and so labelling is carried out in the presence of cytochalasin E which blocks the binding of cytochalasin B to non-glucose transporter proteins.

ATB-BMPA

2-N-(1-azi-2,2,2-trifluoroethyl)benzoyl-1,3-bis(D-mannos-4-yloxy)-2-propylamine

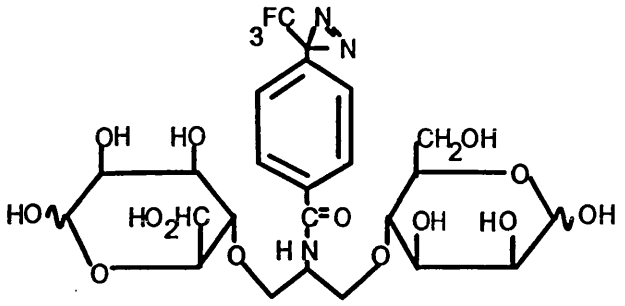

Cytochalasin B

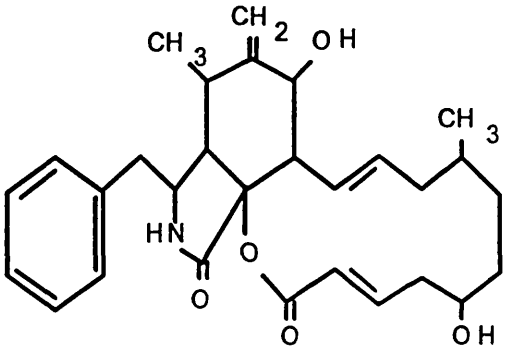

Fig. 6. The structure of the exofacial and endofacial photoaffinity labels for the glucose transporter. ATB-BMPA binds to the exofacial surface of the glucose transporter and cytochalasin B is inside-specific.

1.3.5.2. Forskolin

Forskolin is a potent glucose transporter inhibitor and binds to the erythrocyte glucose transporter in a cytochalasin B-inhibitable manner (Shanahan *et al*, 1987). Tritiated forskolin and 3-[^{125}I]iodo-4-azidophenylamido-7-O-succinyldeacetylforskolin (IAPS-forskolin) are used as photoaffinity reagents for the glucose transporter in erythrocytes (Shanahan *et al*, 1987, Wadzinski *et al*, 1990) and adipocytes (Zorzano *et al*, 1989, Hellwig *et al*, 1992). The dissociation constant (K_D) for forskolin binding to GLUT1 (K_D = 2360 nM) is significantly higher than for binding to GLUT4 (K_D = 200 nM) (Hellwig & Joost, 1991).

The forskolin binding site in the human erythrocyte glucose transporter has been localized to TM10 by Wadzinski *et al*, (1990) who suggest that tryptophan 388 may be involved. The forskolin binding site in GLUT4 from adipocytes has been localized to a site between TM7 and TM9, possibly in the proximity of TM9 (Hellwig *et al*, 1992). They tentatively suggest that forskolin may bind to more than one site in a region spanning transmembrane segments 9 and 10.

1.3.5.3. Bis-Mannose Derivatives as Photoaffinity Labels

A bis-mannose compound (1,3-bis-(D-mannos-4-yloxy)-2-propylamine, BMPA) was designed by Midgley *et al*, (1985) to be an impermeant external ligand for the glucose transporter. Two D-mannose residues were cross-linked through their C4 hydroxyl positions by a 2-propylamine bridge. It has been shown that bulky substitutions at the C4 position can be tolerated by both the glucose transporter protein

in erythrocytes (Barnett *et al*, 1973a) and adipocytes (Holman *et al*, 1981).

Radiolabel was introduced into the 2-position of the bridge by reductive amination. Various photoreactive substituents were attached to the bis-mannose via the amine in the bridge. By synthesizing tritiated derivatives, Midgley *et al*, (1985) showed that the BMPA derivatives were not significantly taken up by either erythrocytes or adipocytes over a period of 90 min, neither via the transporter nor through the lipid bilayer. The compounds had a higher affinity for the glucose transporter protein than the parent compound, D-mannose, but had much lower affinities than alternative labelling reagents such as cytochalasin B and IAPS-forskolin. Therefore it was important that the photolabile substituent was selective. A 4-azidosalicylate derivative of BMPA (ASA-BMPA) was shown by Holman *et al*, (1986) to label the glucose transporter in intact erythrocytes. However, when used with isolated membranes, ASA-BMPA gave some labelling of erythrocyte membrane band 3 and spectrin. A benzophenone derivative of BMPA (BB-BMPA) has been used to label both erythrocyte and adipocyte glucose transporters (Holman *et al*, 1988). However, relatively long irradiation times were required for activation of the photolabile group, in which time damage to the cells may occur.

1.3.5.4. An Azitrifluoroethylbenzoyl-Substituted Bis-Mannose Photolabel

The main properties desired of a photoactivatable group are chemical stability prior to photoactivation, rapid photolysis at an appropriate wavelength and a very high reactivity of the photogenerated species (Bayley & Knowles, 1977). Carbenes react very rapidly with a variety of chemical functions: by coordination to nucleophilic

centers (to give carbanions), by addition to multiple bonds (including those of aromatic systems), by insertion into single bonds (including carbon-hydrogen bonds), and by hydrogen abstraction (to give two free radicals that may then couple) (Bayley & Knowles, 1977).

The diazirine group as a carbene precursor has many advantages. Diazirines are relatively stable in acid. The addition of an electron-withdrawing group such as fluorine stabilizes the parent diazo compound and also decreases the tendency to Wolff rearrangement after photolysis (Bayley and Knowles, 1977). Brunner *et al*, (1980) synthesised 3-trifluoromethyl-3-phenyldiazirine as a carbene precursor and have used this to investigate the hydrophobic regions of membrane proteins (Brunner & Richards, 1980).

The structure of the diazirine derivative of BMPA (2-N-[4-(1-azitrifluoroethyl)benzoyl]-1,3-bis(D-mannos-4-yloxy)-2-propylamine (ATB-BMPA) is shown in Fig. 6. Diazirine substituted hexoses have been used as transported substrates for the glucose transporter (Midgley *et al*, 1985). ATB-BMPA was produced in order to get improved labelling of the erythrocyte and adipocyte glucose transporters and using a shorter irradiation time.

1.4. Conformational Changes of the Glucose Transporter Protein

1.4.1. Chemical and Physical Studies on Glucose Transporter Conformational Changes

A number of approaches have been used to investigate the conformational changes that occur within the glucose transporter protein. When sugar analogues were added to fix the glucose transporter in an inward or outward facing conformation, shifts in the α-helical and ß-structure absorptive band were observed (Alvarez *et al*, 1987). In the presence of an excess of glucose the α-helical content was reduced and there was a significant increase in the random structure content, whereas in the presence of cytochalasin B there was no significant change (Chin *et al*, 1987).

Rampal & Jung, (1987) studied the effect of glucose binding to the erythrocyte glucose transporter on its inactivation by alkylating agents such as N-ethylmaleimide and found that the substrate-induced conformational change mostly occurred within the transmembrane hydrophobic domain. The hydrophilic extracellular domains did not show marked changes.

A number of groups have investigated glucose transporter intrinsic fluorescence, using several ligands including D-glucose and internal- and external-site specific ligands. The extent of quenching of tryptophan fluorescence varied depending on the liganded state of the transporter. Chin *et al*, (1992) suggested possible interactions between Trp 388 and His 337, Trp 412 and Cys 347 and Trp 412 and Glu 380, and stressed the importance of helices 9, 10 and 11 in the transport catalysis process. Pawagi & Deber, (1990) suggested that the region around Trp 388 could be a dynamic segment, which could be located alternately in an aqueous or membrane domain. No change in fluorescence quenching was observed with cytochalasin B

binding (Pawagi & Deber, 1990).

1.4.2. Studying Glucose Transporter Conformational Changes using Proteinases

Proteolysis by enzymes and chemicals has been used to investigate the conformational changes that take place within the erythrocyte and adipocyte glucose transporter upon binding of ligands at internal and external surfaces.

Non-transported exofacial ligands like phloretin and 4,6-O-ethylidene-D-glucose (Gibbs *et al*, 1988, Yano & May, 1993) and ASA-BMPA (Holman & Rees, 1987) decrease the extent of cleavage by trypsin and thermolysin. This protection can not be due to steric hindrance as the native transporter is cleaved solely at its cytoplasmic face, within the large loop between TM6 and TM7 and within the C-terminal extramembranous region (Cairns *et al*, 1987). Therefore the exofacial ligands are thought to stabilize a conformation in which parts of the cytoplasmic loop and C-terminal (which contain the proteolytic cleavage sites) are withdrawn from the cytoplasmic surface.

Compounds that are known to bind internally such as methyl and propyl glucosides, have been shown to increase the susceptibility of the glucose transporter to thermolysin (King *et al*, 1991, Yano & May, 1993) and therefore may be stabilizing an inward-facing conformation in which the cleavage sites are accessible to the protease. When cytochalasin B is covalently bound to the internal surface of the erythrocyte glucose transporter it also increases susceptibility to proteolysis (Holman & Rees, 1987). Noncovalently bound cytochalasin B does not however alter the susceptibility of GLUT1 to proteinases but does reverse the effects of exofacial

ligands which stabilize the exofacial conformation (King *et al*, 1991, Gibbs *et al*, 1988). Surprisingly, cleavage of erythrocyte GLUT1 is decreased by noncovalently bound cytochalasin B at higher temperatures of 45-50 °C (Gibbs *et al*, 1988). In contrast, binding of cytochalasin B was found to increase the cleavage of GLUT4 in adipocyte microsomal membranes (Yano & May, 1993). The authors suggest that this may reflect a greater tendency of the unloaded GLUT4 transporter to assume an outward-facing conformation in the absence of cytochalasin B than observed for the erythrocyte GLUT1 protein.

D-glucose has been shown to increase the cleavage of the erythrocyte glucose transporter by papain (Asano *et al*, 1992b), thermolysin (King *et al*, 1991) and trypsin (Gibbs *et al*, 1988) within the cytoplasmic loop and the C-terminal. The observed D-glucose effect was thought by King *et al*, (1991) to be due to the D-glucose at equilibrium forming a complex with the internal site. However, this may reflect an increased susceptibility of the protein to cleavage during the transport process itself (Baldwin, 1993). However, the asymmetric carrier model predicts a small increase in the steady state of the proteinase-resistant outward-facing carrier conformation in the presence of glucose (Lowe & Walmsley, 1986). By contrast, D-glucose slowed the rate of tryptic cleavage of adipocyte GLUT4 (Yano & May, 1993). This suggests that the D-glucose-bound GLUT4 transporter has a different conformational stability than the unliganded protein.

1.4.3. Site-Directed Mutagenesis of GLUT1

Site-directed mutagenesis studies on GLUT1 have so far implicated a number

of amino acids as being important or essential for glucose transport activity, specificity for substrate and targeting to the cell surface. Garcia *et al*, (1992) studied mutants of GLUT1 using the *Xenopus* oocyte expression system. They found that mutation of tryptophans 388 (at the bottom of TM10) and 412 (at the bottom of TM11) of GLUT1 to glycine or leucine resulted in an inhibition of glucose transport activity. Binding of the internal ligand, cytochalasin B, was partially reduced when either tryptophan 388 or 412 were mutated which suggests that these tryptophans may comprise part of an inside hexose binding site (Garcia *et al*, 1992, Katagiri *et al*, 1991). Substitution of a leucine for tryptophan 412 did not effect binding of the exofacial ligand, ATB-BMPA, (Katagiri *et al*, 1991).

Substitution of asparagine 415 (TM11) for aspartate resulted in an increase in K_m and a decrease in the turnover of the mutant transporter compared to the wild-type (Ishihara *et al*, 1991). They suggest that the asparagine may play a role in determining the rate of the conformational change between an inward-facing form and an outward-facing form of the glucose transporter.

Marshall-Carlson *et al*, (1990) investigated some glucose transport deficient mutants from *Saccharomyces Cerevisiae*. A conservative amino acid change of valine 402 to isoleucine in TM8 caused a defect in the glucose transporter function. They also found that mutation of glycines 112 and 153, predicted to be near the middle of transmembrane segments 1 and 2, perturbed transport suggesting that both are important residues. Both glycines are highly conserved.

Wellner *et al*, (1992) investigated the importance of cysteines 421 and 429 in GLUT1 using the *Xenopus* oocyte expression system. Neither of the residues were found to be essential for glucose uptake. Replacement of cysteine 421 at the exofacial end of TM11 resulted in partial protection from cytochalasin B inhibition of 3-O-

methyl-D-glucose transport. Therefore this cysteine may play a role in stabilizing an adjacent local tertiary structure necessary for the full activity of cytochalasin B (Wellner *et al*, 1992).

Oka *et al*, (1990) found that a GLUT1 mutant lacking the C-terminal 37 amino acids was not able to transport glucose or bind the external ligand, ATB-BMPA. However, the truncated GLUT1 was able to bind the internal ligand, cytochalasin B. These results suggested that the glucose transporter was locked in an inward-facing conformation with only the inner glucose binding site available. Deletion of only the first 12 amino acids from the C-terminal of GLUT1 produced a functional glucose transporter that showed no reduction in glucose transport activity or ligand binding (Lin *et al*, 1992).

1.5. Insulin-Stimulation in Rat Adipocytes

1.5.1. The Translocation Hypothesis for Insulin-Stimulation of Glucose Transport

Insulin increases 3-O-methyl-D-glucose transport in isolated rat adipocytes by at least 30-fold. In 1980, two groups simultaneously and independently proposed that glucose transporter proteins were recruited from an internal pool to the plasma membrane in response to insulin (Fig. 7). Cushman & Wardzala, (1980) measured glucose transporter proteins in plasma membrane (PM) and low-density microsome (LDM) fractions by D-glucose inhibitable [^{3}H]-cytochalasin B binding. Suzuki & Kono, (1980) reconstituted plasma membrane and low-density microsome proteins into artificial lipid membranes and measured their glucose transport capacity. Both groups demonstrated that plasma membrane from basal adipocytes contained 3-7 fold lower glucose transporter content than plasma membrane from insulin-stimulated adipocytes. This increase in the glucose transporter content in the plasma-membrane was paralleled by a decrease in the glucose transporter content in the low-density microsome fraction. It has been shown that stimulation of glucose transport by insulin does not involve new protein synthesis but that ATP is required for the translocation of glucose transporters to and from the cell surface (Kono *et al*, 1981).

Initial evidence for glucose transporter translocation was based on fractionation studies described above. More direct evidence (not involving subcellular fractionation) has come from cell-surface labelling experiments. Holman *et al*, (1988) used a cell-impermeant glucose transporter-specific exofacial photoaffinity reagent (BB-BMPA) to label cell-surface glucose transporters in basal and insulin-stimulated rat adipocytes.

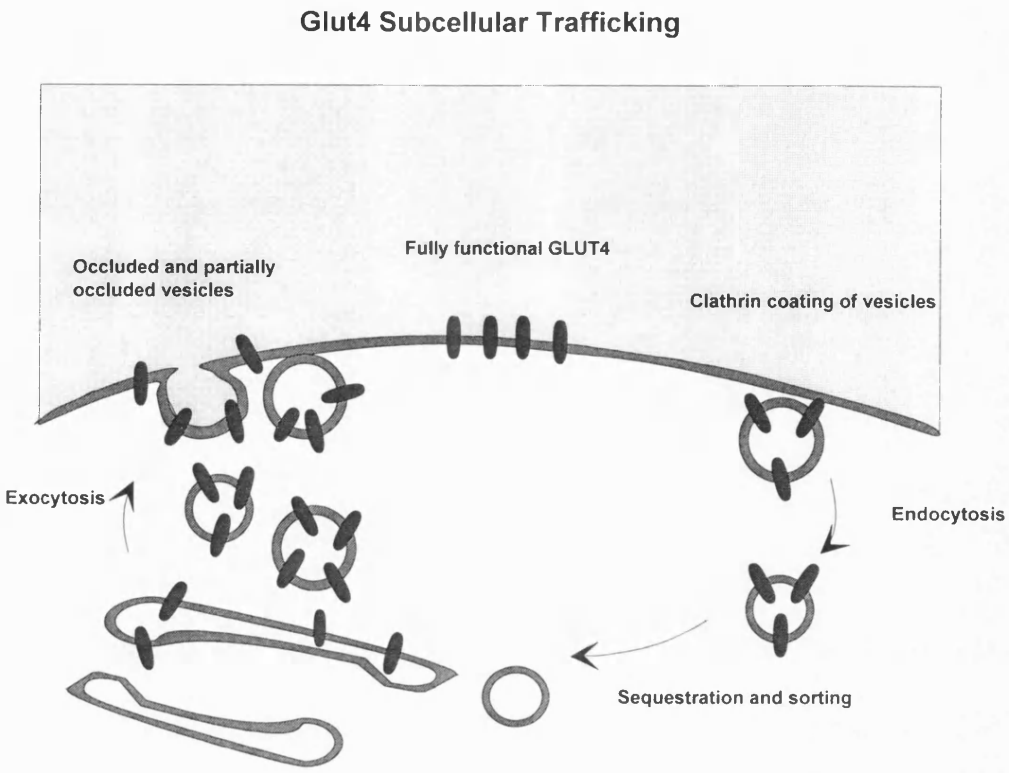

Fig. 7. The translocation hypothesis for insulin-stimulationof glucosetransport (from Gould & Holman, 1993). The majority of GLUT4 glucose transporters are sequestered within the cell in specialized vesicles in the absence of insulin. After insulin addition, transporters are translocated to the plasma membrane. After arrival of GLUT4 at the membrane an approximate two-fold activation is apparent which may be due to dissociation of trafficking proteins. Upon removal of insulin, the GLUT4 is endocytosed back into the cell and restored in vesicles.

BB-BMPA labelling was at least 7-fold greater in insulin-treated versus basal adipocytes. Following incubation and washing at 37 °C in the presence of insulin, 30 % of the transporters photolabelled at the plasma membrane were internalized and were found in the LDM fraction of the cell (Holman *et al*, 1988).

Calderhead and Lienhard, (1988) labelled cell-surface carbohydrate in 3T3-L1 adipocytes with ^{3}H borohydride then selectively immunoprecipitated GLUT1-like glucose transporters to show a 2.6-fold increase in plasma-membrane glucose transporters in response to insulin.

The apparent discrepancy between the extent of GLUT1 recruitment compared to the large increase in transport rate was at least partially explained in 1988 when an insulin-responsive glucose transporter was discovered. James *et al*, (1988) produced a monoclonal antibody IF8 that recognised an insulin responsive glucose transporter, later named GLUT4. These antibodies were used to show that GLUT4, which was barely detectably in the plasma membranes of basal adipocytes, was recruited to the plasma membrane on addition of insulin, resulting in a 7-8-fold increase in the membrane content of this protein.

Slot *et al*, (1991a) have used electron microscopy to localize GLUT4 in rat brown adipose tissue. They found that under basal conditions, 99 % of the GLUT4 labelling was located within the cell, predominantly in the trans-golgi reticulum and tubulo-vesicular structures. In insulin-stimulated cells approximately 40 % of the GLUT4 labelling was at the cell surface, where it was randomly distributed, except for occasional clustering in coated pits.

The stimulation by insulin of glucose transporter translocation from an internal pool to the plasma membrane has also been shown to occur in other tissues including heart muscle (Wheeler, 1988), diaphragm muscle (Wardzala & Jeanrenaud, 1981),

skeletal muscle (Klip *et al*, 1987) and cardiac muscle (Slot *et al*, 1991b).

1.5.2. The Internal Pool of Glucose Transporters

Both GLUT1 and GLUT4 glucose transporter isoforms are sequestered in the low-density microsome fraction in rat adipocytes (Zorzano *et al*, 1989, Holman *et al*, 1990). GLUT1 and GLUT4 are localized in different vesicle populations in rat adipocytes (Zorzano *et al*, 1989), although both translocate to the plasma-membrane in response to insulin to varying extents. GLUT4 was localized to a unique vesicle population that consists of less than 3 % of the total low-density microsome fraction. These vesicles were analyzed and were found to be of limited protein composition. They contained neither the insulin-like growth factor II receptor or the transferrin receptor, both of which are translocated to the plasma membrane in response to insulin (Zorzano *et al*, 1989).

Del Vecchio & Pilch, (1991) have identified phosphatidylinositol 4-kinase (PI4-kinase) as a component of the GLUT4-containing vesicles (GTV). PI4-kinase was also identified in the other LDMs, and the high density microsome and plasma membrane fractions and its location was not altered upon insulin-treatment. Cormont *et al*, (1991) found low molecular weight GTP-binding proteins colocalized with GLUT4 in GTV's. Schurmann *et al*, (1992a) found that although G-proteins were localized in the low density microsome fraction, they were not tightly associated with the GTV's. Cain *et al*, (1992) screened GTV's for various synaptic vesicle proteins and found that one protein, VAMP (also known as synaptobrevin), was highly enriched in GTV's and also translocated to the plasma membrane in response to

insulin. Rab3 was the only other synaptic vesicle protein detected but this was also observed in the non-GLUT4-containing vesicles. A set of three polypeptides of M_r ≈ 36-40 kDa (named GTV3) have also been localised to GTV's (Thoidis *et al*, 1993). The GTV3 proteins may be related, if not completely identical to SCAMPS (secretory component-associated membrane proteins) which may be involved in the secretory process. Streptozotocin-induced diabetic rats which show a marked reduction in GLUT4 levels also have a marked reduction in GTV3 expression.

1.5.3. 3T3-L1 Adipocytes: A Good Model for Studying Insulin-Stimulated Glucose Transport

3T3-L1 cells are used for studying insulin action on glucose transport because they can be differentiated using isobutylmethylxanthine (IBMX), dexamethasone and insulin (Frost & Lane, 1985) to produce differentiated 3T3-L1 adipocytes that respond to acute insulin with increases in glucose transport of 10-20-fold above basal level. 3T3-L1 fibroblasts contain only GLUT1 but during the differentiation period the cells produce the insulin-responsive glucose transporter GLUT4. The GLUT1 and GLUT4 mRNA and protein levels reach a maximum after 8-11 days of differentiation (Tordjman *et al*, 1990, Yang *et al*, 1992).

The ratio of cell-surface GLUT1 : GLUT4 in acutely insulin-stimulated 3T3-L1 adipocytes is approximately 1:1 (Yang *et al*, 1992b) compared to 1:9 in insulin-stimulated rat adipocytes (Holman *et al*, 1990). Therefore GLUT1 makes a greater contribution to the transport activity in 3T3-L1 adipocytes than in rat adipocytes. Calderhead *et al* (1990) found that GLUT1 and GLUT4 were colocalized in the same

low-density microsome vesicles in 3T3-L1 adipocytes. Vesicles immunoprecipitated with antibodies to GLUT1 contained 95 % of the GLUT4 and vesicles immunoprecipitated with antibodies to GLUT4 contained 85 % of the GLUT1 (Calderhead *et al*, 1990). Piper *et al* (1991) immunoabsorbed GLUT4-containing vesicles from a partially purified preparation of low density microsomes and absorbed 90 % of the GLUT4 and only 30 % of the GLUT1. GLUT1 was also found to colocalize with both the transferrin receptor and the insulin-like growth factor II receptor, which also translocate to the plasma membrane in response to insulin (Tanner & Lienhard, 1989). Treatment of 3T3-L1 adipocytes with phenylarsineoxide (PAO) results in GLUT1 and GLUT4 exhibiting different trafficking properties during recycling. Following PAO treatment of fully insulin-stimulated 3T3-L1 cells, GLUT4 showed a greater tendency to internalize to the intracellular transporter pool (Yang *et al*, 1992a).

1.6. Regulation of Glucose Transport

1.6.1. The Insulin Receptor

Insulin-stimulation of glucose transport in adipocytes is mediated by the interaction of insulin with cell surface insulin receptors (This topic is reviewed by Kahn & White, 1988 and Carruthers, 1990). The receptor is a heterotetrameric assembly of two α- and two ß- subunits. The α-subunits reside on the extracellular surface of the membrane and are linked by interchain disulphide bonds to the ß-subunits which span the membrane once and contain a longer C-terminal sequence.

The mechanism by which insulin binding to its receptor causes a translocation of glucose transporters from an internal pool to the plasma membrane is still not understood. The purified insulin receptor displays insulin-dependent receptor autophosphorylation on tyrosine residues of the ß-subunit and the ability to phosphorylate tyrosine residues of exogenous substrates.

Certain mutations within the tyrosine kinase domain of the insulin receptor result in markedly reduced or complete loss of insulin-stimulated tyrosine phosphorylation. These mutations also produce little or no ability to mediate insulin-stimulated glucose transport (Ellis *et al*, 1986). Synthetic inhibitors of *in vivo* insulin receptor tyrosine kinase activity are known to inhibit insulin-stimulation of glucose transport (Saperstein *et al*, 1989). However, Forsayeth *et al*, (1987) showed that monoclonal antibodies directed against the insulin receptor could produce glucose transport stimulation in the absence of insulin receptor tyrosine phosphorylation both *in vivo* and *in vitro*. It is possible, that the conformations of the tyrosine-phosphorylated and antibody-liganded insulin receptor are similar and that it is this conformation that results in signal transduction.

1.6.2. Post-Receptor Signalling

Insulin has been shown to stimulate tyrosine phosphorylation of a protein band of a molecular weight between 165 kDa and 185 kDa, collectively called pp185 or IRS-1 (insulin receptor substrate-1) (White *et al*, 1985). The IRS-1 is a minor cytoplasmic phosphoprotein found in most cells and tissues and its phosphorylation is decreased in cells expressing mutant receptors defective in signalling. IRS-1 has

been cloned by Xiao *et al*, (1991) and has been shown to contain over ten potential tyrosine phosphorylation sites, nine of which are in YXXM motifs.

During insulin stimulation of CHO cells expressing the human insulin receptor, the IRS-1 protein undergoes tyrosine phosphorylation and binds phosphatidylinositol 3-kinase (PI3-kinase)(Backer *et al*, 1992). PI3-kinase is composed of a catalytic subunit (p110) and a putative regulatory subunit (p85) that contains two SH2 (src homology-2) domains and one SH3 (src homology-3) domain. Binding of PI3-kinase to IRS-1 is thought to be mediated through the SH2 domains of p85 and phosphorylated YXXM motifs of IRS-1 as formation of the complex is inhibited by synthetic peptides containing phosphorylated YXXM motifs. Furthermore, overexpression of IRS-1 potentiates the activation of PI3-kinase in insulin-stimulated cells and tyrosyl phosphorylated IRS-1 or peptides containing phosphorylated YXXM motifs activate PI3-kinase in vitro (Backer *et al*, 1992). The expression in CHO cells of mutant p85, which is deficient in coupling to the 110 kDa subunit of PI3-kinase, inhibits the insulin-induced complex formation of PI3-kinase with IRS-1. Expression of this mutant p85 has been shown to inhibit insulin-stimulated glucose uptake by preventing the translocation of GLUT1 to the cell-surface (Hara *et al*, 1993).

PI3-kinase is known to be an important enzyme involved with signalling pathways (Panayotou & Waterfield, 1992). The function of PI3-kinase is to attach a phosphate group to the 3'-hydroxyl group of the inositol ring of PI and/or its phosphorylated derivatives PI(4)P and $PI(4,5)P_2$, to produce PI(3)P, $PI(3,4)P_2$ and $PI(3,4,5)P_3$. The p110 domain of PI3-kinase has a high degree of sequence homology to the yeast protein VPS34 which is implicated in the targeting of proteins to the yeast lysosome-like vacuole (Herman *et al*, 1992) and therefore by analogy, PI3-kinase may be involved in membrane trafficking in higher eukaryotes. The products of PI3-kinase

could be involved directly in the process of membrane invagination or in the recruiting of adaptor proteins involved in vesicle formation. Also, targeting of vesicular structures to their cellular destination, as well as interactions with the cytoskeletal protein network, could be mediated by the phospholipids. Alternatively, other downstream signalling molecules could be activated by the products of the PI3-kinase, initiating a cascade that would generate further distinct second messengers (Panayotou & Waterfield, 1992).

The subcellular distribution of PI3-kinase has been investigated in basal and insulin-stimulated rat adipocytes (Kelly *et al*, 1992). They found that insulin increased the activity of PI3-kinase in adipocytes and that this increased activity was primarily located in the LDM's and to a lesser extent in the plasma membrane.

1.6.3. Movement of Glucose Transporter-Containing Vesicles

Antibodies against the N- and C-termini of GLUT4 have been used to localize GLUT4 in basal and insulin-stimulated rat adipocytes (Smith *et al*, 1991). From their results, Smith *et al* (1991) concluded that the C-terminal epitope of GLUT4 may be masked when GLUT4 is inside the cell and that this may be due either to a conformational change within the glucose transporter protein or a change in protein or lipid surrounding it.

Recently, synaptobrevin has been found in GTV's (Cain *et al*, 1992). This is of particular interest as a simple docking mechanism has been reported in which an N-ethylmaleiimide sensitive factor (NSF) and SNAPs (soluble, NSF accessory proteins) link synaptobrevin in synaptic vesicles to syntaxin, an integral membrane

protein in the presynaptic membrane (Sollner *et al*, 1992, Warren, 1992). Therefore a similar mechanism may take place in insulin-sensitive tissues and allow docking of GTV's onto the plasma membrane. Docking must be a regulated process and this regulation may involve the Rab family of GTP-binding proteins. The Rab family of proteins have been implicated in many aspects of membrane trafficking (Van Der Sluijs *et al*, 1991). Non-hydrolysable analogues of GTP mimic insulin in inducing the translocation of GLUT4 from the low density microsomes to the plasma membrane in α-toxin permeabilized rat adipocytes (Baldini *et al*, 1991). A small GTP-binding protein, Rab 3D, has been found to be abundant in 3T3-L1 adipocytes and its mRNA levels have been found to increase during differentiation in a similar pattern to the increase in GLUT4 levels (Baldini *et al*, 1992). These investigators suggest that as Rab 3D is a close homolog of Rab 3a (involved in regulated secretion by neurosecretory vesicles), it may play a role in the exocytosis of GLUT4-containing vesicles.

Clathrin may also be involved in the exocytosis and/or endocytosis of GLUT4. Clathrin coated vesicles are part of the trafficking process of a number of proteins and receptors (Pearse & Robinson, 1990, Keen, 1990). Insulin has been shown to stimulate the assembly of cytosolic clathrin onto the plasma membrane of rat adipocytes (Corvera, 1990). Poku *et al*, 1992, have found GLUT4 in clathrin-coated vesicles, while Kim & Jung (1992) have found that GLUT4 is associated tightly with clathrin and some clathrin-coat components in the plasma membrane of rat adipocytes. Exposure of the cells to insulin resulted in a decrease in GLUT4 concentration in clathrin-coated vesicles (Poku *et al*, 1992) and no change in the relative abundance of clathrin-associated GLUT4 in the plasma membrane (Kim & Jung, 1992). GLUT4 has been visualized in clathrin lattices in 3T3-L1 adipocytes by electron microscopy

(Robinson *et al*, 1992). An interaction between phosphoinositol components of the phosphoinositol pathway and plasma membrane-associated clathrin assembly protein has been reported (Beck & Keen, 1991).

1.6.4. Mechanism for the Sequestration of GLUT4 within the Cell

Jo *et al*, (1992) introduced purified erythrocyte GLUT1 into rat adipocytes by PEG-induced vesicle-cell fusion. More than 85 % of the GLUT1 that was inserted in the correct physiological orientation in the adipocyte plasma membrane was moved to the LDM fraction whereas 90 % of wrongly inserted GLUT1 was retained in the plasma membrane. Although more than 70 % of the LDM-associated erythrocyte GLUT1 was found in the small subset of LDM's that contained 80 % of LDM-associated GLUT4, insulin did not recruit GLUT1 to the plasma membrane under conditions where GLUT4 plasma membrane content increased 4-5 fold. Therefore Jo *et al*, (1992) suggest that the adipocyte plasma membrane content is kept low by a mechanism where a cell-specific constituent interacts with a cytoplasmic domain common to GLUT1 and GLUT4, while the insulin-dependent recruitment requires a cytoplasmic domain specific to GLUT4.

When GLUT1 and GLUT4 are expressed in CHO cells, 3T3-L1 fibroblasts and *Xenopus oocytes*, expressed GLUT1 is normally directed to the plasma membrane and GLUT4 retained within the cell (Shibasaki *et al*, 1992, Piper *et al*, 1992, Thomas *et al*, 1993). Chimeric glucose transporters containing parts of GLUT1 and GLUT4 were transiently expressed in CHO cells by Piper *et al*, (1992). They found that replacement of the N-terminal 30 amino acids of GLUT1 with the 41 N-terminal

amino acids of GLUT4 resulted in the sequestration of the glucose transporter within the cell. Deletion of only the N-terminal 8 amino acids of GLUT4 or a single amino acid substitution of phenylalanine at position 5 to alanine was sufficient to cause a marked accumulation of GLUT4 at the cell surface (Piper *et al*, 1993).

Asano *et al*, (1992a) replaced portions of GLUT4 with GLUT1 and expressed the chimeras in CHO cells. They found two domains to be important for correct targeting of the GLUT4. One domain included TM2 and TM3 and contained a leucine zipper sequence. These investigators suggested that a dimer structure of the glucose transporter may be required for its correct targeting. They suggested that another targeting sequence was a 28 amino acid domain around TM7 and TM8 containing 9 amino acids that vary between GLUT1 and GLUT4.

1.6.5. Glucose Transporter Activation

Although translocation of glucose transporters to the plasma membrane appears to account for most of the effect of insulin on glucose transport activity, there is still a small discrepancy which may be due to some activation of the glucose transporter protein. Some agents (such as lipolytic agents) may regulate glucose transporter intrinsic activity, possibly by phosphorylation of the transporter (section 1.6.6.). Agents such as protein synthesis inhibitors have been reported to stimulate transport without apparently affecting the subcellular distribution of GLUT1 or GLUT4, as detected by Western blotting of plasma membrane fractions (Clancy *et al*, 1991). A discrepancy between transport activity and transporter abundance has been noted in comparing 3T3-L1 fibroblasts with differentiated adipocytes (Harrison *et al*, 1991,

Yang *et al*, 1992b). The ratio of transport activity to GLUT1 abundance has been calculated to be higher in fibroblasts than in differentiated cells. Therefore, it has been suggested that the low basal transport rate observed in the adipocytes may reflect a suppression of the intrinsic activity of GLUT1 by 40-50 % (Yang *et al*, 1992b) and by 90 % (Harrison *et al*, 1991).

Tanti *et al*, (1992) found that anti-GLUT1 peptide antibodies, when loaded into fibroblasts transfected with human insulin receptor cDNA, produced a 60 % increase in basal 2-deoxyglucose and 3-O-methyl-D-glucose transport. This increase was not observed with nonimmune serum and only occurred at low glucose concentrations, suggesting that binding of the specific antibody to the C-terminal caused an increase in the intrinsic activity of the glucose transporter rather than changing its maximal capacity.

1.6.6. Phosphorylation of the Glucose Transporter

Although insulin does not promote GLUT4 phosphorylation, GLUT4 can be phosphorylated in vitro by a number of protein kinases. Lawrence Jr. *et al*, (1990a) incubated microsomal membranes with cAMP-dependant protein kinase and found that all the phosphorylation was on Ser 488 in the C-terminal of GLUT4. As Ser 488 is unique to GLUT4, Lawrence Jr. *et al*, (1990a) suggest that GLUT4 may be uniquely regulated by phosphorylation. Nishimura *et al*, (1991) observed that there was no change in phosphorylation of GLUT1 upon insulin-stimulation of rat adipocytes.

Schurmann *et al*, (1992b) found that phosphorylation of adipocyte membranes with protein kinase A produced a stimulation of reconstituted glucose transport activity

in plasma membranes and low-density microsome fractions provided the cells had been treated with insulin prior to isolation. They concluded that glucose transport activity can be modified by protein phosphorylation in an insulin-dependent mechanism but that phosphorylation of GLUT4 itself does not correlate with changes in reconstituted glucose transport activity.

Isoproterenol, a lipolytic agent, has been shown to stimulate glucose transport at low concentrations and inhibit insulin-stimulated glucose transport at high concentrations, but only in the absence of antilipolytic agents (Nishimura *et al*, 1991). Isoproterenol treatment can produce a phosphorylation of GLUT4 in preparations of rat adipocytes. However, isoproterenol-induced phosphorylation occurs both in the presence and in the absence of adenosine receptor agonists whereas isoproterenol treatment inhibits insulin-stimulated glucose transport only in their absence. Nishimura *et al*, (1991) therefore suggested that the phosphorylation of GLUT4 that is induced by isoproterenol treatment does not account for the inhibition of transport activity produced by this treatment.

The inhibitory effects of isoproterenol in glucose transport activity do not result from changes in the subcellular distribution of the glucose transporter as measured by cytochalasin B binding (Kuroda *et al*, 1987). These authors suggested that the reduced transport could be due to a change in the intrinsic activity of the glucose transporter within the plasma membrane. However recent data obtained with the exofacial glucose transporter labelling reagent ATB-BMPA suggests that isoprenaline induces an alteration, but not a loss, of GLUT4 in the plasma membrane of intact cells (Vannucci *et al*, 1992). These authors suggest that an occluded form of GLUT4 is produced that can neither bind photolabel nor transport glucose but can still be

detected with cytochalasin B and Western blotting.

Okadaic acid, an inhibitor of type I and IIa protein phosphatases, has been shown to stimulate glucose transport in adipocytes by increasing the amount of GLUT4 in the plasma membrane (Lawrence Jr. *et al*, 1990b, Corvera *et al*, 1991). Okadaic acid treatment partially inhibited insulin-stimulated glucose transport. The transport activity observed following treatment with both insulin and okadaic acid was similar to that of okadaic acid alone. Incubation of cells with okadaic acid results in a 3-fold increase in the phosphorylation of GLUT4 and also in an increase in phosphorylation of at least three other glucose transporter vesicle (GTV) proteins. As insulin does not increase phosphorylation of GLUT4, the phosphorylation of one of the GTV proteins may be the signal for vesicle translocation (Lawrence Jr. *et al*, 1990b). Lawrence Jr. *et al*, (1990b) suggest that the reduction, by okadaic acid, of the levels of glucose transporter present in the plasma membrane may be due to phosphorylation of GLUT4 which promotes its internalization.

Increased phoshorylation of GLUT4 has also been found in rat adipocytes from streptozotocin-induced diabetic rats (Begum & Draznin, 1992). In adipocytes from these rats the phosphorylated GLUT4 appears to be more resistant to phosphatases. This may be due to the glucose transporter being phosphorylated on sites that are not normally phosphorylated. Begum & Draznin, (1992) suggest that this greater phosphorylation may render GLUT4 less sensitive to acute regulation by insulin.

1.6.7. The Role of Protein Kinase C in Glucose Transport

The role of protein kinase C (PKC) in the stimulation of glucose transport by insulin is still controversial. Most, if not all, PKC activators stimulate glucose transport. However, in some cells these PKC activators are less effective than insulin. The phorbol ester, phorbol 12-myristate 13-acetate (PMA) stimulates 3-O-methyl-D-glucose transport in intact rat adipocytes in association with the subcellular redistribution of glucose transporters from the low density microsomes to the plasma membranes. However the effect of PMA on glucose transport is only approximately 13 % of that for insulin (Holman *et al*, 1990, Saltis *et al*, 1991). The stimulation of glucose transport activity correlates closely with the appearance of GLUT4 at the plasma membrane in response to both PMA and insulin, but does not correlate with the sum of GLUT1 and GLUT4. These results are consistent with GLUT4 being inherently more active than GLUT1 due to a higher TK (turnover/K_m)(Holman *et al*, 1990, Saltis *et al*, 1991).

PKC depletion caused by 20-24 hour treatments with phorbol esters or other PKC activators such as glucose and/or insulin inhibit subsequent acute effects of insulin and phorbol esters (Ishizuka *et al*, 1991) on glucose transport. Therefore PKC may be involved in insulin-stimulation of glucose transport but additional factors must also be required to give the full insulin effect.

1.7. Aims of this Study.

1) To use the impermeant ligand, ATB-BMPA, to selectively label the exofacial binding site of the erythrocyte glucose transporter.

2) To investigate the different conformations of the glucose transporter upon external (ATB-BMPA) and internal (cytochalasin B) ligand binding, by investigating its susceptibility to a number of proteinases.

3) To investigate the conformations of the native erythrocyte glucose transporter and the 18 kDa tryptic fragment of the transporter, by investigating their affinities for external and internal ligands.

4) To investigate the role of a number of conserved residues within the glucose transporter by investigating the ability of mutants with single amino acid substitutions to transport glucose and to bind external and internal ligands.

5) To use the impermeant ligand, ATB-BMPA, in combination with specific antibodies to investigate the role of the two glucose transporter isoforms, GLUT1 and GLUT4, in insulin-stimulation of glucose transport in rat adipose cells.

CHAPTER 2 : METHODS

2.1. Materials

2.1.1. General Materials

Radiolabelled sugars and cytochalasin B were from Amersham International. Nonaethylene glycol dodecyl ether (Thesit) was from Boehringer Mannheim. Protein A-Sepharose, phloretin, trypsin and thermolysin were from Sigma. All other reagents were of analytical grade and were purchased from Sigma, BDH or Fisons.

2.1.2. Preparation of ATB-BMPA and ATB-[2-^{3}H]BMPA

ATB-BMPA and ATB-[2^{3}H]BMPA (specific activity : 10 Ci/mmol) were prepared by Dr G.D.Holman using the method previously described (Clark & Holman, 1990). Tritiated ATB-BMPA (5 mCi/ml in PBS, pH 7.2) was aliquoted and stored at -20 °C.

2.2. Preparation and use of Anti-Peptide Antibodies

2.2.1. Peptide Synthesis

A 15 amino acid peptide (CGEELFHPLGADSQV) was synthesised. This corresponded to the 13 amino acids at the C-terminal of GLUT1 (Mueckler *et al*, 1985), with a cysteine attached to the N-terminal via a glycine spacer. The cysteine allowed easy and efficient coupling of the peptide to the carrier protein Keyhole Limpet Haemocyanin (KLH). A 14 amino acid peptide (CSTELEYLGPDEND) corresponding to the C-terminal 13 amino acids of GLUT4 (James *et al*, 1989), with a cysteine attached at the N-terminal, was made. These peptides were synthesized by the Nα-fluorenylmethoxy-carbonyl-polyamide solid phase method (Atherton & Sheppard, 1985).

2.2.2. Estimation of Thiol Groups

Ellmans reagent (Ellman, 1958) was used to estimate the number of cysteines on each peptide that were in a reduced state and so able to react with m-maleimidobenzoyl-N-hydroxysuccinimide ester (MBS). For the standard curve, 0, 2, 5, 10 and 25 μl of standard cysteine solution (1 mg/ml in 0.1 M Na_2HPO_4 buffer, pH 8.0) were made to 1 ml with the same buffer and 100 μl of Ellmans reagent (5,5' dithiobis (2-nitrobenzoic acid, DTNB, Sigma), 4 mg/ml in 0.1 M Na_2HPO_4 buffer, pH 8.0) was added. 25 and 50 μl of peptide solution (4 mg/ml in 10 mM $NaHPO_4$ buffer, pH 7.2) were made to 1 ml with 0.1 M Na_2HPO_4 buffer, pH 8.0 and 100 μl

of Ellmans reagent was added. Absorbance was read at 412 nm in a spectrophotometer and the concentration of cysteines on each peptide was calculated using the standard curve.

2.2.3. Conjugation of Peptides to Keyhole Limpet Haemocyanin

The peptides were conjugated to KLH (Sigma) using m-maleimidobenzoyl-N-hydroxysuccinimide ester (MBS, Pierce). MBS (1.4 mg in 120 μl of dry dimethylformamide (DMF)) was added dropwise to KLH (8 mg in 0.5 ml 10 mM $NaPO_4$ buffer, pH 7.2) to ensure that the local concentration of DMF was kept low, as KLH is insoluble in > 30 % DMF. The mixture was stirred for 30 min at RT and then passed through a Sephadex G25 column (8 mm dia. x 80 mm, equilibrated with 50 mM $NaPO_4$ buffer, pH 6.0) to remove free MBS. The KLH-MBS conjugate was not retained by the column. Fractions of column eluate were monitored by absorbance at 280 nm and the peak fractions were pooled. Peptide (10 mg in 2 ml $NaPO_4$ buffer, pH 7.2) was added to the pooled KLH-MBS and stirred for 3 hrs at RT. The protein content was then determined and aliquots were stored at -20 °C until required.

2.2.4. Immunization Procedure

Antibodies were raised in rabbits by intramuscular injection of peptide conjugates. The conjugates (200 μg protein) in 0.5 ml of PBS (154 mM NaCl, 12.5 mM Na_2HPO_4, pH 7.2) were emulsified with 1 ml of Complete Freunds Adjuvant

(Sigma). A booster injection of conjugate (200 μg) in Incomplete Freunds Adjuvant was made after 4 weeks. Booster injections of conjugate in Alum were then made every 4 weeks. Conjugate (200 μg) in 0.5 ml PBS, pH 7.2, was mixed with 0.5 ml of Imject Alum (Pierce) for 30 min at RT before injection. A 5 ml test bleed was taken in week 6 then every 4 weeks after that to monitor the titre of specific antibodies. Preimmune sera was obtained prior to the first injection.

2.2.5. Isolation And Treatment Of Antisera

Rabbits were bled from the ear vein for routine test bleeds. 30 ml bleeds were obtained by cardiac puncture under anaesthetic, then after 4 bleeds the rabbits were bled out. Rabbit blood was allowed to clot for 1 hr at RT then overnight at 0 °C. The serum was removed following sedimentation of the clot by centrifugation at 3000 revs/min (IEC-Centra-3 bench centrifuge) for 10 min. The titre of specific antibodies was monitored by ELISA and aliquots were stored at -20 °C.

2.2.6. Purification of Anti-peptide Antibodies

Anti-peptide antibodies to GLUT1 and GLUT4 were purified essentially according to the method of Oka *et al*, (1988).

2 ml of Reacti-gel(6X) (1,1'-carbonyldiimidazole activated 6 % cross-linked beaded agarose, Pierce) was filtered through Whatman number 1 filter paper on a Buchner funnel under gentle suction and washed thoroughly with double-distilled water

at 0-4 °C to remove any acetone. The reactigel was added to 5.5 mg of peptide in 2 ml of sodium borate buffer, pH 8.5 and then mixed for 48 hr at 0-4 °C by rotation (stirring is known to damage the beads). The mixture was then filtered and the beads were added to 2 ml of 1.0 M ethanolamine in sodium borate buffer, pH 8.5 and mixed for 3 hr at RT. The beads were then packed into a column (8 mm dia. x 50 mm) and washed successively with 1 M NaCl, double-distilled water and PBS, pH 7.2. 5 ml of antiserum was then loaded onto the column and circulated at least 3 times. The column was then washed extensively with PBS, then with 2 M NaCl in 5 mM $NaPO_4$ buffer, pH 7.2 to remove any weakly bound antibodies. The anti-peptide antibodies were then eluted with 3.5 M sodium thiocyanate in 10 mM $NaPO_4$ buffer, pH 6.6 and immediately dialysed against PBS, pH 7.2. The antibody solution was concentrated using polyethylene glycol 4000 (PEG) and then aliquoted and stored at -20 °C. At each stage of the purification, samples were taken and monitored for the presence of specific antipeptide antibodies by ELISA.

2.2.7. Enzyme Linked Immunosorbant Assay (ELISA)

ELISA's were done in 96 multi-well plates (Labsystems). For assaying anti-GLUT1 antibodies, wells were coated with protein-depleted erythrocyte membranes (section 2.3.2., 1 μg in 100 μl of coating buffer (50 mM $NaHCO_3$ buffer, pH 9.6)/well) overnight at 4 °C. For assaying anti-GLUT4 antibodies, wells were coated in GLUT4 peptide (20 ng in 100 μl of coating buffer/well) overnight at 4 °C. Unoccupied protein binding sites were blocked by three, 10 min incubations at RT with 100 μl of blocking buffer (1 % casein, 0.05 % Tween 20 (polyoxyethylene-

sorbitan monolaurate, Sigma) in PBS (154 mM NaCl, 12.5 mM Na_2HPO_4, pH 7.2). The wells were incubated with 100 μl antisera (serial dilutions from 1:100 to 1:6400, in blocking buffer) for 2 hr at 37 °C. Unbound antisera was removed by three, 10 min washes in 100 μl of blocking buffer then 100 μl of a 1:2000 dilution of goat anti-rabbit peroxidase conjugate (Sigma) in blocking buffer was incubated with the wells for 2 hr at 37 °C. Excess conjugate was removed by four, 5 min washes in 0.05 % Tween 20 in PBS, pH 7.2. 100 μl of freshly prepared substrate (0.1 M sodium acetate, pH 6.0, : 10 ml, tetramethylbenzidine (10 mg/ml in DMSO) : 100 μl, hydrogen peroxide (30 % v/v) : 1.5 μl) was added and incubated at RT until a bright blue colour had developed (approximately 10 min) then the reaction was stopped by the addition of 25 μl of 1 M H_2SO_4. The resulting bright yellow colour was read at 450 nm in a microtitre plate reader (Labsystems).

2.2.8. Western blotting

2.2.8.1. Transfer of Proteins onto Nitrocellulose

Samples were run on 1.5 cm SDS-polyacrylamide gels as described in section 2.6.2.. The stacking gel was removed and the resolving gel was put in continuous transfer buffer (39 mM glycine, 48 mM Tris, 0.0375 % (w/v) SDS, 20 % methanol, pH 8.8). Proteins were transferred using a Multiphor II NovaBlot electrophoretic transfer unit (Pharmacia LKB Biotechnology). The semi-dry transfer method involved soaking sheets of filter paper, nitrocellulose sheets and the gel in the continuous transfer buffer then layering them on the anode electrode (presoaked in distilled

water). Nine sheets of filter paper were placed on the anode electrode, followed by the nitrocellulose (Biotrace, Gelman Sciences), then the gel, then 9 sheets of filter paper. The cathode electrode (presoaked in distilled water) was then placed on top and a current applied (0.8 x gel area, mA) for 1 hr 45 min. Great care was taken when setting up the trans unit to cut all the sheets to the same size, to soak the sheets evenly and to remove all the trapped air bubbles when layering the sheets together. Once the transfer was complete the nitrocellulose was washed in distilled water and the proteins were stained in the temporary stain, Ponceau S (0.1 % Ponceau S in 3 % trichloroacetic acid) to enable the nitrocellulose to be cut and marked as required.

2.2.8.2. Blotting of GLUT1 and GLUT4 with ^{125}I-Protein A

The nitrocellulose was first washed 2 times in blocking buffer (3 % bovine serum albumin (BSA), 0.2 % Tween 20, in TBS buffer (10 mM Tris, 0.9 % NaCl, pH 7.4)) to remove the Ponceau S, then incubated in blocking buffer overnight at 0-4 °C. It was then incubated at RT for 1 hr in the same buffer. The nitrocellulose was incubated with antisera (1:200 dilution in 1 % BSA, 0.2 % Tween 20, TBS buffer) for 2 hr at room temperature, then washed by three 5 min and one 15 min wash in 50 ml TBS/Tween (0.2 % Tween 20 in TBS buffer). ^{125}I-labelled Protein A (affinity purified, Amersham) was then added at 0.1 μCi/ml in TBS/Tween for 2 hr at room temperature, then the nitrocellulose was washed extensively with at least six 5 min washes in TBS/Tween. The nitrocellulose was dried and wrapped in cling-film then exposed to X-ray film (Fuji) for 24-72 hr. The glucose transporter band was excised

from the nitrocellulose and counted in a Gamma counter. A background (the average count from a band of equivalent size cut from above and below the glucose transporter band) was subtracted to get glucose transporter-specific counts.

2.3. Erythrocyte Glucose Transporter Studies

2.3.1. Preparation of Erythrocytes and Erythrocyte Membranes

Erythrocytes from 1-3 week old transfusion blood were washed five times at 0-4 °C in PBS (154 mM NaCl, 12.5 mM Na_2HPO_4, pH 7.2). The cells were pelleted at 3,000 revs/min (IEC Centra-3). Care was taken to remove the " buffy coat " of white cells and platelets. To obtain erythrocyte membrane ghosts, the cells were then lysed for 20 min at 0-4 °C in haemolysis buffer (5 mM Na_2HPO_4, 1 mM EDTA, 20 μg/ml PMSF, pH 7.8). The membranes were centrifuged at 20,000 g in an Ole Dich bench centrifuge for 20 min. The pellets were resuspended and washed once in haemolysis buffer then once in 5 mM Na_2HPO_4 buffer, pH 7.2 before being resuspended at 1 mg/ml in 5 mM Na_2PO_4 buffer. It was important to keep the cells cold and to wash them rapidly to remove the haemoglobin before the ghosts resealed.

2.3.2. Preparation of Protein-Depleted Erythrocyte Membranes

Protein-depleted membranes were prepared by the method of Gorga & Lienhard, (1981). Erythrocyte membranes were washed once in 5 mM Na_2PO_4 buffer, pH 7.8 and collected at 20,000 g for 20 min. The pellet was resuspended at 4 mg/ml then treated with 5 volumes of a freshly prepared alkaline buffer (15.4 mM NaOH, 2 mM EDTA, 0.2 mM DTT) for 15 min at 4 °C. The membranes were spun at 20,000 g for 20 min and then resuspended in 50 mM Tris-HCl pH 6.8 and spun again before being resuspended at 4 mg/ml in 50 mM Tris-HCl pH 6.8.

2.3.3. Photolabelling of Erythrocytes with ATB-[2-^{3}H]BMPA

200 μl of a washed erythrocyte suspension (20 % cytocrit) was mixed with 10-30 μCi of ATB-[2-^{3}H]BMPA in 200 μl of PBS (usually containing 600 mM D-mannitol or D-glucose) in 1 mm-pathlength cuvettes. The cuvettes were covered with a 10 mm-pathlength quartz cell containing a chemical filter of 1 % cumene in 2, 2, 4-trimethylpentane. Samples were irradiated for 60 sec in a Rayonet RPR-100 photoreactor containing RPR-3000 lamps. After irradiation, the cells were washed five times in PBS. The membranes were then obtained by hypo-osmotic lysis (section 2.3.1.).

2.3.4. Photolabelling of Erythrocyte Membranes with [4-^{3}H]Cytochalasin B and ATB-[2-^{3}H]BMPA

300 μl of erythrocyte membrane suspension at 1 mg/ml in 5 mM Na_2PO_4 buffer, pH 7.2, was mixed with 1.6 μCi of [4-^{3}H]cytochalasin B in the presence of 10^{-4} M cytochalasin E or with 10 μCi of ATB-[2-^{3}H]BMPA and was irradiated for 30-60 sec in 1 mm-pathlength cuvettes. After irradiation, membranes were diluted in 3.0 ml of Na_2PO_4 buffer and centrifuged at 20,000 g for 20 min. The pellets were resuspended and washed twice more in Na_2PO_4 buffer to remove unbound radiolabel.

2.3.5. Immunoprecipitation of GLUT1 From Erythrocyte Membranes

Labelled erythrocyte membranes (100 μg) were solubilized in 300 μl of 0.5 % Mega 10 solution (0.5 % decanoyl-N-methyl-glucamid (Mega 10), 2 mM DTT in 5 mM Na_2PO_4 buffer, pH 7.2), for 20 min at RT then centrifuged at 20,000 g for 20 min to remove any unsolubilized material. Protein A-Sepharose CL-4B (Sigma) was swollen in 5 mM Na_2PO_4 buffer for 15 min at 0-4 °C then incubated with affinity purified anti-GLUT1 antibodies (135 μg antibody/30 μl of protein A-Sepharose) for 2 hr at 0-4 °C. The protein A-Sepharose-antibody conjugate was pelleted by centrifugation at low speed (6,500 revs/min) for 1 min in a MSE microcentaur bench microfuge and any unbound antibodies were removed by washing the pellets in 1 ml of 5 mM Na_2PO_4 buffer, pH 7.2. The solubilized membranes were incubated with the antibody-protein A-Sepharose conjugate for 2 hr at 0-4 °C. The antibody-protein A-Sepharose complex was then pelleted by centrifugation and the supernatant removed and retreated to obtain a second immunoprecipitate. The pellets were washed by resuspension 2 times in 50 μl of 0.5 % Mega 10 solution and the washings were combined with the first supernatant. Protein released from the immunopellets and from the supernatant was run on 10-12 % acrylamide gels (section 2.6.2.).

2.3.6. Estimation of the Affinity Constant for ATB-BMPA

The affinity of the erythrocyte glucose transporter for ATB-BMPA was investigated. The affinity constant (or half-maximal inhibition constant) for ATB-BMPA was determined in two ways: Either from the inhibition of the uptake of 100

μM D-galactose or from the inhibition of the reversible binding of the exofacial label ASA-BMPA.

2.3.6.1. Transport Inhibition Determination

50 μl of an erythrocyte suspension (40 % cytocrit) was mixed with 10 μl of PBS, pH 7.2 containing the indicated concentrations of ATB-BMPA and 10 μl of D-[1-^{14}C]galactose (100 μM final concentration). The assay tubes were kept in subdued light until the erythrocyte suspension had been added. Transport was stopped after 10 sec by the addition of 3 ml of stopping buffer (0.3 mM phloretin in PBS, pH 7.2). An equilibrium value (α) was determined by measuring transport for 60 sec. A blank value (b) was determined by adding 3 ml of stopping buffer before addition of the erythrocyte suspension. The erythrocytes were collected by centrifugation at 3000 revs/min for 45 sec in a refrigerated bench centrifuge (IEC Centra-3). The supernatant was carefully aspirated and then the cells were resuspended in stopping buffer and recentrifuged. The supernatant was removed and any remaining liquid was removed from the sides of the tube with tissue paper. 500 μl of 10 % TCA was added to precipitate the protein and then any unsolubilized material was spun down at 3,000 revs/min. Two 200 μl aliquots of supernatant were counted.

The reciprocal of the uptake rate constant (s/v) was calculated from the fractional filling (f) and was: $v/s = -\ln(1-f)/t$ where $f = cpm_{10}-b/cpm_{\alpha}-b$, cpm_{10} was the amount of labelled sugar transported in 10 sec, cpm_{α} was the equilibrium value determined by measuring transport for 60 sec and b was the blank value determined by adding stopping buffer before the labelled sugar. If the substrate

concentration added is much less than the K_m :

$$s/v = K_m(1+I/K_i)/V_{max} \qquad \text{Equation 1}$$

The K_i was determined by non-linear regression fitting to Equation 1. As the substrate concentration used (100 μM) was approximately 10-times lower than the K_m, the error in the K_i should not be greater than 10 %.

2.3.6.2. Erythrocyte Binding Experiments

200 μl of an erythrocyte suspension at high cytocrit (80 %) was mixed with 10 μl of buffer containing 0.1 μCi (10 pmol) of ASA-[2-^{3}H]BMPA and 0.02 μCi of [U-^{14}C]sucrose and non-labelled ATB-BMPA at a range of dilutions. Samples were mixed and incubated for 5 min and then spun in a microcentrifuge. These operations (including centrifugation) were carried out at either 20 °C or 0-4 °C. A 5 μl sample of the supernatant was then counted on a program that counted both tritium and ^{14}carbon. Extracellular space and the final total concentrations of ATB-BMPA were then calculated from the [^{14}C]sucrose in this sample. Bound/free ASA-BMPA was calculated as [(Hmix/Cmix)/(Hspl/Cspl)]-1. Bound ASA-BMPA was calculated as 1-[(Hspl/Cspl)/(Hmix/Cmix)]xTot (where Hmix is ^{3}H dpm in the isotope mixture without cells, Cmix is the ^{14}C in the isotope mixture, Hspl is the ^{3}H in the sample equilibrated with the cells, Cspl is the ^{14}C in the sample and Tot is the added concentration of ligand). In additional samples, 50 μM cytochalasin B was added to estimate the non-specifically bound ASA-BMPA ($\approx$10 % of the total). The small bound/free ratio in the presence of cytochalasin B was subtracted from that obtained in its absence. The free/bound ratio in the presence of ATB-BMPA was multiplied by the bound/free ratio in the absence of inhibitor (n) and was plotted against the

ATB-BMPA concentration. The K_i was calculated by non-linear regression fitting to Equation 2.

$$(\text{free/bound})xn = 1 + [\text{ATB-BMPA}]/K_i \qquad \text{Equation 2}$$

2.3.7. Treatment of Erythrocyte membranes with Trypsin and Thermolysin

Erythrocyte membrane suspension at 1 mg/ml in 5 mM Na_2PO_4 buffer, pH 7.2 was treated with either trypsin at 100 units/ml for 30 min at 20 °C or thermolysin at 0.4 units/ml for 30 min at 20 °C. After treatment with trypsin, the enzyme was removed by dilution of the membranes in 3.0 ml of 5 mM Na_2PO_4 buffer and by centrifugation at 20,000 g for 20 min at 4 °C. The pellet was then resuspended and washed again in the same buffer. After thermolysin treatment the enzyme was removed by dilution of the membranes in 3.0 ml of 5 mM sodium phosphate buffer with 27 mM EDTA and by centrifugation at 20,000 g for 20 min. After washing of trypsin and thermolysin treated samples, the membranes were resuspended in phosphate buffer without enzymes.

2.3.8. 2-Nitro-5-thiocyanobenzoic Acid Treatment

Labelled membranes were dissolved in a buffer comprising 42 mM Tris-acetate pH 8.0, 0.8 mM EDTA, 1.7 % (w/v) SDS and the sample was gassed with nitrogen. NTCB was then added to a final concentration of 10 mM and the reaction was kept

at 37 °C for 30 min. An equal volume of 0.1 M sodium borate pH 9.3 was added and the pH readjusted to pH 10 by the addition of 1 M NaOH. The mixture was then maintained at 37 °C for 42 hr. 2-mercaptoethanol (30 μl/ml) was then added. The samples were desalted by repeatedly filtering through Ultrafree-MC filter units (Millipore) and diluting with a 1 mM Tris-HCl buffer containing 0.1 % (w/v) SDS, pH 6.8. The samples were then either analysed by electrophoresis on Tricine gels (section 2.6.2.3.) or were solubilized in 2 % Thesit detergent buffer and immunoprecipitated with antibodies to the C-terminal and cytoplasmic loop of GLUT1 as described in section 2.3.5. Anti-peptide antibody against the large cytoplasmic loop (residues 231-246) of GLUT1 was kindly provided by S.A. Baldwin.

2.4. Studies on GLUT1 Mutants Expressed in (CHO-K1) cells

Ham's F-12 medium, penicillin/streptomycin and glutamine were from ICN/Flow laboratories. Foetal calf serum, trypsin/EDTA and geneticin (G-418 sulphate) were from Gibco BRL. 35 mm and 90 mm tissue culture dishes were from Nunc/Gibco BRL. 2-deoxy-D-[2,6-^{3}H]glucose, sodium boro[^{3}H]hydride and [4-^{3}H]cytochalasin B were from Amersham International. Phloretin, cytochalasin E, cytochalasin B, galactose oxidase, neuraminidase, protein A-Sepharose, proteinase inhibitors and 2-deoxy-D-glucose were from Sigma. 4,6-O-ethylidene-D-glucose was from Koch-light Laboratories. Nonaethylene glycol dodecyl ether (Thesit) was from Boehringer Mannheim.

2.4.1. Production and Expression of Wild-Type and Mutant GLUT1 Glucose Transporters in CHO-K1 cells

The CHO-K1 cells expressing wild-type and mutant GLUT1 glucose transporters were prepared by Dr Mitsuru Hashiramoto using the method previously described (Hashiramoto *et al*, 1992).

2.4.2. Culture of CHO-K1 cells

The CHO cell line CHO-K1 were used as they have a low endogenous glucose transporter activity (Hasegawa *et al*, 1990). They were maintained in Ham's F-12

medium containing 10 % foetal calf serum, 100 unit/ml penicillin, 100 μg/ml streptomycin, 2 mM glutamine and 600 μg/ml geneticin (G-418 sulphate). The medium was changed every 2 days and when the cells reached confluence they were trypsinized and split 1:10 for further maintenance in culture. For transport and photolabelling experiments, cells were seeded into 35 mm and 90 mm culture dishes and were generally confluent 2-3 days later.

2.4.3. 2-Deoxy-D-Glucose Transport in CHO-K1 Cells

The measurement of 2-deoxy-D-glucose uptake was performed essentially as described by Harrison *et al*, (1990). Cells in 35 mm dishes were grown to confluence for 2-3 days. Cells were then washed three times with 2 ml of Krebs-Ringer Hepes Buffer (KRH:140 mM NaCl, 4.7 mM KCl, 2.5 mM $CaCl_2$, 1.25 mM $MgSO_4$, 2.5 mM Na_2HPO_4, 10 mM Hepes, pH 7.4). The cells were incubated with 0.9 ml of KRH for 10 min at 37°C, then with 50 μl of inhibitor (0-50 mM, final concentration) for a further 10 min. 2-deoxy-[2,6-^{3}H]D-glucose (0.3 μCi) was then added to give a final assay concentration of 0.1 mM and cells were maintained at 37°C for 5 min. Uptake was terminated by the addition of 2 ml/well of ice-cold PBS containing 0.3 mM phloretin and three rapid washes with ice-cold PBS/phloretin. Cells were solubilized with 1 ml of 0.1 M NaOH and the extract was added to scintillant for estimation of radioactivity. Nonspecific 2-deoxy-D-glucose uptake was measured in the presence of 50 μM cytochalasin B and 0.3 mM phloretin and was subtracted from each determination to obtain specific uptake.

2.4.4. Labelling of Cell-surface Carbohydrate with Tritiated Sodium Borohydride

The CHO-K1 clones transfected with either wild-type or mutant GLUT1 were grown to confluence in 35 mm culture dishes. The cells were then simultaneously treated with 10 units of galactose oxidase and 1 unit of neuraminidase in 1 ml of PBS for 30 min at 18 °C. The dishes were then washed three times with 2 ml of PBS and then 2 mCi of sodium borohydride (specific activity 13.7 Ci/mmole) in 40 μl of 50 mM NaOH was rapidly mixed with 20 μl of 45 mM HCl and added immediately to the cells in 1 ml of PBS. After maintaining the cells at 18°C for 10 min the dishes were washed four times in PBS and then the cells were solubilized in 1 ml of 2 % Thesit detergent buffer and immunoprecipitated with anti-GLUT1 antibodies as described below.

2.4.5. Immunoprecipitation of GLUT1 From CHO-K1 Cells

Labelled CHO-K1 cells were solubilized in 2 % Thesit detergent buffer (2 % $C_{12}E_9$, nonaethylene glycol dodecyl ether, with the proteinase inhibitors antipain, aprotinin, pepstatin A and leupeptin, each at 1 μg/ml, in 5 mM Na_2PO_4 buffer, pH 7.2). Following centrifugation at 20,000 g for 20 min the supernatants were subjected to immunoprecipitation with 20 μl of protein A-Sepharose coupled to 100 μl of anti-GLUT1 antiserum for 2 hr at 0-4 °C. C-terminal deletion mutants were immunoprecipitated with an anti-peptide antibody raised against the large cytoplasmic loop (residues 231-246) of GLUT1 (kindly provided by S.A. Baldwin). The immunoprecipitates were then washed 4 times with 1 ml of 0.2 % Thesit buffer (0.2

% Thesit, with the proteinase inhibitors antipain, aprotinin, pepstatin A and leupeptin, each at 1 μg/ml, in 5 mM Na_2PO_4 buffer, pH 7.2). The glucose transporter-antibody conjugate was removed from the protein A-Sepharose by incubating the immunopellet for 20 min with "whirly mixing" in electrophoresis sample buffer (10 % (w/v) SDS, 6 M Urea and 10 % (v/v) 2-mercaptoethanol) and analysed by electrophoresis (section 2.6.2.).

2.4.6. Photolabelling of CHO-K1 Cells with ATB-BMPA

Confluent cells in 35 mm culture dishes were washed with PBS and were then incubated at 18°C with 100 μCi of ATB-[2^3H]-BMPA (specific activity 10 Ci/mmol) in 200 μl of PBS for 2 min and then irradiated for 1 min in a Rayonet RPR-100 photochemical reactor with 300 nm lamps. Following irradiation the dishes were washed five times in PBS. In some experiments, the cells were solubilized in 250 μl of 2 % Thesit buffer, then chloroform/methanol precipitated (section 2.6.3.). Protein was measured on the precipitate, and the pellets were solubilized in electrophoresis sample buffer and analysed by SDS-PAGE. In later experiments the cells were solubilized directly in 250 μl of electrophoresis sample buffer.

2.4.7. Photolabelling of CHO-K1 Cells with Cytochalasin B

CHO-K1 cells were grown to confluence in 90 mm culture dishes and washed 3 times in 5 ml of TES (20 mM Tris-HCl, 1 mM EDTA and 255 mM sucrose, pH

7.2). The cells were homogenized in 2 ml of TES and then spun at 900 g for 2 min to pellet a fraction containing mainly mitochondria and nuclei. The supernatant was then centrifuged at 20,000 g for 20 min to obtain a plasma membrane fraction. Plasma membrane (200 μg) in 400 μl of TES containing 100 μM cytochalasin E, was labelled with 1.4 μCi of [4-^{3}H]-cytochalasin B by irradiation for 45 sec in a Rayonet photochemical reactor. Following irradiation, the membranes were washed twice by centrifugation at 35,000 g for 20 min and resuspension in 3 ml TES. The final pellet was resuspended in 100 μl of TES, solubilized in electrophoresis sample buffer and analysed by electrophoresis.

2.5. Studies on the Rat Adipocyte Glucose Transporter

2.5.1. Preparation of Albumin Solution

100 g of bovine serum albumin (Fraction V, Sigma) was dissolved in 500 ml of double-distilled water at 0-4 °C. This was dialysed for 24 hr against 2 changes of 10 volumes of double-distilled water at 0-4 °C. The volume of the solution was then made up to 1000 ml with double-distilled water (to give a 10 % solution) and the solution was filtered, first through Whatman 41 filter paper, then Whatman 42 filter paper, and finally through Millipore type A membrane filters (0.8 μm pore size). The pH of the solution was adjusted to 7.4 with 10 M NaOH and the solution was divided into 15 ml aliquots and stored at -20 °C until required. Once thawed, the solution was not refrozen.

2.5.2. Preparation of Buffers and Insulin Stock Solution

All buffers, unless otherwise stated, contained the following, Hepes buffer: 140 mM NaCl, 4.7 mM KCl, 2.5 mM $CaCl_2$, 1.25 mM $MgCl_2$, 2.5 mM NaH_2PO_4, 10 mM Hepes. The pH was adjusted to 7.4 at 20 °C. Albumin was added as required. Buffer stock solutions were prepared as 10 X concentrates, one containing Hepes and NaH_2PO_4 (pH 7.6), and the other containing NaCl, KCl, $CaCl_2$ and $MgSO_4$ and were stored at 4 °C for up to 1 month.

Monocomponent porcine insulin was a gift from Dr. Ronald Chance, Eli Lilly

laboratories. 1.0 mg of insulin was dissolved in 1.0 ml of 0.03 M HCl and the solution made up to 3.0 ml with double-distilled water. 1.0 ml of this solution was then diluted to 50 ml with 1 % albumin/Hepes buffer, pH 7.6. The resulting insulin solution (1 μM) was divided into 1 ml aliquots and stored at -20 °C until required. The solution was not refrozen once it had been thawed.

2.5.3. Preparation of Isolated Rat Adipose Cells

Isolated adipose cells were prepared from the whole epididymal fat pads of male Wistar rats (175-190 g) by the method of Taylor & Holman (1981). The rats were stunned and the necks dislocated. The epididymal fat tissue was quickly removed and rinsed in 1 % albumin/Hepes buffer at 37 °C. The washed tissue was then placed into Hepes buffer (3.5 ml/2 pads) containing 3.5 % albumin, 0.5 mM glucose, and 0.85 mg/ml collagenase (Worthington) in a 75 x 23.5 mm clear polystyrene flat-bottomed tube (Sarstedt), and minced finely with scissors. The tissue suspension was shaken rapidly in a shaking waterbath at 37 °C for approximately 50 min until most of the tissue lumps were digested. The resulting cell suspension was filtered through nylon mesh (250 μm mesh size, Lockertex), and allowed to float at 37 °C. The infranatant buffer was removed using a needle (2 mm dia. x 100 mm) attached to a 20 ml plastic syringe, and 10-15 ml of 1 % albumin/Hepes buffer was added. The cells were resuspended and allowed to float. This washing procedure was repeated 4 times and was carried out at 37 °C. The cell suspension was then adjusted to 40 % cytocrit (using a 25 μl capillary tube which was centrifuged at 1500 g for 30 sec, and expressed as the ratio of the length of the packed cell fraction in the tube to

the total length of the suspension in the tube).

2.5.4. Treatment of Rat Adipocytes with Insulin

Either 2 or 10 nM insulin (1 μM stock, section 2.5.2.) was used to stimulate isolated rat adipocytes. The time course for activation of insulin stimulated glucose transport was studied using 2 nM insulin and 0.5 mg/ml bacitracin. 2 mM potassium cyanide (150 mM stock) was added at the specified times to stop any further translocation. Deactivation of insulin-stimulated glucose transport was achieved in two ways which gave the same results. Either the cells were washed 4-6 times during the reversal period with 1 % albumin/Hepes buffer at 37 °C to wash away the insulin, or collagenase (final concentration: 0.25 mg/ml, 50 x stock in albumin-free Hepes buffer) was added to remove the insulin.

2.5.5. 3-O-Methyl-D-Glucose Transport in Rat Adipocytes

Uptake of 3-O-methyl-D-glucose was determined by the method of Whitesell & Gliemann, (1979). 50 μl of a 40 % adipocyte suspension was added to 10 μl of 200 μM 3-O-methyl-D-glucose (to give a final concentration of 50 μM), containing 0.15 μCi of 3-O-[^{14}C]methyl-D-glucose in albumin-free Hepes buffer in a 4 ml (50 mm x 13 mm) polypropylene tube (Nunc/Gibco BRL). Uptake was terminated by rapidly adding 3 ml of 0.3 mM phloretin in albumin-free Hepes buffer (the phloretin was first dissolved in ethanol such that the final concentration of ethanol was 0.5 %).

Timings of 10 sec or less were carried out using a metronome set at 2 beats/sec. Uptake was measured for 3 sec in insulin-stimulated cells and 120 sec in basal cells (these times should give fractional filling values (f) of approximately 0.5). "Blank" values (b) (indicating extracellular trapped radioactivity) were determined by adding 3 ml of 0.3 mM phloretin in albumin-free Hepes buffer to the sugar before the addition of the cells. "Infinity" values (α) (indicating equilibrium distribution of radioactivity) were determined by incubating insulin-treated cells with sugar for 12-15 min. 1 ml of silicon oil (Dow Corning 100/200 cs, obtained from BDH) was layered on top of the buffer, and the tubes were centrifuged (MSE bench centrifuge, swing-out rotor) at 2,500 revs/min for 45 sec. The cell layer was removed from the top of the oil using small pieces of pipe-cleaner (5 mm), and placed in a scintillation vial. 8 ml of scintillation fluid was added. The rate constant of sugar uptake (v/s) was calculated from the fractional filling (f).

$$f = cpm_t\text{-}b/cpm_\alpha\text{-}b \qquad v/s = (-\ln[1-f])/t$$

2.5.6. Photolabelling of Glucose transporters in Rat Adipocytes

1 ml of cells (40 % cytocrit) were added to 333-500 μCi of ATB-[^{3}H]BMPA in albumin-free Hepes buffer in 35 mm-diam. polystyrene dishes (Nunc/Gibco BRL) and irradiated for 1 min in a Rayonet RPR-100 photoreactor containing RPR-3000 lamps. Following irradiation, the cells were washed into polystyrene centrifuge tubes (Sarstedt) with 8 ml 1 % albumin/Hepes buffer at 18 °C and spun in a bench

centrifuge (IEC centra-3) to 1,000 revs/min then immediately stopped. The infranatant buffer was removed using a needle (2 mm dia. x 100 mm), and the cells were resuspended in 8 ml of 1 % albumin/Hepes buffer and washed twice more.

2.5.7. Subcellular Fractionation of Rat Adipocytes

This procedure was carried out essentially as described by Weber *et al*, (1988), with a few modifications. 2.5 ml of cells were washed once in TES buffer (20 mM Tris-HCl, 1 mM EDTA and 255 mM sucrose, pH 7.2) at 20 °C and then resuspended in 2 ml of TES buffer at 18 °C. The cells were then rapidly homogenized (basal first) with 10 strokes of a 55 ml Potter-Elvehjem homogenizer, (Thomas Scientific, with a specific clearance of 0.15 mm) then rapidly centrifuged at 1000 rev/min for 1 min (MSE refrigerated bench centrifuge) to pellet any remaining red blood cells and separate the fat. All further centrifugations were done in a Beckman TL-100 benchtop ultracentrifuge with a TLA-100.3 fixed rotor and a TLS-55 swing-out rotor. The infranatant was removed with a syringe and hypodermic needle (21 g x 1.5") and centrifuged at 18,000 revs/min for 20 min. The supernatant was removed and used for fractionation of the microsomal membranes. The pellet containing plasma membranes, mitochondria and nuclei was resuspended in 2 ml of TES by homogenization (5 strokes of a 10 ml homogenizer, Braun) and respun at 18,000 revs/min then resuspended in 300 μl of TES. This suspension was loaded onto 0.6 ml of a sucrose cushion (1.12 M sucrose (38.3 %), 20 mM Tris, 1 mM EDTA, pH 7.2) and spun at 35,000 revs/min for 20 min in a swing-out rotor. The mitochondria and nuclei were recovered as a pellet. The plasma membranes were collected at the

cushion interface and were resuspended in 3 ml of TES and then centrifuged at 37,000 revs/min for 9 min. They were then homogenized in 1 ml of TES at 0-4 °C with 5 strokes of a 10 ml homogenizer. The homogenizer was washed out with a further 1 ml of TES which was added to the membranes and centrifuged at 37,000 revs/min for 9 min. The plasma membrane pellet was then resuspended in 100 μl of TES. The microsomal membranes were obtained from the 18,000 revs/min spin supernatant. This was centrifuged at 30,000 revs/min for 30 min to pellet the high-density microsomes. The supernatant was then centrifuged at 100,000 revs/min for 17 min to pellet the low-density microsomes. Both microsomal fractions were resuspended in 100 μl TES.

2.5.8. Immunoprecipitation of GLUT1 and GLUT4 from Rat Adipocytes

Immunoprecipitation of GLUT1 and GLUT4 from subcellular fractions and directly from whole rat adipose cells was carried out. In the case of immunoprecipitation of GLUT1 and GLUT4 from subcellular fractions, plasma-membrane and low density microsome fractions were solubilized in 2 % Thesit detergent buffer (2 % nonaethyleneglycol dodecyl ether, with proteinase inhibitors (antipain, aprotinin, leupeptin and pepstatin A, each at 1 μg/ml) in 5 mM Na_2PO_4 buffer, pH 7.2) for 20 min at 20 °C. For direct immunoprecipitation experiments, labelled cells were washed in 1 % albumin/Hepes buffer 3 times then cells were solubilized in 2 % Thesit detergent buffer for 20 min at 20 °C. Any unsolubilized material was then spun down at 20,000 g for 20 min. Protein A-Sepharose CL-4B (Sigma) was washed and swollen in PBS, pH 7.2 for 15 min then incubated for 2 hr

at 4 °C with either affinity-purified antibodies or antiserum to GLUT1 or GLUT4 in PBS. When using affinity-purified antibodies, 10-20 μg of affinity-purified antibodies were mixed with 8 μl of swollen protein A-Sepharose. When using antiserum, 75-100 μl of antiserum was mixed with 20 μl of protein A-sepharose. Unbound antibodies were removed from the protein A-Sepharose pellets by washing the pellets 2 times in 1 ml of PBS. The protein A-Sepharose was always pelleted by centrifugation at low speed (6,500 revs/min) in a MSE microcentaur microfuge for 1 min. The solubilized membranes and cells were then incubated with either the GLUT1 or GLUT4 antibody-protein A-Sepharose conjugate for 2 hr at 4 °C. The immunoprecipitate was then pelleted and the supernatant incubated with the other antibody conjugate for 2 hr at 4 °C. The immunopellets were washed 4 times with 1 ml of 0.2 % Thesit detergent buffer in PBS containing proteinase inhibitors (antipain, aprotinin, leupeptin and pepstatin A, each at 1 μg/ml). The glucose transporter-antibody conjugate was removed from the protein A-Sepharose by incubating the immunopellet for 20 min with whirly mixing in electrophoresis sample buffer and was analysed by SDS-Page (section 2.6.2.).

2.5.9. Trypsin-Treatment of Immunoprecipitated GLUT4

Immunoprecipitated, ATB-BMPA-labelled GLUT4 was treated with 10 units of trypsin in 100 μl of PBS for 30 or 45 min at RT. Then, either electrophoresis sample buffer was added directly to the sample, or the pellet and supernatant were separated and were analysed separately by SDS-PAGE.

2.6. General Methods

2.6.1. Protein Assays

2.6.1.1. BIO-RAD Protein Assay

For the standard protein curve, 0, 5, 10, 15, 20 and 25 μl of standard bovine serum albumin (BSA) solution (200 μg/ml in double-distilled water) were made to 775 μl with 5 mM Na_2HPO_4 buffer, pH 7.2, then 25 μl of 0.1 M NaOH was added. An aliquot of the membrane or protein sample to be assayed (generally 5 to 50 μl aliquots depending on the expected protein content) was made to 775 μl with 5 mM Na_2HPO_4 buffer then 25 μl of 0.1 M NaOH was added. 200 μl of BIO-RAD reagent (BIO-RAD) was added to the standard protein samples and the protein samples to be assayed. After incubation of the samples for 10 min at RT the absorbance was read at 595 nm in a spectrophotometer.

2.6.1.2. BCA Protein Assay

The BCA protein assay was carried out in microtitre plates. 100 μl standard BSA solution (2 mg/ml in double-distilled water) was mixed with 100 μl of 0.2 M NaOH. For the standard protein curve, 0, 2, 4, 6, 8 and 10 μl of this solution was made to 10 μl with 0.1 M NaOH. 5 μl of the membrane or protein sample to be assayed (diluted if necessary) was mixed with 5 μl of 0.2 M NaOH. 10 ml of reagent

A (1 % BCA detection reagent (bicinchoninic acid, sodium salt, Pierce), 2 % Na_2CO_3, 0.16 % sodium tartrate, 0.4 % NaOH, 0.95 % $NaHCO_3$, (pH = 11.25 with 1 M NaOH) and filtered through a 0.7 μm filter (Millipore)) was mixed with 200 μl of reagent B (4 % $CuSO_4$, filtered through a 0.7 μm filter (Millipore)). 200 μl of this solution was added to the standard protein samples and the protein samples to be assayed and incubated for 30 min at 37 °C. The absorbance was read in a microtitre plate reader (Labsystems) at 562 nm (filter 6 and 3).

2.6.2. SDS-Polyacrylamide Gel Electrophoresis

Ammonium persulphate and TEMED were from BIO-RAD. All other reagents were of analytical grade and were purchased from Sigma, BDH or Fisons.

2.6.2.1. Sample Preparation for Electrophoresis

Samples were dissolved in electrophoresis sample buffer (10 % (w/v) SDS, 6 M urea, 0.05 % (w/v) bromophenyl blue and 10 % (v/v) 2-mercaptoethanol) for 20 min at RT with mixing, then unsolubilized material was pelleted and the supernatant was applied to the gel (using a Hamilton syringe for 1.5 mm gels and a 200 μl Gilson pipette for 3 mm gels).

2.6.2.2. SDS-Polyacrylamide Gel Electrophoresis

Electrophoresis was carried out using a modification of the method of Hashimoto *et al*, 1983, using the discontinuous buffer system of Laemmli (Laemmli, 1970). The linear slab gels were 8-12 % acrylamide and were made as shown in table 2. Electrophoresis was carried out using a Protean II system (BIO-RAD) using 16 cm plates. The gels were run at constant current (25 mA for a 3 cm gel and 12 mA for a 1.5 cm gel) for approximately 15 hr, until the bromophenyl blue tracking dye had just run off the gel.

Buffers

The following stock solutions were made and stored for up to one month at 0-4 °C.

Resolving gel buffer : 1.5 M Tris-HCl, 0.4 % (w/v) SDS, pH 8.8

Stacking gel buffer : 0.5 M Tris-HCl, 0.4 % (w/v) SDS, pH 6.8

Acrylamide stock solution : Obtained by dissolving 60 g acrylamide, 60 g sucrose and 1.6 g N'N methylene bis acrylamide in 150 ml of double distilled water (final volume = 250 ml). This solution was stored in a dark bottle.

Electrophoresis running buffer : 0.025 M Tris-HCl, 0.1 % (w/v) SDS, 0.2 M glycine, pH 8.3

Ammonium Persulphate : 100 mg/ml, was freshly made for each gel.

Table. 2 Quantities required for one 3 mm gel

Stock solution	Resolving Gel			Stacking Gel
	8 %	10 %	12 %	
Acrylamide stock solution (ml)	20	25	30	2
Resolving gel buffer (ml)	25	25	25	-
Stacking gel buffer (ml)	-	-	-	3.75
Double-distilled water (ml)	22	17	12	9.75
Ammonium persulphate (ml)	0.5	0.5	0.5	0.1
TEMED (μl)	40	40	40	20

2.6.2.3. Tricine Gel System

The Tricine gel system (Schagger & Von Jagow, 1987) was used for good separation of labelled glucose transporter fragments. Electrophoresis was carried out using a Protean II system (BIO-RAD) using 20 cm plates. Gels were run on constant voltage, 30 V for approximately 1 hr, until everything had entered the stacking gel, then 95 V for approximately 15 hr, until the bromophenyl blue tracking dye had just reached the bottom of the gel but had not run off the gel.

Buffers

The following stock solutions were made and stored for up to one month at 0-4 °C.

Acrylamide solution 1 (49 % T, 3 % C) : 48 g acrylamide and 1.5 g N'N methylene bis acrylamide were dissolved in double distilled water (100 ml final vol.). The

solution was stored in a dark bottle.

Acrylamide solution 2 (49.5 % T, 6 % C) : 46.5 g acrylamide and 3 g of N'N methylene bis acrylamide were dissolved in double distilled water (100 ml final vol.) and stored in a dark bottle.

Gel buffer : 3 M Tris-HCl, 0.3 % (w/v) SDS, pH 8.45

Anode buffer : 0.2 M Tris-HCl, pH 8.9

Cathode buffer : 0.1 M Tris-HCl, 0.1 M Tricine, 0.1 % (w/v) SDS, pH 8.25

Ammonium Persulphate : 100 mg/ml, was freshly made for each gel.

Table. 3 Quantities required for one 3 mm gel

Stock solution	Separating Gel (16.5% T, 6% C)	Spacer Gel (10% T, 3% C)	Stacking Gel (4% T, 3% C)
Acrylamide sol^n 1 (ml)	-	6.1	1
Acrylamide sol^n 2 (ml)	10	-	-
Gel buffer (ml)	10	10	3.1
glycerol	4 g	-	-
d.d. water (ml)	30 including glycerol	13.9	8.4
Ammonium persulphate (μl)	100	100	100
TEMED (μl)	10	10	10

The stacking gel was 2 cm long and the spacer gel was 3 cm long. The separating and stacking gels were poured within 2 min of each other (but it was essential that the separating gel had polymerized first). The Anode buffer was put in the lower compartment and cathode buffer was put in the upper compartment of the

electrophoresis apparatus.

2.6.2.4. Molecular Weight Standards For Electrophoresis

Molecular weight standards were: myosin (205 kDa), ß-galactosidase (116 kDa), phosphorylase B (97.4 kDa), bovine albumin (66 kDa), Ovalbumin (44 kDa), and carbonic anhydrase (29 kDa). 1 vial of standards (SDS-6H, Sigma) was dissolved in 2 ml of electrophoresis sample buffer and then divided into aliquots (100 μl) and stored at - 20 °C. Prestained standards (Sigma): triosephosphate isomerase (26.6 kDa) and ß-galactosidase (116 kDa) were applied when gels were to be transferred for western blotting. Prestained standards (one vial of each) were dissolved in a total of 3 ml of electrophoresis sample buffer and stored at - 20 °C in 100 μl aliquots.

2.6.2.5. Processing of Gels

Gels were stained in 0.02 % Coomassie blue, 30 % methanol, 10 % acetic acid, to fix the protein and to allow the lanes to be clearly seen. The lanes were sliced (0.33 or 0.66 cm/slice) and dried in scintillation vials for 2 hr at 80 °C, then dissolved for approximately 2 hr at 80 °C in hydrogen peroxide (30 % v/v), 2 % ammonium hydroxide (with vial lids on). Samples were counted in 8 ml of scintillant (Optiphase Safe, LKB) in a Packard 1500 TRI-CARB or 1600 TR liquid scintillation counter at an efficiency of about 30 %.

2.6.3. Chloroform/Methanol Precipitation of Protein

1 ml of methanol and 250 μl of chloroform were added to 250 μl of protein sample in a 10 ml polypropylene centrifuge tube and this suspension was centrifuged at 9,000 g in an Ole Dich bench centrifuge for 10 sec. 750 μl of water was added and the sample was respun at 9,000 g for 1 min. The upper phase was removed, and 750 μl of methanol was added to the rest of the lower chloroform phase and the interphase with the precipitated protein. The sample was respun at 9,000 g for 2 min and the supernatant was discarded. The protein pellet was dried under an air stream.

CHAPTER 3 : RESULTS

3.1. Production of Antibodies

3.1.1. Preparation of Anti-GLUT1 and Anti-GLUT4 Antibodies

Anti-C terminal peptide antibodies were produced to the GLUT1 and GLUT4 glucose transporter isoforms. The anti-GLUT1 antibodies did not bind to the GLUT1 C-terminal peptide in an ELISA. This was probably due to the peptide binding very tightly to the ELISA plate. The anti-GLUT1 antibodies did bind to protein-depleted erythrocyte membranes and a good titre of antibodies was obtained from each rabbit used. Fig. 8 shows the increase in antibody titre obtained in one rabbit over 20 weeks. 30 ml bleeds were generally taken monthly after a good titre of specific antibodies had been obtained.

The anti-GLUT4 antibodies bound to the GLUT4 C-terminal peptide in an ELISA and were produced in high yields by all rabbits. We were therefore able to use these antibodies in immunoprecipitation and Western blotting experiments.

No cross-reactivity was observed between the two antibodies. This was tested by ELISA, checking anti-GLUT4 antiserum binding to protein-depleted membranes and GLUT1 peptide and anti-GLUT1 antiserum binding to GLUT4 peptide (results not shown). Also when one particular isoform was immunoprecipitated from detergent solubilized rat adipocytes, it was not recognized on a Western blot by antibodies to the other isoform.

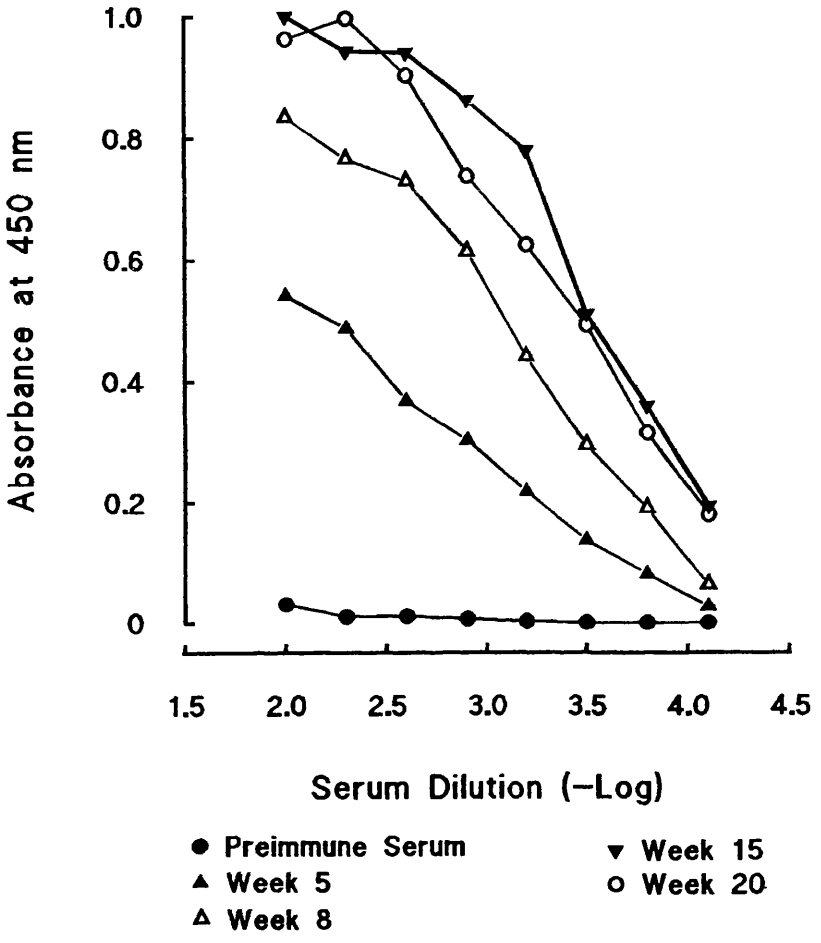

Fig. 8. Anti-GLUT1 antibody screening by ELISA. Rabbits were immunized with GLUT1 C-terminal peptide conjugated to KLH and the antisera was monitored for specific antibodies by ELISA. Plates were coated with 5 μg of protein-depleted membranes/well and bound antibody was detected with a peroxidase conjugate.

3.1.2. Purification of Anti-Peptide Antibodies

GLUT1 and GLUT4 C-terminal peptides were coupled to activated agarose to give anti-peptide antibody affinity columns for GLUT1 and GLUT4 antibodies. The column eluant at each stage was monitored for specific anti-peptide antibodies using ELISA. Fig. 9 shows that after recycling of the antiserum 3 times through the column, virtually all antipeptide antibodies had bound and so were removed from the serum. A small amount of antipeptide antibody was removed during the 2 M sodium chloride wash which was meant to only remove loosely bound antibodies. However virtually all the specific antibody was removed from the column with sodium thiocyanate (NaSCN). The NaSCN eluant was then rapidly dialysed and concentrated to a volume similar to that of the starting serum and shown by ELISA to contain functional antibodies. We would routinely obtain approximately 250 μg of specific antibodies per 1 ml of antisera. The antibodies were stored at -80 °C. Although affinity purified antibodies were initially used successfully in a large number of experiments, they seemed to only remain stable in solution at -80 °C for a few months. As purifying the antibodies was also a time consuming process, we decided to try using whole antisera in immunoprecipitations and western blots. Antisera proved to be just as efficient as the affinity purified antibodies and therefore whole antisera was used in most future experiments.

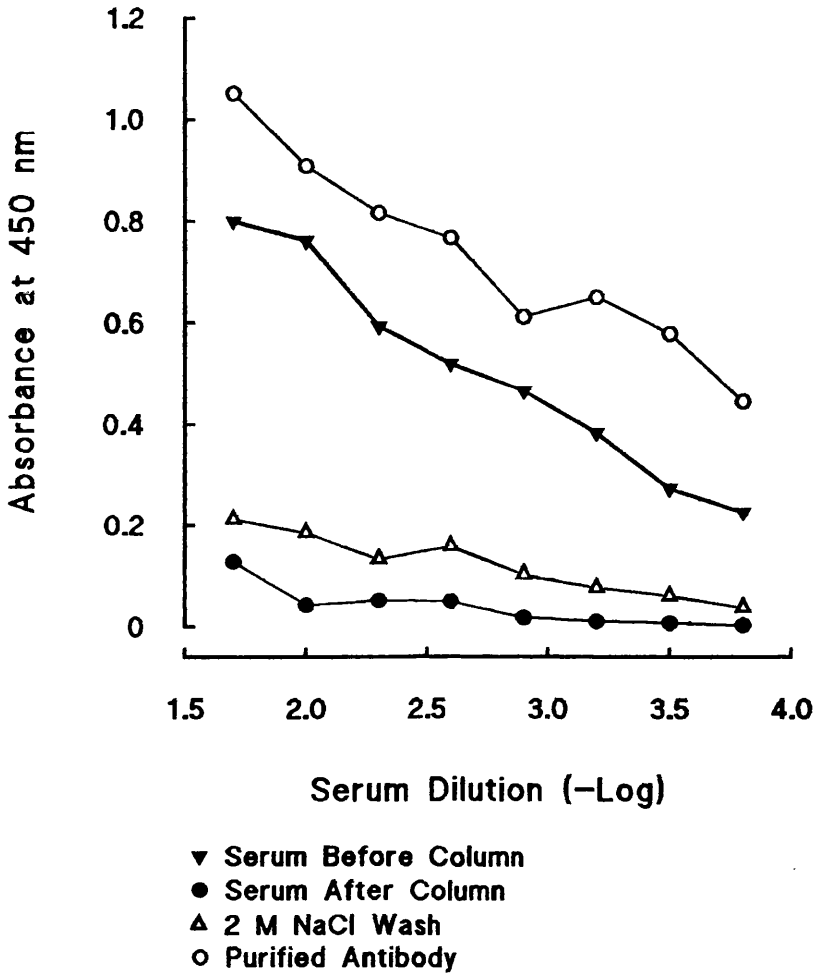

Fig. 9. Monitoring of the affinity purification of anti-GLUT1 antibodies by ELISA. GLUT1 peptide was coupled to reactigel to make an affinity column. Fractions collected from the column were monitored by ELISA. Serum (▼) was passed through the column at least 3 times to allow retention of specific antibody by the column and leaving very little in the antisera (●). The column was washed with PBS and then 2 M NaCl to remove weakly bound protein (△). Specific antibodies were then eluted with 3.5 M NaSCN and rapidly dialysed against PBS (○).

3.2. Studies on the Erythrocyte Glucose Transporter

The glucose transporter in erythrocytes has been extensively studied as erythrocytes are easy to obtain in large quantities and contain large levels of the glucose transporter protein (Allard & Lienhard, 1985). Also, it was not until the first glucose transporter (GLUT1) was cloned, sequenced and its tissue distribution investigated (Mueckler *et al*, 1985), that it was realised that there are a number of glucose transporter isoforms. Even though there are now known to be at least six different glucose transporter isoforms, they display a high degree of sequence homology, and so it is thought that a common mechanism for facilitation of transport is likely. The transport of sugars is generally thought to occur via a conformational change mechanism in which binding sites are alternately exposed to the outside and inside solutions (Barnett *et al*, 1973a,b). However, detailed information on the kinetics and conformational changes involved in the transport of sugars is still not known. With the use of specific external and internal ligands ATB-BMPA and cytochalasin B, anti-C-terminal peptide antibodies and proteinases, the studies described in this thesis aimed to investigate some of the conformational changes that take place within the transporter upon ligand binding and transport.

3.2.1. Photolabelling the Glucose Transporter in Intact Erythrocytes using ATB-BMPA

The azidosalicoyl derivative of bis-mannose (ASA-BMPA) was used by Holman *et al*, (1986) to label the external binding site of the erythrocyte glucose

transporter. Although ASA-BMPA was specific for the glucose transporter in intact erythrocytes, it also labelled a band 3 protein and spectrin when used to label the glucose transporter in isolated erythrocyte membranes. Therefore a diazirine derivative of BMPA (ATB-BMPA) was made in an attempt to get increased specificity in isolated membranes.

When erythrocytes were irradiated in the presence of ATB-[2-^{3}H]BMPA, and the resulting membranes were analysed by electrophoresis on a 10 % acrylamide gel, a single broad peak was observed which ran between the 45 and 66 kDa molecular weight markers (Fig. 10). Photochemical decomposition of ATB-BMPA in water has been shown to have a half time of approximately 30 sec (Clark & Holman, 1990). Increasing the irradiation time from 30 sec to 60 sec increased the incorporation of ATB-BMPA into the glucose transporter (Fig. 10). Therefore to achieve maximum incorporation whilst trying to avoid damaging the cells, for most future experiments a 60 sec irradiation time was used. This labelling was fully inhibited by 300 mM D-glucose but not 300 mM D-mannitol (Fig. 10). 50 μM cytochalasin B, an inside specific inhibitor of the glucose transporter, also fully inhibited ATB-BMPA labelling of the transporter in intact erythrocytes (Fig. 20).

3.2.2. Photolabelling the Glucose Transporter in Erythrocyte Membranes using ATB-BMPA

It was necessary to be able to label glucose transporter protein specifically in isolated membranes as proteolytic cleavage studies on the erythrocyte glucose transporter had to be done on membranes. When erythrocyte membranes were

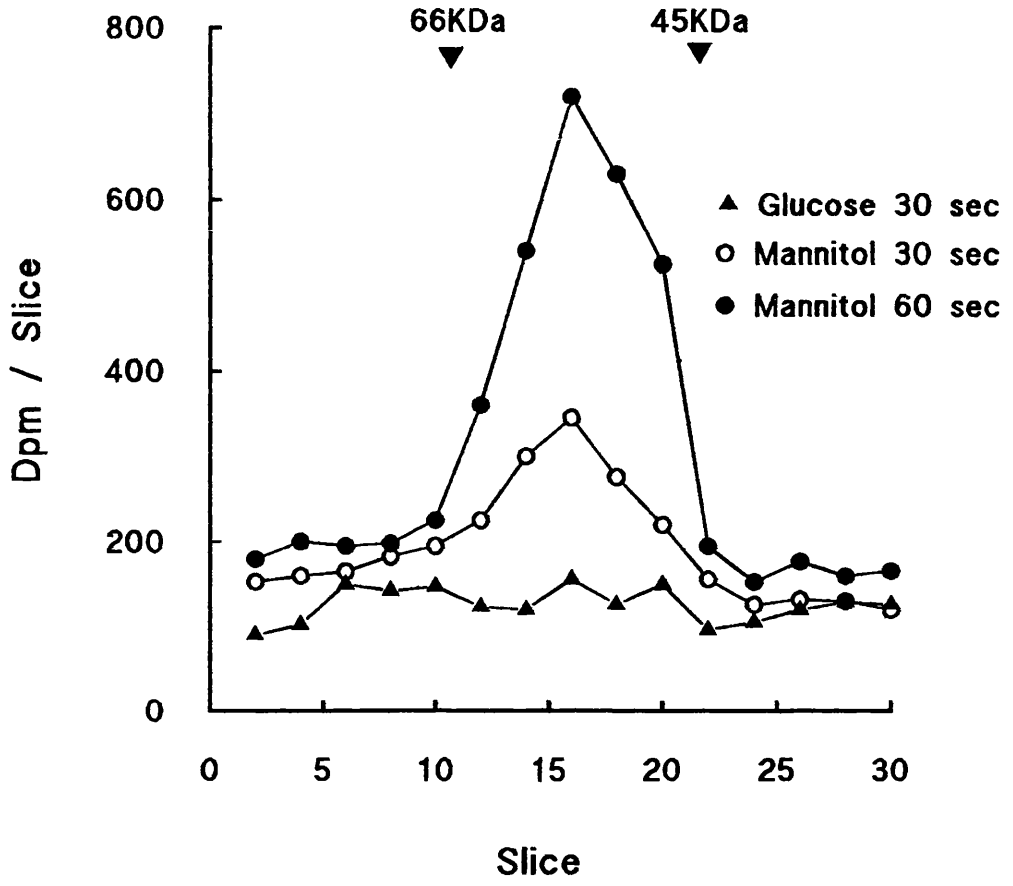

Fig. 10. Photolabelling of erythrocytes with ATB-BMPA. Human erythrocytes were washed with PBS then 600 μl of a 20 % erythrocyte suspension containing 300 mM D-glucose (▲) or 300 mM D-mannitol (○,●) was mixed with 10 μCi of ATB-[2-^{3}H]BMPA. The erythrocyte suspension was transferred to 1 mm-pathlength cuvettes and irradiated for 30 sec (▲,○) or 60 sec (●). Erythrocyte membranes were obtained by osmotic lysis and analysed by electrophoresis on a 10 % acrylamide gel.

irradiated with the photolabel ATB-[2-^{3}H]BMPA, just one peak was observed on SDS-PAGE of approximate molecular weight 45-66 kDa (Fig. 11). This peak was fully displaceable by 300 mM D-glucose (Fig. 11) and 50 μM cytochalasin B (results not shown).

3.2.3. Determining the Affinity of the Erythrocyte Glucose Transporter for ATB-BMPA

The affinity constant (or half maximal inhibition constant, K_i) of the erythrocyte glucose transporter for ATB-BMPA was determined in two ways.

[^{14}C]Galactose uptake in erythrocytes was measured at a range of nonlabelled ATB-BMPA concentrations. The reciprocal of the uptake rate constant (s/v) was plotted against the ATB-BMPA concentration (Fig. 12). The K_i (as determined by non-linear regression fitting to Equation 1) was 297 ± 53 μM at 20 °C.

ATB-BMPA inhibition of ASA-^{3}H-BMPA binding to intact erythrocytes was also determined at 0 °C and 20 °C. The free/bound ratio was calculated by comparison with [^{14}C]sucrose as described (section 2.3.6.2.). The free/bound ratio in the presence of ATB-BMPA was multiplied by the bound/free ratio in the absence of the inhibitor (n) and was plotted against the ATB-BMPA concentration (Fig. 13) The K_i was calculated by non-linear regression fitting to Equation 2. These K_i values were 368 ± 59 μM and 338 ± 37 μM at 0 °C and 20 °C respectively.

Therefore the K_i was not found to be affected by a change in temperature of the membranes and the K_i's for ATB-BMPA inhibition of ASA-BMPA binding at 20 °C corresponded well with the K_i for ATB-BMPA inhibition of galactose uptake at 20

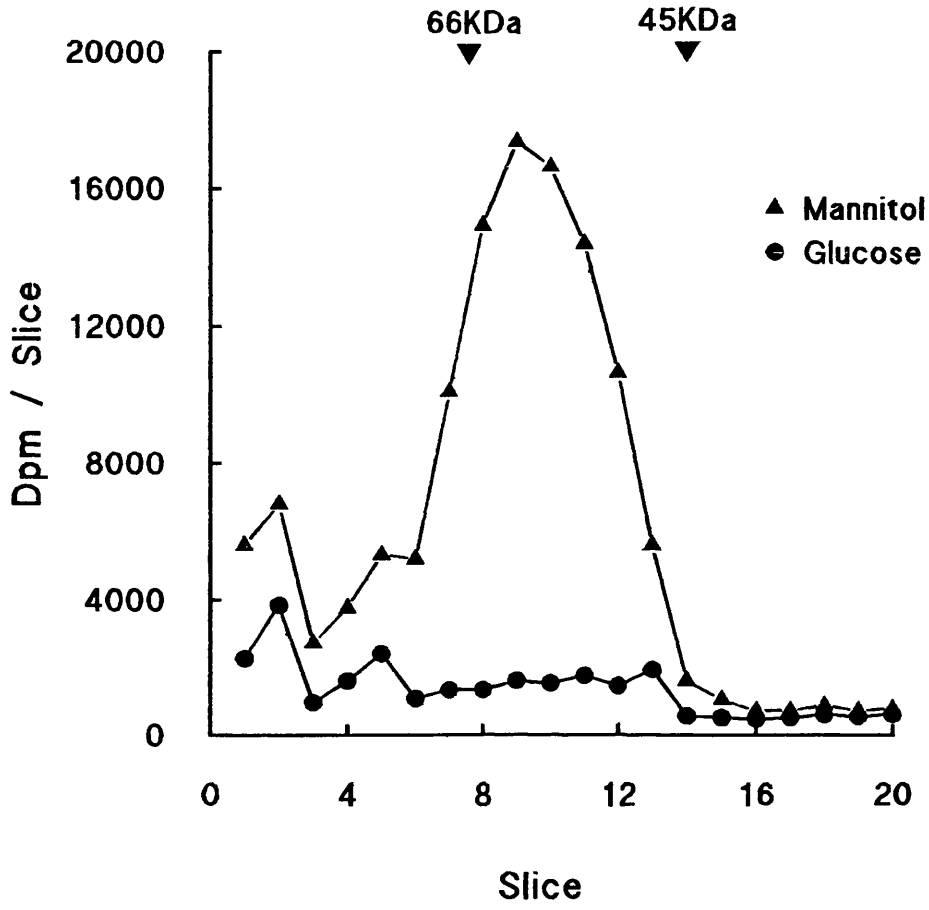

Fig. 11. Photolabelling of erythrocyte membranes with ATB-BMPA. Human erythrocytes were washed in PBS, then the membranes were obtained by osmotic lysis and centrifugation at 20,000 g. 300 μl of erythrocyte membranes at 1 mg/ml containing 300 mM D-glucose (●) or 300 mM D-mannitol (▲) were mixed with 60 μCi of ATB-[2-^{3}H]BMPA and irradiated for 60 sec. Membranes were washed 2 times in 35 ml of phosphate buffer then analysed by electrophoresis on a 12 % acrylamide gel.

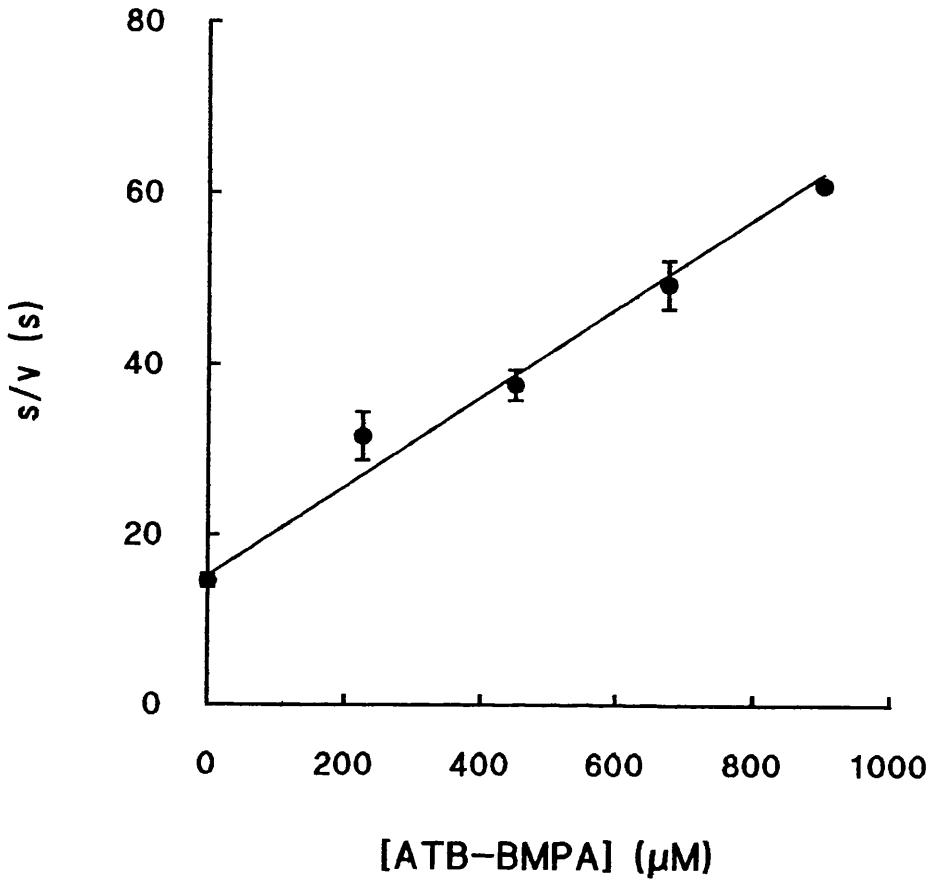

Fig. 12. Inhibition of D-galactose uptake with ATB-BMPA. The uptake of 100 μM D-galactose by erythrocytes was measured at a range of ATB-BMPA concentrations. The reciprocal of the uptake rate constant (s/v) was plotted against the ATB-BMPA concentration. The K_i was determined by non-linear regression fitting to Equation 1. The K_i was 297 $\pm$ 53 μM (from two experiments with triplicate observations at each inhibitor concentration) ; results are means and the bars represent the S.E.M. of the six observations at each concentration.

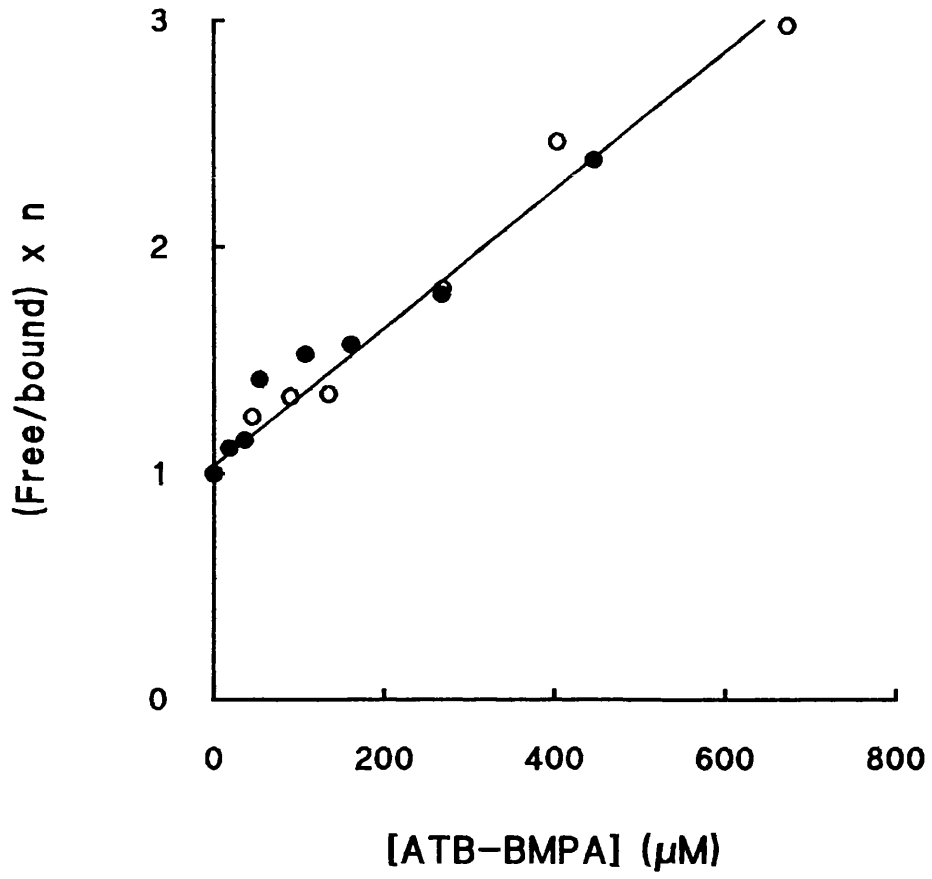

Fig. 13. Inhibition of ASA-BMPA binding by ATB-BMPA. The binding of 0.1 μCi (10 pmol) of ASA-[2-^{3}H]BMPA to 200 μl of an 80 %-cytocrit erythrocyte suspension was measured over a range of ATB-BMPA concentrations. The free/bound ratio was calculated by comparison with [^{14}C]sucrose as described in the methods section. The free/bound ratio in the presence of ATB-BMPA was multiplied by the bound/free ratio in the absence of inhibitor (n) and was plotted against the ATB-BMPA concentration. The K_i was calculated by non-linear regression fitting to Equation 2. At 20 °C (●) the K_i = 368 ± 59 μM (from observations at 16 ATB-BMPA concentrations). At 0 °C (○) the K_i = 338 ± 37 μM (from observations at 14 ATB-BMPA concentrations).

°C.

3.2.4. Efficiency of ATB-BMPA Labelling of Erythrocyte Membranes

Using the half maximal inhibition constant of the erythrocyte glucose transporter for ATB-BMPA, the efficiency of labelling could be calculated. 90 pmol of transporter (calculated assuming 600 pmol/mg of membrane protein (Allard & Lienhard, 1985)) incorporated 5.7 pmol of ATB-BMPA, and therefore 6.3 % of the sites were labelled. The concentration of ATB-BMPA in the reaction was 20 μM, which means that, as the half-saturation constant was approximately 350 μM, the sites were 5.4 % saturated. The efficiency of labelling was therefore calculated as 117 %. Another experiment showed labelling to be 177 % efficient. These values seem higher than expected, but suggest that if all the sites were occupied by ligand, then all the sites would covalently cross-link with the ATB-BMPA. Subsequent studies by Palfreyman *et al*, (1992) and Nishimura *et al*, (1993) also suggested that the labelling by ATB-BMPA was $\approx$ 100 % efficient.

3.2.5. Immunoprecipitation of GLUT1 from Erythrocyte Membranes

An anti-GLUT1 antibody was produced by immunizing a rabbit with a KLH-conjugated peptide corresponding to the C-terminal 13 amino acids of the erythrocyte (GLUT1) glucose transporter (section 3.1.1.). Erythrocyte glucose transporters were labelled with ATB-BMPA and then the erythrocyte membranes were solubilized in 0.5

% Mega 10 with 2 mM DTT in 5 mM phosphate buffer. This detergent buffer was found to successfully solubilize the erythrocyte membrane proteins without interfering with the antibody-glucose transporter binding. Fig. 14 shows that incubation of solubilized labelled erythrocyte membranes for 1 hr with anti-GLUT1 antibodies coupled to protein A-Sepharose pulled down 64 % of the labelled glucose transporters. A second 1 hr incubation with more antibody pulled down another 20 % of the labelled GLUT 1 leaving only 16 % in the supernatant. Under identical conditions, immunoprecipitation with preimmune antiserum pulled down no labelled transporter, leaving it all in the supernatant (Fig. 15). This suggested that most if not all the labelled glucose transporters in erythrocytes membranes were the GLUT1 isoform. Subsequent studies showed that immunoprecipitation of GLUT1 using a single precipitation from Thesit-solubilized membranes was ≈ 80-90 % efficient.

3.2.6. Trypsin Cleavage of the Erythrocyte Glucose Transporter

Trypsin cleaves the native glucose transporter on the cytoplasmic face only, to give two membrane-embedded fragments (Cairns *et al*, 1987). Cleavage of the ASA-BMPA-labelled glucose transporter by trypsin yields a labelled 19 kDa fragment (Holman *et al*, 1986). When the ATB-BMPA-labelled glucose transporter was treated with 100 units/ml of trypsin, a labelled peak at approximately 18 kDa was produced which could be resolved from the 50 kDa native glucose transporter peak using a 12 % SDS-polyacrylamide gel (Fig. 16).

The ATB-BMPA-labelled glucose transporter was cleaved with trypsin and then the solubilized membrane fragments were incubated with anti-GLUT1 C-terminal

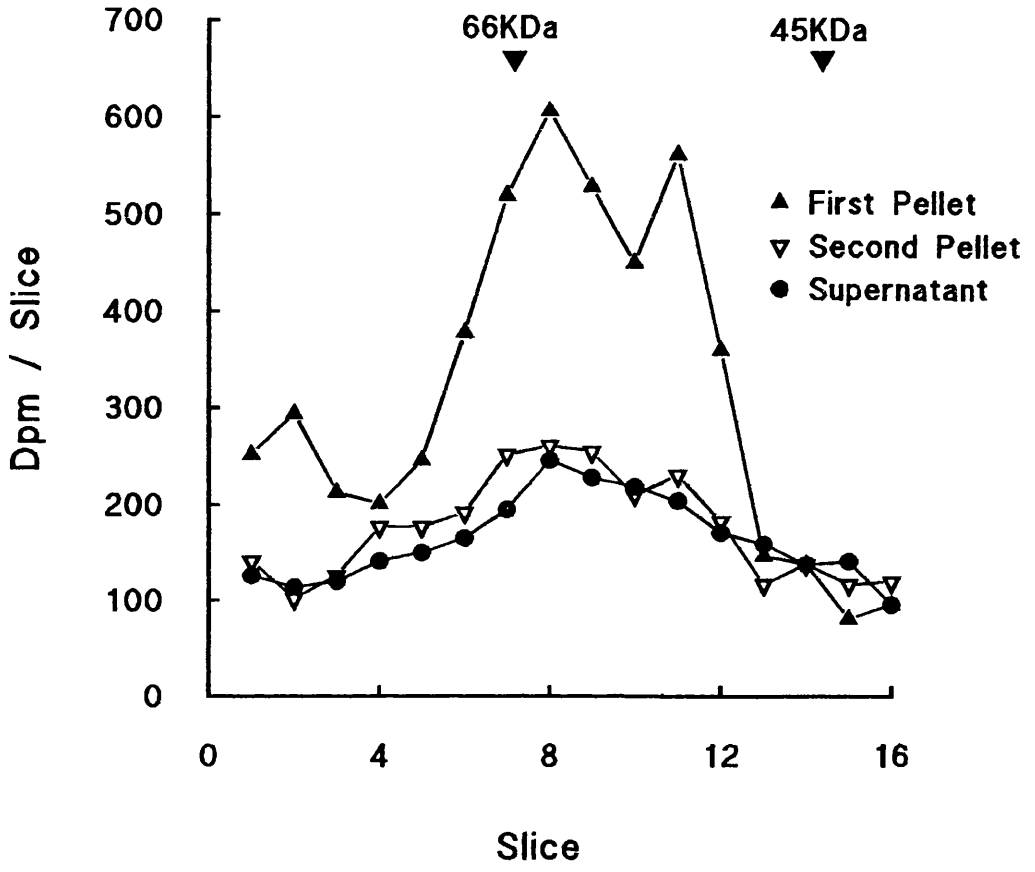

Fig. 14. Immunoprecipitation of ATB-BMPA labelled erythrocyte membranes. Erythrocyte membranes were labelled with ATB-[2-^{3}H]BMPA, then solubilized in 0.5 % Mega 10 detergent buffer. Solubilized membranes (75 μg) were mixed at 0-4 $^\circ$C for 1 hr with 180 μg of purified anti-GLUT1 antibody attached to 30 μl protein A-Sepharose (▲). Supernatant from the first immunoprecipitate was transferred to a second GLUT1 antibody-protein A-Sepharose conjugate for another 1 hr (▽) then the immunopellets were washed and analysed along with the remaining supernatant (●) by electrophoresis on a 10 % polyacrylamide gel.

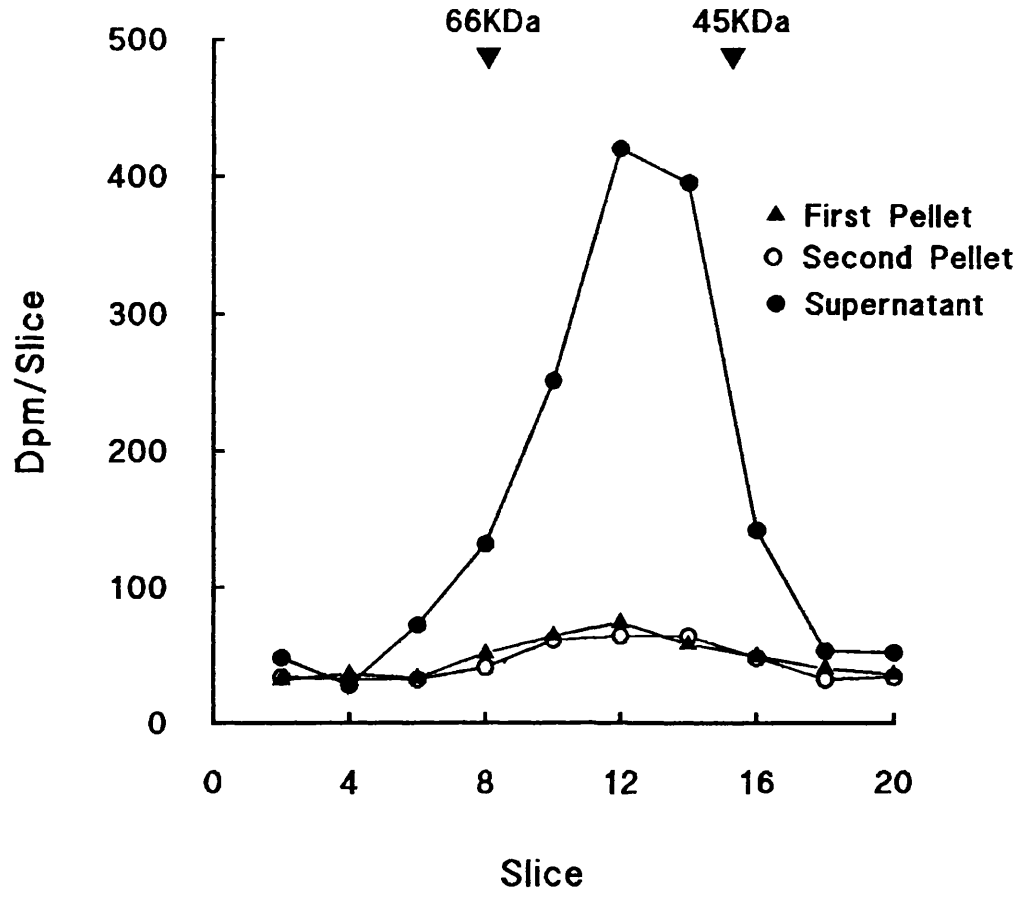

Fig. 15. Immunoprecipitation of ATB-BMPA labelled erythrocyte membranes with preimmune serum. Erythrocyte membranes were labelled with ATB-[2-^{3}H]BMPA then solubilized in 0.5 % Mega 10 detergent buffer. Solubilized membranes (75 μg) were mixed at 0-4 $^{\circ}$C for 1 hr with 180 μl of preimmune serum attached to 30 μl protein A-Sepharose (▲). Supernatant from the first immunoprecipitate was transferred to a second preimmune serum-protein A-Sepharose conjugate for another 1 hr (○). Then the immunopellets were washed and analysed along with the remaining supernatant (●) by electrophoresis.

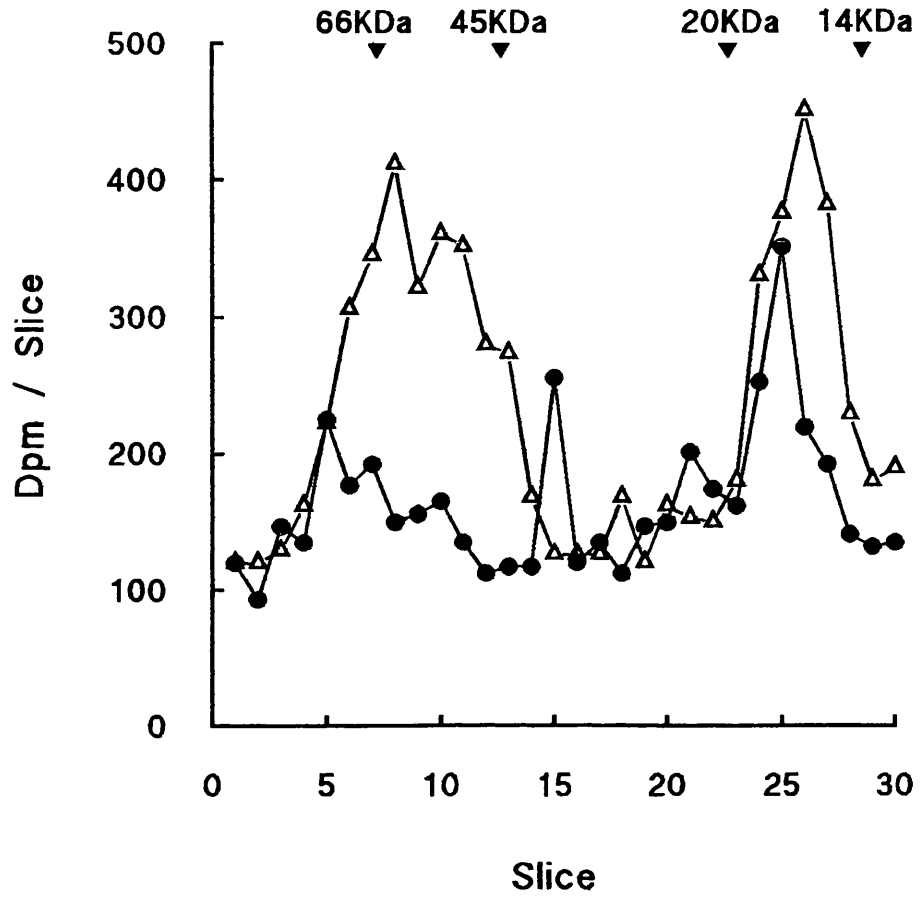

Fig. 16. Immunoprecipitation of trypsin-treated ATB-BMPA labelled erythrocyte glucose transporters. Erythrocyte membranes (1 mg/ml) were labelled with ATB-[2-^{3}H]BMPA then treated with trypsin (100 u/ml) for 30 min at 20 °C. The trypsin was removed by washing in phosphate buffer then the membranes were solubilized in 0.5 % Mega 10 detergent buffer and subjected to immunoprecipitation with anti-GLUT1 antibodies bound to protein A-Sepharose. The immunopellet (●) and the supernatant (Δ) were analysed by electrophoresis on a 12 % acrylamide gel.

peptide antibodies attached to protein A-Sepharose. Both the immunoprecipitated protein and the protein left in the supernatant were analysed by 12 % SDS-PAGE (Fig. 16). The labelled 45-66 kDa peak corresponding to the transporter that still retains most or all of its structure and the C-terminal 18 kDa labelled fragment that has lost its N-terminal half are shown. Approximately 50 % of the ATB-BMPA labelled transporter was converted to the labelled 18 kDa fragment. A large percentage (82 %) of the 45-66 kDa glucose transporter peak was still in the supernatant. If this is compared to the 36 % for the non-treated glucose transporter (Fig. 14) then the result suggests that some of the glucose transporter must lack its C-terminal (antibody binding fragment). There was also a small amount (35 %) of the 18 kDa fragment immunoprecipitated on the antibody pellet suggesting that some of the 18 kDa fragment still retained its C-terminal. Therefore, the two regions of GLUT1 in which trypsin cleaves (the central loop and cytoplasmic C-terminal) do not appear to vary markedly in their susceptibility to trypsin cleavage.

3.2.7. Effect of ATB-BMPA Labelling on Trypsin Cleavage of the Erythrocyte Glucose transporter

Proteolysis by trypsin was used to investigate the conformational changes involved when the erythrocyte glucose transporter bound the outside-specific ligand ATB-BMPA. The erythrocyte glucose transporter was labelled with ATB-BMPA and the resulting membranes were treated with trypsin. Approximately 50 % of the labelled transporter was converted to the 18 kDa fragment (Fig. 16). The unlabelled glucose transporter was treated with trypsin (under identical incubation conditions as

those used for the labelled transporter) and then the resulting fragments were labelled with ATB-BMPA. In this case, virtually all the glucose transporters were cleaved to give an 18 kDa peak (Fig. 17). ATB-BMPA labelling of the trypsin fragment was also fully displaced with 300 mM D-glucose (Fig. 17). Therefore labelling of the glucose transporter with the outside binding ligand ATB-BMPA makes it more resistant to cleavage by trypsin.

3.2.8. Effect of ATB-BMPA and Cytochalasin B Labelling on Thermolysin Cleavage of the Erythrocyte Glucose Transporter

Proteolysis by thermolysin was also used to investigate conformational changes involved when ligands bind to the internal and external surface of the erythrocyte glucose transporter. Erythrocyte membranes were labelled with the exofacial ligand ATB-BMPA and with cytochalasin B which binds to the inside binding site. The labelled membranes were then treated with thermolysin which cleaves proteins on the amino side of hydrophobic residues. Thermolysin (0.4 units/ml) cleaved cytochalasin B labelled membranes giving almost total conversion to a labelled 18 kDa fragment (Fig. 18). Treatment of ATB-BMPA labelled membranes with 6 times as much thermolysin (2.4 units/ml) resulted in no cleavage of the transporter (Fig. 18).

When the thermolysin treated ATB-BMPA labelled membranes were immunoprecipitated with anti-C terminal peptide antibodies, all the labelled transporter was found on the immunopellet leaving virtually none in the supernatant (Fig. 19). As the ATB-BMPA labelled glucose transporter was fully immunoprecipitated after thermolysin treatment, it must still retain its C-terminal segment.

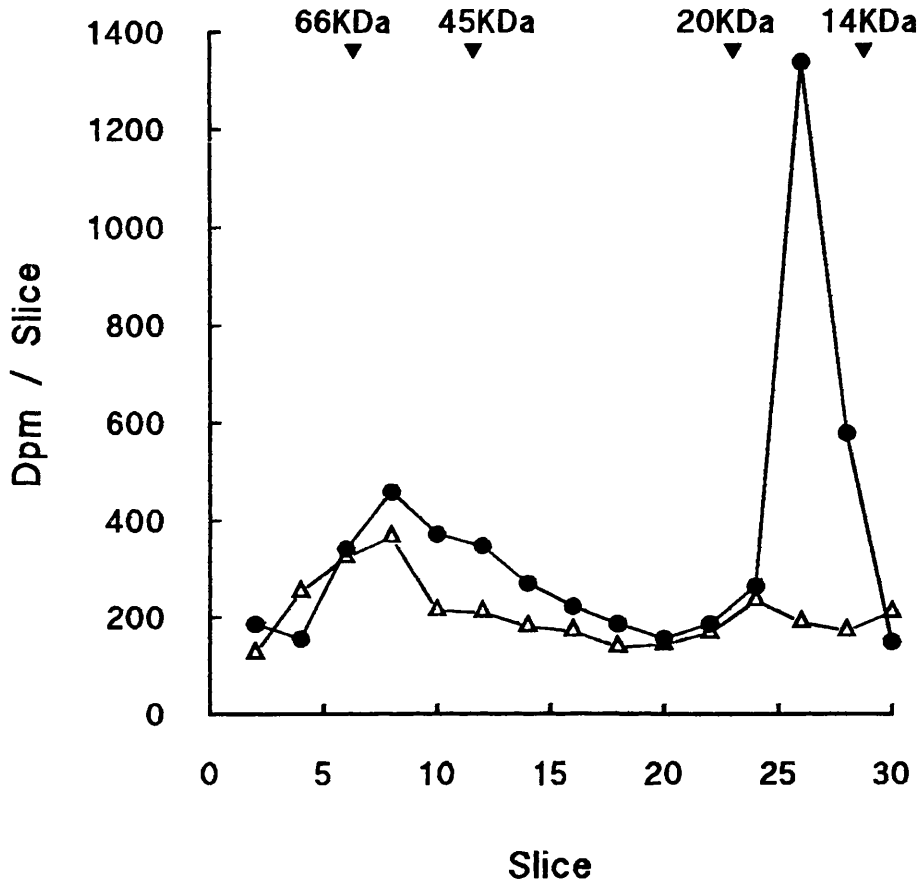

Fig. 17. Trypsin treatment of erythrocyte membranes followed by photolabelling with ATB-BMPA. Erythrocyte membranes (1 mg/ml) were treated with trypsin (100 u/ml) for 30 min at 20 °C. The trypsin was removed by washing in phosphate buffer then the membranes were labelled with ATB-[2-^{3}H]BMPA in the presence of 300 mM D-glucose (△) or 300 mM D-mannitol (●). The membranes were washed in phosphate buffer then analysed by electrophoresis on a 12 % acrylamide gel.

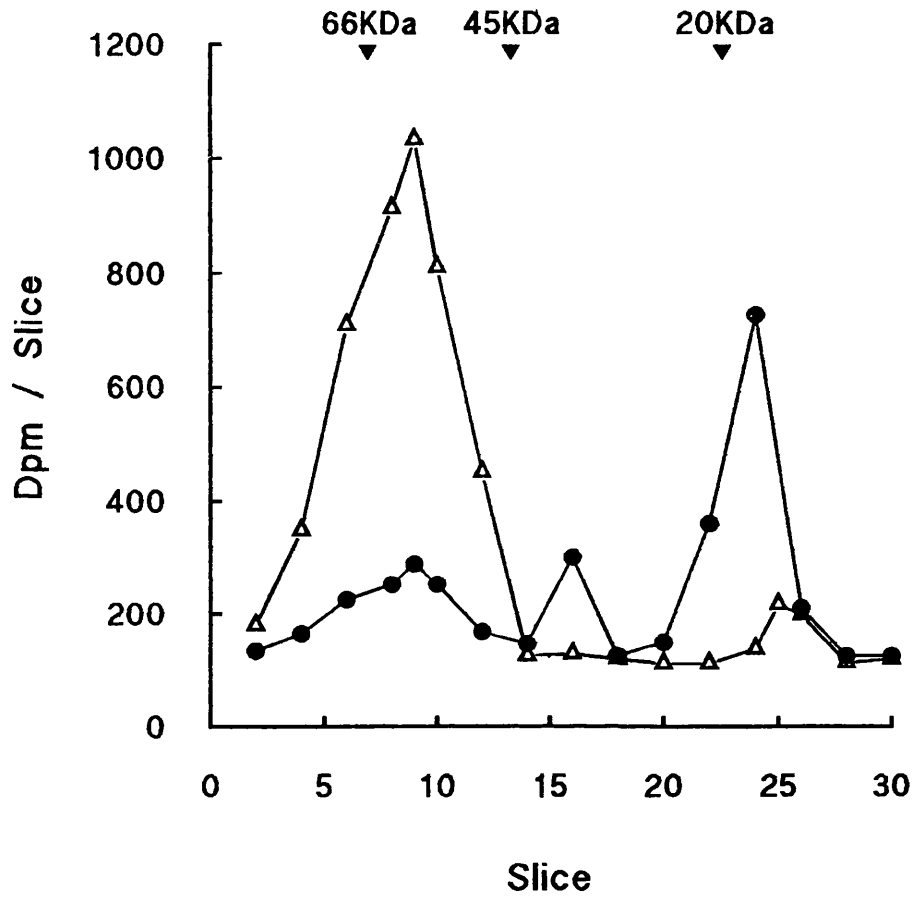

Fig. 18. Thermolysin treatment of labelled erythrocyte membranes. Erythrocyte membranes (300 μg) were labelled with either 30 μCi of ATB-[2-^{3}H]BMPA and treated with 2.4 units/ml of thermolysin (△) or with 1.6 μCi of [^{3}H]cytochalasin B in the presence of 100 μM cytochalasin E and treated with 0.4 units/ml of thermolysin (●) for 30 min at 20 °C. Thermolysin was removed by washing the membranes in phosphate buffer with 27 mM EDTA, then the samples were analysed by electrophoresis on a 12 % acrylamide gel.

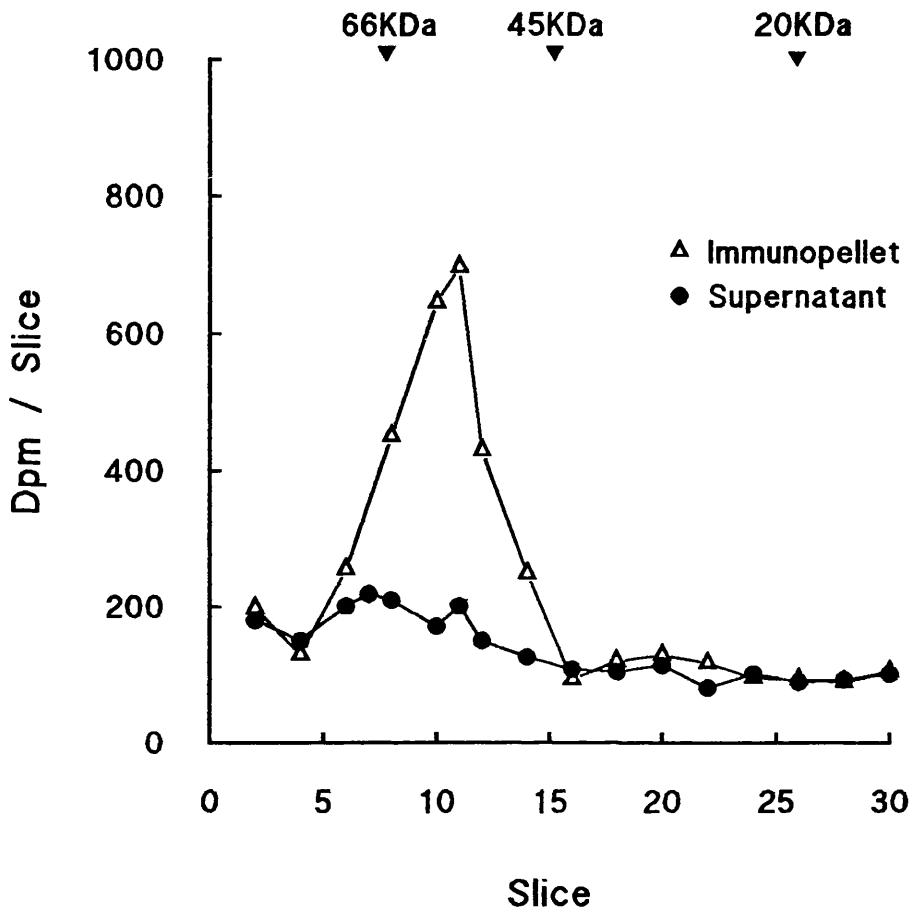

Fig. 19. Immunoprecipitation of thermolysin-treated ATB-BMPA-labelled erythrocyte glucose transporters. Erythrocyte membranes (1 mg/ml) were labelled with ATB-[2-^{3}H]BMPA then treated with 2.4 units/ml of thermolysin for 30 min at 20 °C. After washing in phosphate buffer with 27 mM EDTA, the membranes were solubilized in 0.5 % Mega 10 detergent buffer and immunoprecipitated with purified GLUT1 antibody attached to protein A-Sepharose for 1 hr at 0-4 °C. The immunopellet (Δ) was washed and analysed along with the supernatant (●) by electrophoresis on a 12 % acrylamide gel.

Therefore, binding of ATB-BMPA to the glucose transporter must stabilize a conformation that is resistant to thermolysin cleavage at both the cytoplasmic loop and the C-terminal cleavage sites. In comparison, binding of the inside ligand seems to stabilize a conformation that is very susceptible to thermolysin cleavage. Therefore the inside and outside ligands must be stabilizing different conformations of the glucose transporter protein.

3.2.9. Affinity of the Native and Trypsin-Treated Glucose Transporter for ATB-BMPA

The affinity of the native glucose transporter and the trypsin produced 18 kDa fragment for the external ligand ATB-BMPA were compared. Erythrocyte membranes were labelled with ATB-BMPA without trypsin treatment (Fig. 11) and after trypsin treatment (Fig. 17). Trypsin treated membranes showed 10-12 fold less labelling (2 experiments), which suggests that the affinity for ATB-BMPA is markedly reduced in the trypsin fragment.

3.2.10. Investigation of D-Glucose Displacement of ATB-BMPA in The Native Glucose Transporter and in the 18 kDa Trypsin Fragment

In order to further investigate the differences in the native glucose transporter and the 18 kDa trypsin fragment, the displacement of the exofacial ligand ATB-BMPA

by the substrate for the transporter (D-glucose) was investigated. Native and trypsin-treated erythrocyte membranes were labelled with ATB-BMPA in the presence of 0-100 mM D-glucose or 50 μM cytochalasin B. The membranes were collected and separated on 10-12 % gels.

Fig. 20 shows the gel profile for the native transporter. Labelling was completely displaced by 50 μM cytochalasin B, whereas some labelling was still obtained even in the presence of 100 mM D-glucose. The ratio of the areas of the photolabelled peaks obtained in the presence and absence of D-glucose (A/A_0) were plotted against the D-glucose concentration (Fig. 22), giving a K_i of about 10 mM. This could be due to D-glucose combining with two sites (curve 2) or a single site (curve 3).

Glucose displacement of labelling of the intact transporter was then compared with the displacement by D-glucose of ATB-BMPA labelling of the trypsin fragment (Fig. 21). With the trypsin fragment, a much lower concentration of D-glucose was needed to fully displace all the ATB-BMPA labelling. 10 mM D-glucose gave virtually total displacement of labelling, resulting in a gel profile similar to that of 50 μM cytochalasin B. When we plotted A/A_0 against D-glucose concentration for the trypsin fragment a K_i of about 1.5 mM was obtained (Fig. 22). This apparent increase in the affinity of the trypsin fragment for glucose may be associated, at least in part, with the decrease in affinity for ATB-BMPA that was observed (section 3.2.9.).

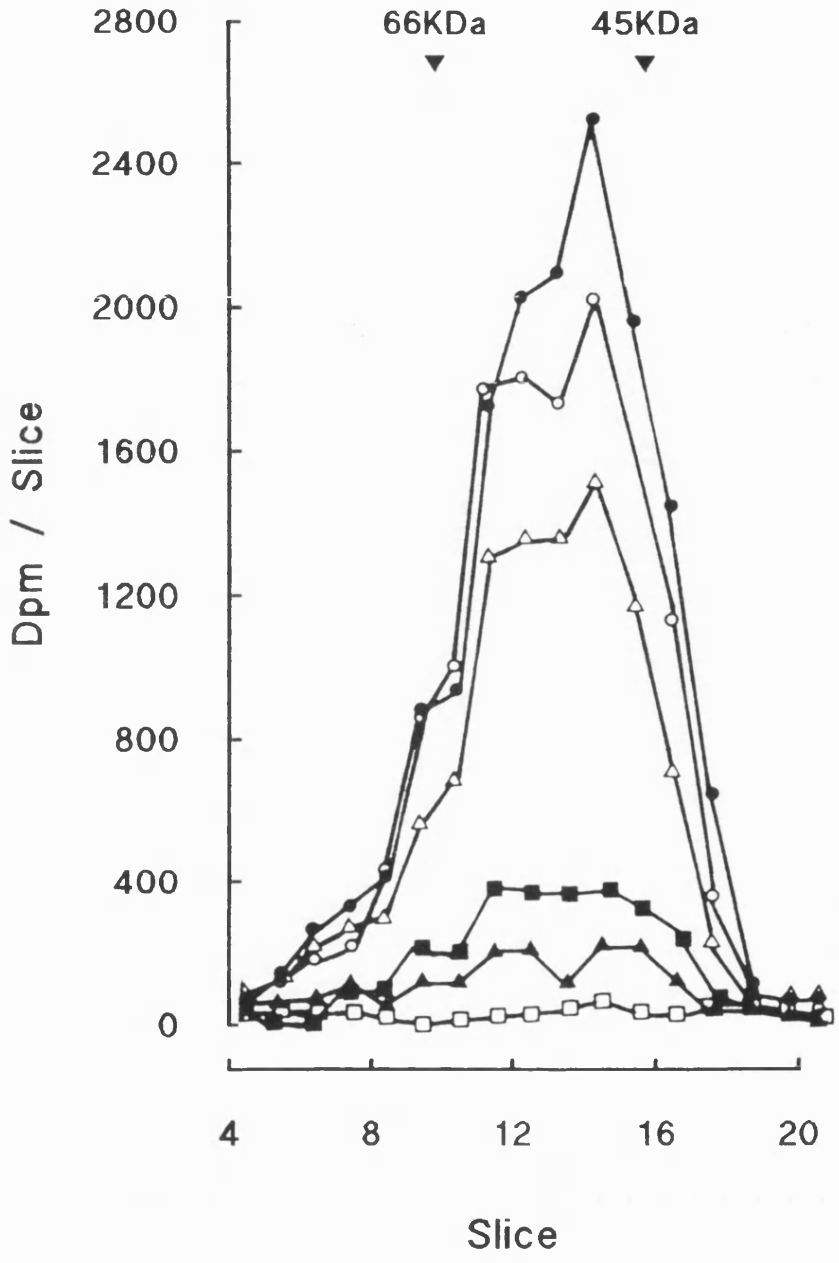

Fig. 20. Displacement of ATB-BMPA labelling of the erythrocyte glucose transporter by D-glucose. Intact erythrocytes were labelled with ATB-[2-^{3}H]BMPA in the absence of D-glucose (●) and at 1 mM (○), 5 mM (△), 25 mM (■) and 100 mM (▲) D-glucose. Labelling was also determined in the presence of 50 μM cytochalasin B (□). Erythrocyte membranes were obtained by osmotic lysis and analysed by electrophoresis.

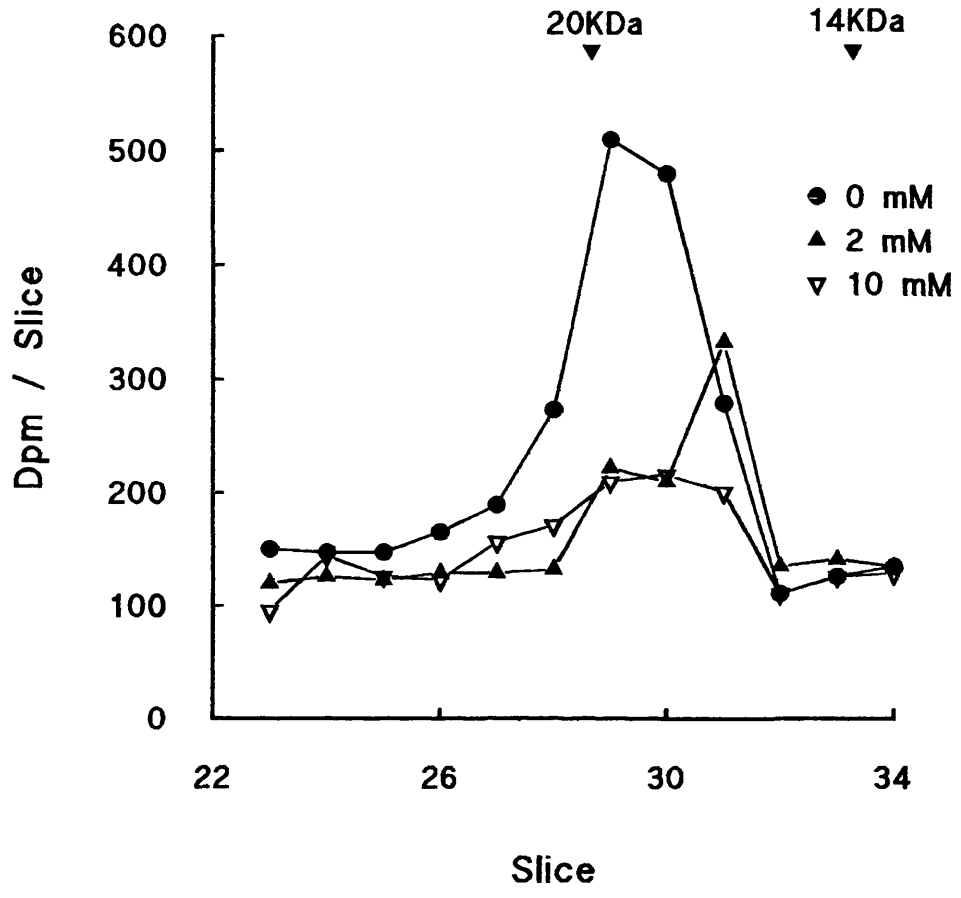

Fig. 21. Displacement of ATB-BMPA labelling of the trypsin fragment by D-glucose. Erythrocyte membranes were treated with trypsin (100 u/ml) for 30 min at 20 °C then labelled with ATB-[2-^{3}H]BMPA in the presence of 0 mM (●), 2 mM (▲) or 10 mM (▽) D-glucose or 50 μM cytochalasin B. The membranes were washed in phosphate buffer then analysed by electrophoresis on a 12 % acrylamide gel.

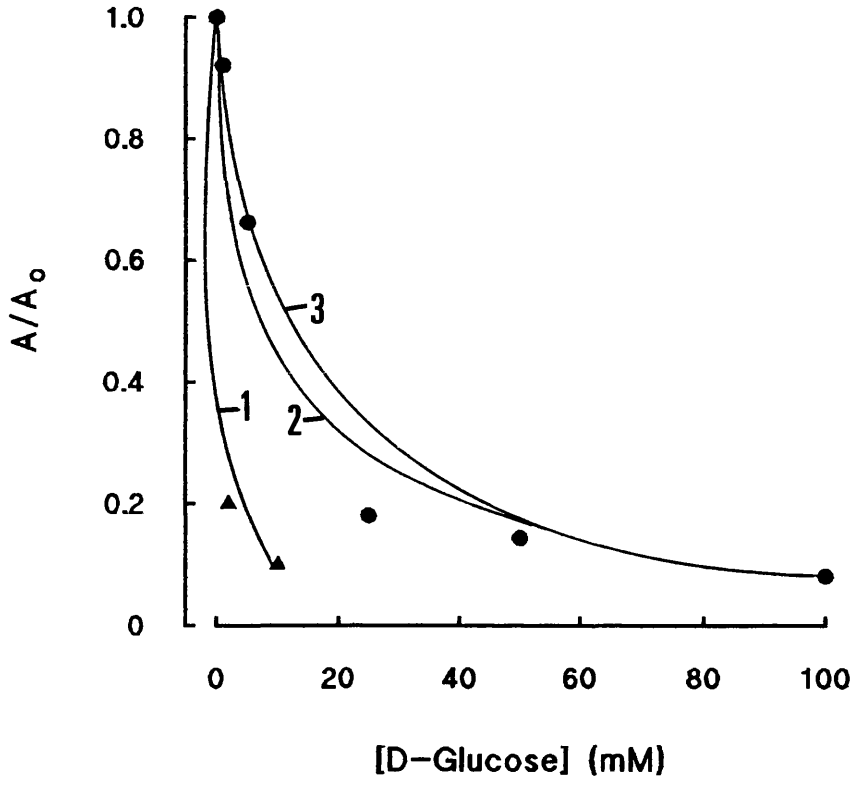

Fig. 22. Displacement by D-glucose of ATB-BMPA labelling to the native and trypsin-treated glucose transporter. A comparison of D-glucose displacement of ATB-BMPA from the native transporter and from the trypsin fragment (Figs 20 & 21). The ratio of the areas of the photolabelled peaks obtained in the presence and absence of D-glucose (A/A_o) was plotted against the D-glucose concentration. The ATB-BMPA labelling that was not displaced by cytochalasin B was subtracted. Displacement by D-glucose of ATB-BMPA labelling of the intact transporter (●) gave a K_i of 10 mM when results were fitted to the equation $A/A_o = K_i/(K_i+G)$ where G is the D-glucose concentration. Displacement of ATB-BMPA from the trypsin fragment (▲) gave a K_i of about 1.5 mM [curve 1, $A/A_o = 1.5/(1.5+G)$]. Curve 2 was obtained from the equation for a two-site model:
$A/A_o = ½[1.5/(1.5+G)] + ½[26/(26+G)]$. Curve 3 was obtained from the single-site model [$A/A_o = 10/(10+G)$].

3.2.11. NTCB Cleavage of the ATB-BMPA-Labelled Purified Glucose Transporter

Treatment of proteins with NTCB followed by incubation at alkaline pH results in cleavage of proteins at cysteines (Cairns *et al*, 1984). The erythrocyte (GLUT1) glucose transporter sequence contains 6 cysteine residues (Mueckler *et al*, 1985). Fig. 23 shows the location of the 6 cysteines in GLUT1 and the potential NTCB cleavage fragments. The NTCB treatment was carried out in a buffer containing 1.7 % SDS, which would at least partially denature the glucose transporter protein and so allow cleavage of the cysteines buried within the transmembrane segments. The ATB-BMPA labelled, purified glucose transporter was chosen for use in these experiments, as it was a much more concentrated source of labelled glucose transporters than erythrocyte membranes. NTCB treatment of erythrocyte membranes resulted in similar fragmentation patterns to those seen with the purified glucose transporter (results not shown).

The ATB-BMPA labelled glucose transporter was treated with NTCB and then the resultant fragments were immunoprecipitated by antibodies to the GLUT1 C-terminal and the GLUT1 cytoplasmic loop (residues 231-246). NTCB treatment produced a number of ATB-BMPA labelled fragments (Fig. 24) of approximate molecular weight: 6 kDa, 14 kDa, 23 kDa, 29 kDa and 50 kDa. The cytoplasmic loop antibody immunoprecipitated ATB-BMPA labelled fragments of approximate molecular weight: 14 kDa, 23 kDa, 29 kDa and 50 kDa. The anti-C-terminal antibody immunoprecipitated ATB-BMPA labelled fragments of approximate molecular weight: 14 kDa, 29 kDa and 50 kDa.

Therefore, a 6 kDa fragment labelled by ATB-BMPA was not immuno-precipitated by either the C-terminal or loop antibodies. As ATB-BMPA has already

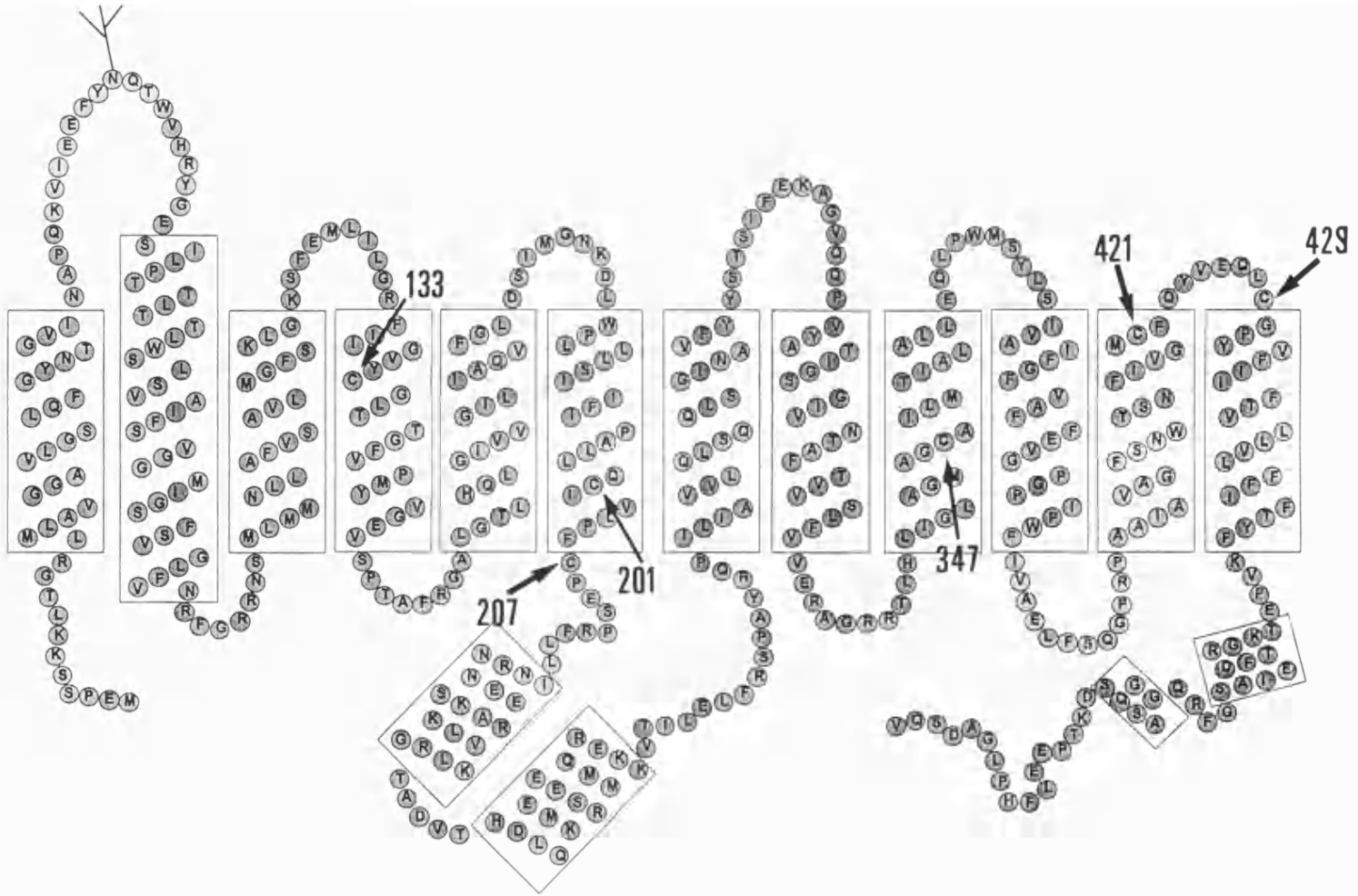

Fig. 23. Location of the six cysteines in GLUT1. The GLUT1 amino acid sequence contains six cysteines (Mueckler *et al*, 1985). The location of the six cysteines in the putative two-dimensional model of GLUT1 (Proposed by Mueckler *et al*, 1985) are shown.

been shown to bind to the C-terminal half of the glucose transporter (section 3.2.6.), the only possible fragment is that produced by cleavage at cysteines 347 and 421 or 429, comprising the top half of TM9, TM10 and most of TM11. A labelled 14 kDa fragment was immunoprecipitated by both antibodies. The C-terminal antibody must be immunoprecipitating the fragment from the C-terminal to cysteine 347, which would locate the site of ATB-BMPA labelling to somewhere in TM9 to TM12. However the loop antibody must be immunoprecipitating the fragment produced by cleavage at cysteines 201 or 207 and 347, suggesting that there is also extensive labelling somewhere between TM6 and TM9. Therefore, ATB-BMPA may be labelling more than one residue in the C-terminal half of GLUT1. Subsequent studies in collaboration with Baldwins group (Davies *et al*, 1992) suggested that the major site of labelling was TM8.

Fig. 24. NTCB cleavage of the ATB-BMPA labelled, purified glucose transporter. ATB-BMPA labelled, purified erythrocyte glucose transporter (in Tris-acetate buffer, pH 8.0, containing 1.7 % SDS) was gassed with nitrogen then incubated with 10 mM NTCB for 30 min at 37 °C. An equal volume of borate buffer, pH 9.3, was added and the pH adjusted to between pH 9 and 10, then the mixture was incubated for 45 hr at 37 °C, with regular readjustment of the pH back to pH 9 to 10. After addition of 2-mercaptoethanol (30 μl/ml), the mixture was desalted by filtration through a centricon 10 microconcentrator and dilution with 1 mM Tris-HCl, pH 6.8. The mixture was divided into 4, one sample was not immunoprecipitated (Fig. 24a) and three samples were solubilized in 2 % Thesit detergent buffer, then immunoprecipitated with preimmune serum, anti-GLUT1 cytoplasmic loop antibody (Fig. 24b) and anti-GLUT1 C-terminal antibody (Fig. 24c). The resulting labelled peaks were separated by electrophoresis using the Tricine gel system.

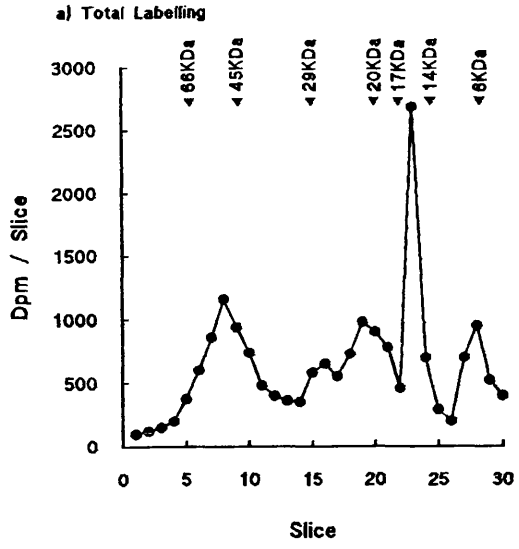
a) Total Labelling
66KDa
45KDa
29KDa
20KDa
17KDa
14KDa
6KDa
Dpm / Slice
3000
2500
2000
1500
1000
500
0
0
5
10
15
20
25
30
Slice

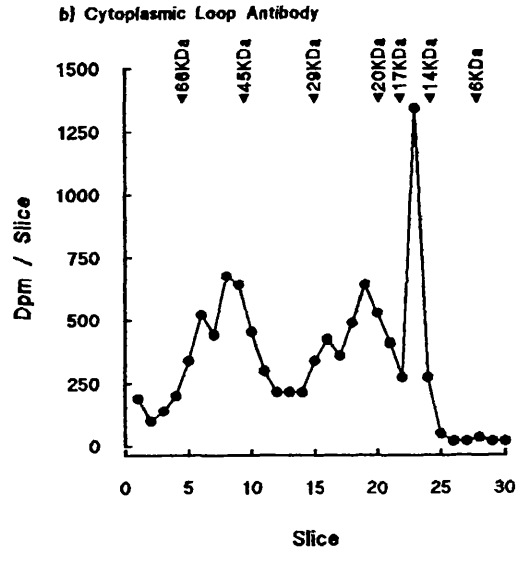
b) Cytoplasmic Loop Antibody
66KDa
45KDa
29KDa
20KDa
17KDa
14KDa
6KDa
Dpm / Slice
1500
1250
1000
750
500
250
0
0
5
10
15
20
25
30
Slice

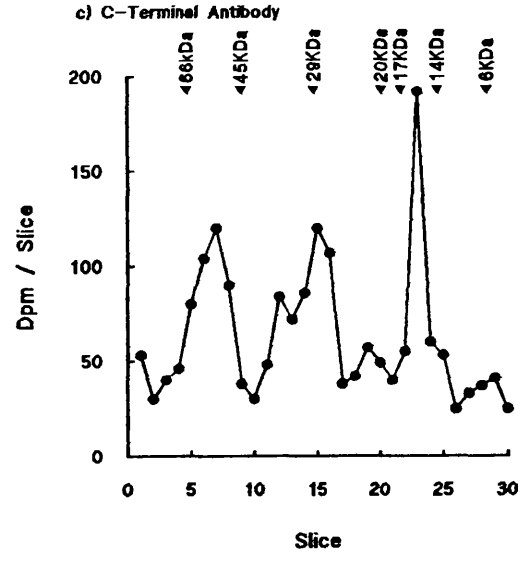
c) C-Terminal Antibody
66KDa
45KDa
29KDa
20KDa
17KDa
14KDa
6KDa
Dpm / Slice
200
150
100
50
0
0
5
10
15
20
25
30
Slice

3.3. Studies on GLUT1 Mutants Expressed In CHO-K1 Cells

This work was done in collaboration with Hashiramoto and colleagues in Kobe, Japan who did all the mutagenesis on GLUT1 and expressed the mutants in CHO-K1 cells. They also carried out some of the transport and labelling studies. The CHO-K1 cell line was chosen because of its low endogenous glucose transport activity (Hasegawa *et al*, 1990). Wild-type and mutant GLUT1 expression levels were monitored by labelling cell-surface carbohydrate with ^{3}H-borohydride and then immunoprecipitating the labelled GLUT1 with anti-GLUT1 antibodies. Glucose transport activity was then compared in the wild-type and mutant clones. In order to investigate whether particular amino acid residues are involved in the binding of ligands or in the changes in conformation of GLUT1, binding of the external ligand, ATB-BMPA and the internal ligand, cytochalasin B to the mutant glucose transporters were compared. ATB-BMPA is known to bind to the external surface of GLUT1 in the region of TM8 (Holman & Rees, 1987, Davies *et al*, 1992, section 3.2.11.). Cytochalasin B is thought to bind at the internal surface of the glucose transporter in the region of TM10 and TM11 (Holman & Rees, 1987, Davies *et al*, 1992).

3.3.1. Mutation of Asparagine and Glutamine Residues in Transmembrane Segments 7 and 8

Sequence alignment of the glucose transporter sequences (Dr P. Hodgson, University of Bath) has shown that asparagine and glutamine residues are highly conserved and so may therefore be important for glucose transporter structure and

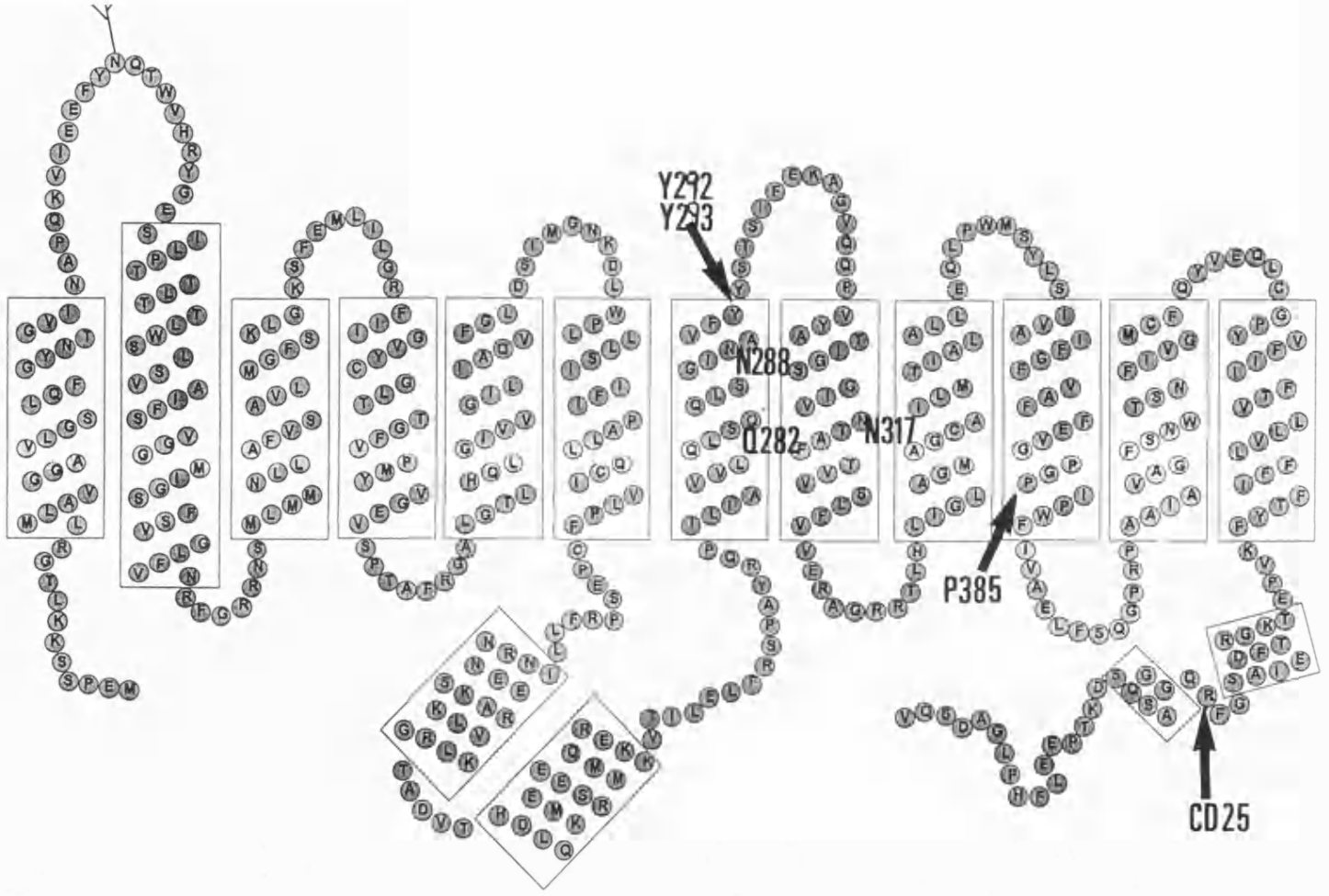

Fig. 25. Location of the residues in GLUT1 that have been investigated by site-directed mutagenesis. The location in the putative two-dimensional membrane topology of GLUT1 (proposed by Mueckler *et al*, 1985) of Gln282, Asn288, Asn317, Tyr292, Tyr293 and Pro385. Also the 25th amino acid from the C-terminal of GLUT1 is shown.

function. Since asparagine (Asn) and glutamine (Gln) residues can participate in hydrogen bonding to sugars (Quiocho, 1986), they may form part of a channel through the protein. Substitutions at glutamine 282 and asparagine 288, which are predicted to occur in TM7 and at asparagine 317, which is predicted to occur in TM8, (Fig. 25) were investigated to determine whether any of these residues were important for glucose transporter structure and function. The amide residues were substituted with the aliphatic residues, leucine (Leu) and isoleucine (Ile) which could not participate in hydrogen bonding.

The results are shown in table 4. Although borohydride labelling of CHO-K1 cells labels any cell-surface exposed carbohydrate, the anti-GLUT1 antibody was specific enough to immunoprecipitate only the GLUT1 glucose transporter (Fig. 26). All 3 mutants (Gln282-Leu, Asn288-Ile, Asn317-Ile) could be detected at the cell surface of CHO-K1 cells by borohydride labelling to a level comparable to that of wild-type GLUT1. Labelling in the Gln282-Leu, Asn288-Ile and Asn317-Ile clones was 97 ± 14.8 % (n=4), 57.7 % (n=2) and 166 ± 32 % (n=4) of the wild-type level, respectively. Non-transfected CHO-K1 cells showed levels of endogenous GLUT1 that were only approximately 5 % of the labelling found in the wild-type clone (Fig. 26).

Uptake of 2-deoxy-D-glucose was measured in the wild-type and mutant clones. The wild-type clone had a large increase (5.2-fold) in transport activity compared to non-transfected CHO-K1 cells. Glucose transport activity in each of the mutant clones, Gln282-Leu, Asn288-Ile and Asn317-Ile was comparable to activity in the wild-type clone and was 92.2 ± 6.1, 51.0 ± 3.8 and 70.0 ± 16.1 % (n=5) of the wild-type value, respectively.

Transport activity in the wild-type and Gln282-Leu mutant was further

Experiment	wild-type	Q282L	N288I	N317I
Transport Activity	100	92.2±6.1 (n=5)	51±3.8 (n=5)	70±16.1 (n=5)
Borohydride Labelling	100	97.0±14.8 (n=4)	57.7 (57,58.4)	166±32 (n=4)
Cytochalasin B Labelling	100	55.5±9.4 (n=4)	184 (202,166)	55.2±3.4 (n=4)
ATB-BMPA Labelling	100	5	43.9 (34,53)	113 (100,127)

Table 4. Transport activity and labelling levels in wild-type, asparagine mutant and glutamine mutant clones. All values are expressed as the percentage of the level in the wild-type clone. The results are the mean ± S.E.M. from 4-5 experiments, except where the mean of 2 results is shown followed by the individual values.

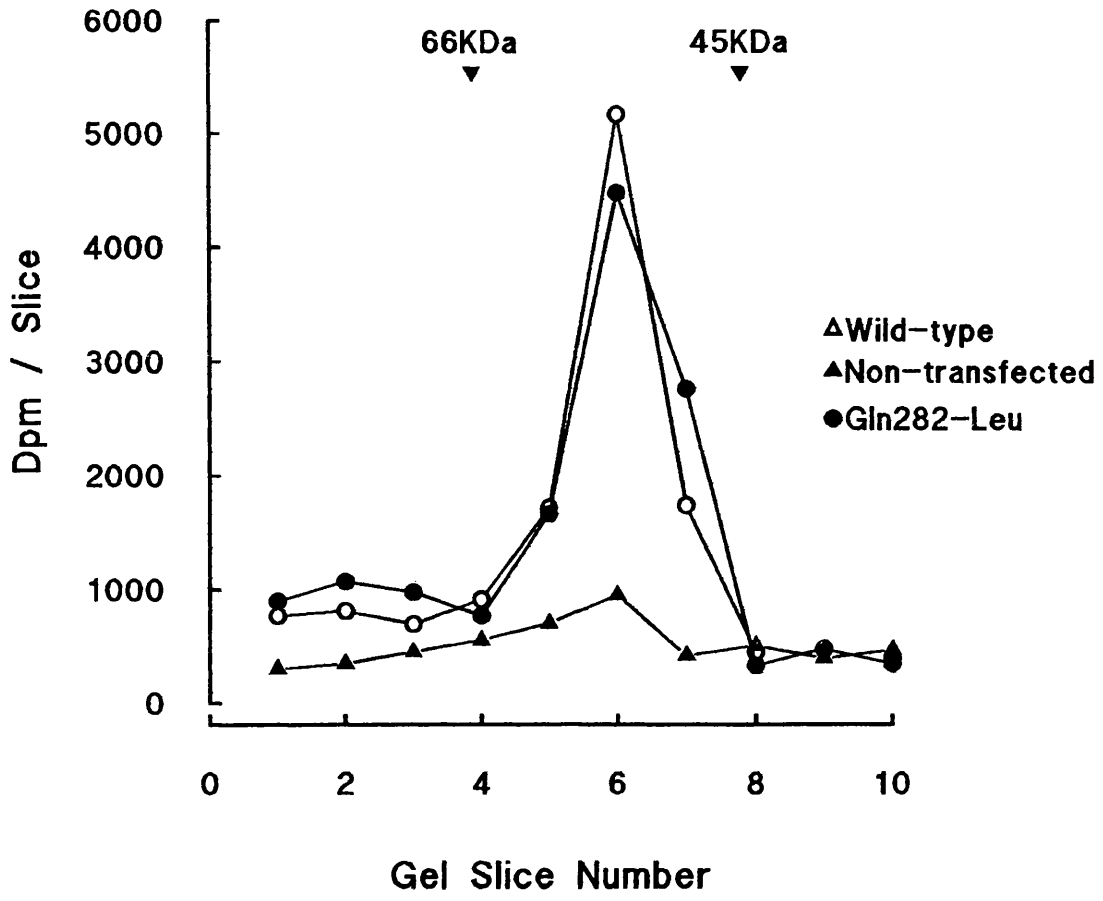

Fig. 26. Immunoprecipitation of borohydride-labelled GLUT1 in non-transfected, wild-type and Gln282-Leu CHO-K1 clones. Cells of the wild-type (○), Gln282-Leu (●) and non-transfected CHO-K1 (▲) clones were grown to confluence in 35 mm culture dishes. Cells were treated with 10 units of galactose oxidase and 1 unit of neuraminidase in 1 ml of PBS for 30 min at 18 °C. After washing in PBS, the cells were incubated with 2 mCi of tritiated sodium borohydride in 1 ml PBS for 10 min. After washing in PBS, the cells were solubilized in 2 % Thesit detergent buffer and immunoprecipitated with anti-GLUT1 antibody. The immunoprecipitates were then analysed by electrophoresis on a 10 % acrylamide gel.

investigated and they were found to have similar K_m and V_{max} values for 2-deoxy-D-glucose net influx. The K_m and V_{max} values calculated from these data were 1.83 ± 0.2 mM and 1458 ± 97 pmol/min/mg of protein for the wild-type and 1.07 ± 0.38 mM and 735 ± 136 pmol/min/mg of protein for the Gln282-Leu clone, respectively (Fig. 27). Thus at low concentrations of substrate, where the transport rate constant is equal to V_{max}/K_m, the wild-type and Gln282-Leu values are similar (the V_{max}/K_m ratios were 0.8 and 0.69 nmol/min/mg of protein/mM for the wild-type and Gln282-Leu cells, respectively). Some nonlinearity was observed in the reciprocal kinetic plot of 2-deoxy-D-glucose transport in the Gln282-Leu mutant, and at high substrate concentrations this mutated transporter showed approximately 2-fold slower net influx.

Binding of the internal ligand cytochalasin B was then examined. All three mutants were able to bind cytochalasin B giving labelling significantly greater than that in non-transfected cells. The mutants, Gln282-Leu, Asn288-Ile and Asn317-Ile, showed levels of labelling that were 55.5 ± 9.4 % (n=4), 184 % (n=2) and 55.2 ± 3.4 % (n=4) of wild-type levels, respectively (Fig. 28). Therefore, substitution of leucine for glutamine 282 and isoleucine for asparagine 288 and 317 did not greatly perturb binding of cytochalasin B to the inside site of the glucose transporter.

The two asparagine mutants both bound the external ligand ATB-BMPA, giving levels of labelling that were comparable to the labelling seen in the wild-type clone (Fig. 29). However the Gln282-Leu mutant showed very little labelling by ATB-BMPA, the labelling being only approximately 5 % of the wild-type level and similar to that of non-transfected cells. This result suggests that glutamine 282 is important for binding of ligands to the outside site.

To further investigate this inability of the Gln282-Leu mutant to bind outside site-specific ligands, we examined the ability of 4,6-O-ethylidene-D-glucose, which

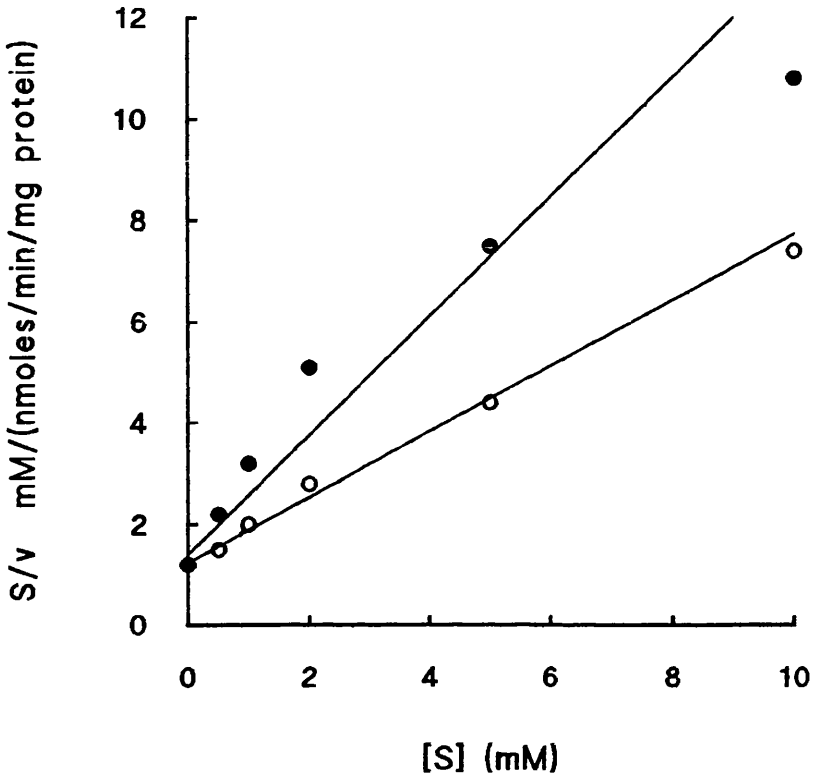

Fig. 27. 2-Deoxy-D-glucose net uptake in wild-type and Gln282-Leu mutant GLUT1 clones. Cells of the wild-type (○) and Gln282-Leu (●) clones were grown to confluence in 35 mm culture dishes. The net uptake of 2-deoxy-D-[2,6-^{3}H]glucose was measured for 1 min at the indicated extracellular concentrations. Results shown are from a single experiment representative of two similar experiments. K_m and V_{max} values were determined by nonlinear regression (weighted for relative error) of the Michaelis-Menten equation. The K_m and V_{max} values calculated from these data were 1.83 ± 0.2 mM and 1458 ± 97 pmol/min/mg of protein for the wild-type and 1.07 ± 0.38 mM and 735 ± 136 pmol/min/mg of protein for the Gln282-Leu cells.

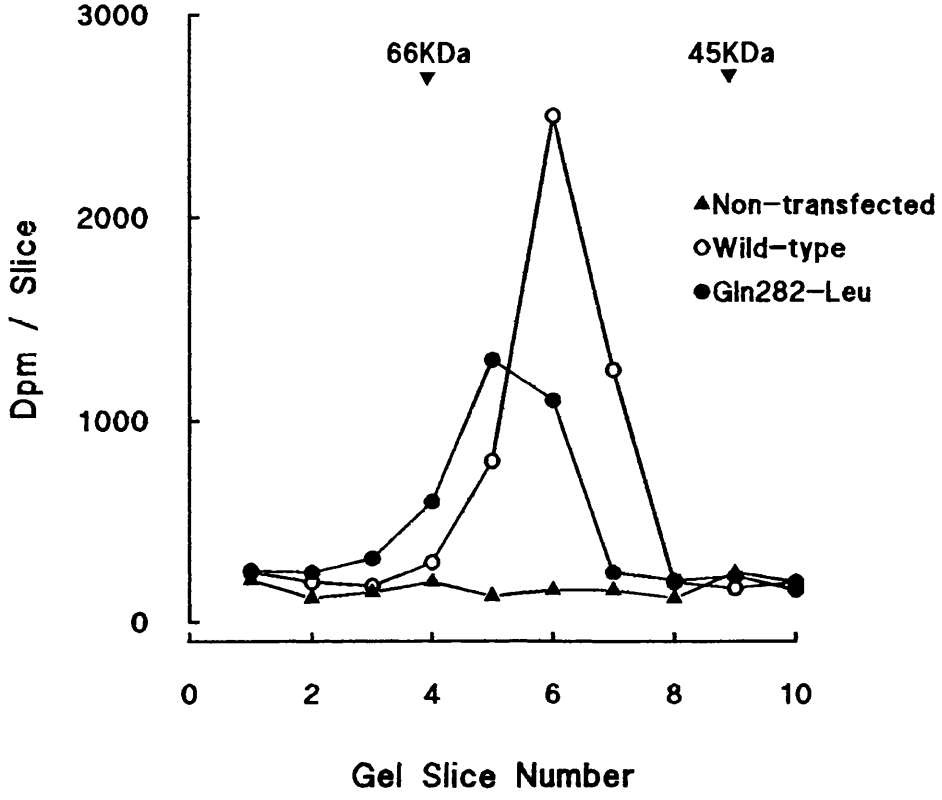

Fig. 28. Cytochalasin B labelling of GLUT1 in non-transfected, wild-type and Gln282-Leu CHO-K1 clones. Cells of the wild-type (○), Gln282-Leu (●) and non-transfected CHO-K1 (▲) clones were grown to confluence in 90 mm culture dishes and then fractionated to yield a crude plasma membrane fraction. 200 μg of plasma membranes in 400 μl of TES and 100 μM cytochalasin E were labelled with 1.4 μCi of [4-^{3}H]cytochalasin B by irradiation. The membranes were washed twice and then analysed by electrophoresis on a 10 % acrylamide gel.

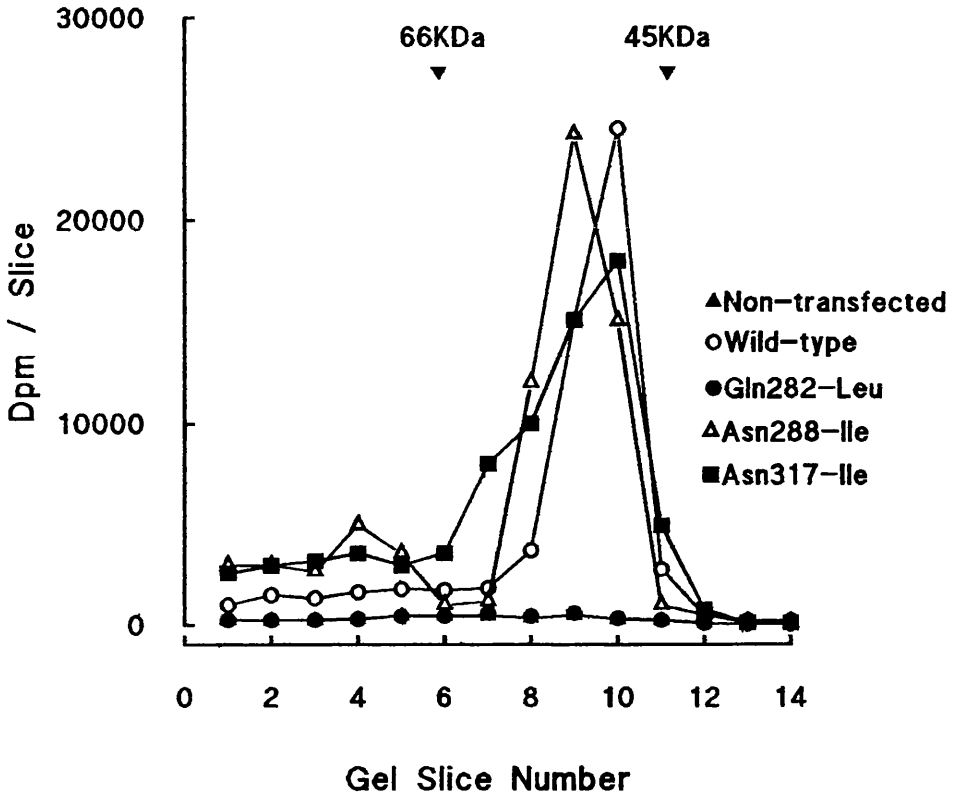

Fig. 29. ATB-BMPA labelling of GLUT1 in non-transfected, wild-type and mutant CHO-K1 clones. Cells of the wild-type (○), Gln282-Leu (●), Asn288-Ile (△), Asn317-Ile (■) and non-transfected CHO-K1 (▲) clones were grown to confluence in 35 mm culture dishes. Cells were labelled with 100 μCi of ATB-[2-^{3}H]BMPA in 250 μl of PBS at 18 °C by irradiation. After washing five times in PBS, the cells were solubilized in 2 % Thesit detergent buffer and precipitated with chloroform/methanol. The precipitates were then analysed by electrophoresis on a 10 % acrylamide gel.

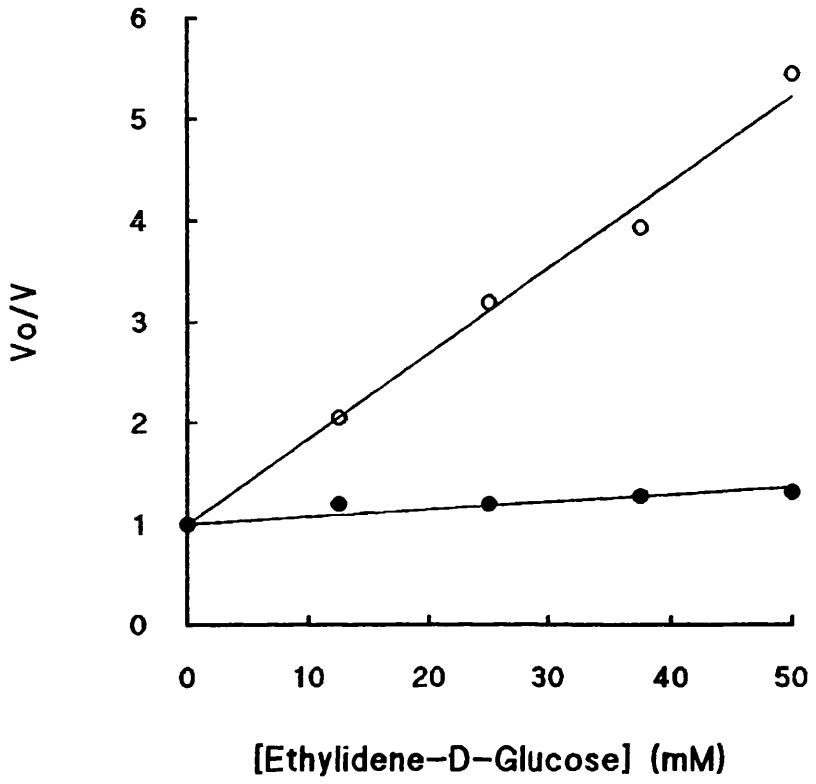

Fig. 30. 4,6-O-ethylidene-D-glucose inhibition of transport activity in wild-type and Gln282-Leu mutant GLUT1 clones. Cells of the wild-type (○) and Gln282-Leu (●) clones were grown to confluence in 35 mm culture dishes. The net uptake of 2-deoxy-D-[2,6-^{3}H]glucose was measured for 10 min at the indicated concentrations of 4,6-O-ethylidene-D-glucose. Results shown are from a single experiment representative of two similar experiments. The K_i was determined by nonlinear regression (weighted for relative error) of the equation $V/V_o = K_i/(K_i + I)$. The K_i values calculated from these data were 11.7 ± 0.77 mM for the wild-type and 121 ± 20 mM for the Gln282-Leu cells.

binds to the outside site of the glucose transporter, to inhibit 2-deoxy-D-glucose transport. Fig. 30 shows that 4,6-O-ethylidene-D-glucose is a potent inhibitor of transport activity in the wild-type clone, giving an apparent K_i of 11.7 ± 0.77 mM. This value is similar to that reported for the inhibition of glucose transport activity in erythrocytes (Barnett *et al*, 1973a,b), where GLUT1 is the predominant isoform. However, in the Gln282-Leu mutant clone, 4,6-O-ethylidene-D-glucose was a very poor inhibitor of transport and the apparent K_i was increased by 10-fold to 121 ± 20 mM.

3.3.2. Mutation of Tyrosines 292 and 293 in Transmembrane Segment 7

The substitution of leucine for glutamine 282, which is predicted to occur in transmembrane segment 7, has been shown to perturb binding of ligands to the outside binding site of GLUT1 (section 3.3.1.). Therefore, it is thought that TM7 may move up and down in the membrane to accept inside or outside binding ligands. To further investigate the role of TM7, tyrosine's (Tyr) 292 and 293 which are predicted to occur at the top of TM7 (Fig. 25), were substituted with the aromatic residue, phenylalanine (Phe) and the aliphatic residue, isoleucine (Ile). The motif Q^{282}QXSGXNXXXYY^{293} is present in all mammalian glucose transporters and is highly conserved in members of the wider glucose transporter superfamily.

The results are shown in table 5. All the mutants were found to be expressed at the cell surface to a level comparable to that of wild-type GLUT1. The amount of borohydride-labelled Tyr292-Ile, Tyr293-Ile, Tyr292-Phe and Tyr293-Phe mutant GLUT1 was 131.9 ± 31.0 % (n=4), 112.7 ± 29.7 % (n=4), 133.5 ± 5.7 % (n=4)

Experiment	wild-type	Y292I	Y293I	Y292F	Y293F
Transport Activity	100	73.8±4.7 (n=5)	15.0±3.4 (n=5)	55.8±4.8 (n=5)	89.2±6.1 (n=5)
Borohydride Labelling	100	132±31 (n=4)	113±30 (n=4)	134±6 (n=4)	137±19 (n=4)
Cytochalasin B Labelling	100	53.8±7.3 (n=4)	4.5±2.1 (n=4)	104±8 (n=4)	107±8 (n=4)
ATB-BMPA Labelling	100	119±16 (n=3)	126±35 (n=3)	148±61 (n=3)	106±27 (n=3)

Table 5. Transport activity and labelling levels in wild-type and tyrosine mutant clones. All values are expressed as the percentage of the level in the wild-type clone. The results are the mean ± S.E.M. from 3-5 experiments.

and 137.3 ± 18.5 % (n=4) of the wild-type level, respectively.

The uptake of 2-deoxy-D-glucose was measured in these tyrosine mutants. The Tyr292-Ile, Tyr292-Phe and Tyr293-Phe mutants all retained a high level of transport activity which was 73.8 ± 4.72 % (n=5), 55.8 ± 4.84 % (n=5) and 89.2 ± 6.10 % (n=5) of the wild-type activity, respectively. Substitution of tyrosine 293 for isoleucine resulted in a markedly decreased transport activity which was only 15.0 ± 3.36 % (n=5) of that observed in the wild-type clone and was similar to the transport activity seen in non-transfected CHO-K1 cells (24.4 ± 4.72 % (n=5) of the wild-type clone).

This reduction in transport activity of the Tyr293-Ile mutant was accompanied by an inability to bind the internal ligand. The cytochalasin B labelling in the Tyr293-Ile mutant was only 4.5 ± 2.1 % (n=4) of that of the wild-type clone (Fig. 31) and was comparable to the labelling in the non-transfected CHO-K1 cells (18.2 ± 2.3 % (n=4) of the wild-type clone) (Fig. 31). Cytochalasin B labelling in the other mutants (Tyr292-Ile, Tyr292-Phe and Tyr293-Phe) was comparable to wild-type GLUT1 with levels that were 53.8 ± 7.3 % (n=4), 103.5 ± 8.6 % (n=4) and 107.3 ± 8.1 % (n=4) of wild-type levels, respectively.

Although substitution of tyrosine 293 with isoleucine perturbed binding of the internal ligand, binding of the external ligand ATB-BMPA was unaffected. All four mutants were labelled with ATB-BMPA to a similar extent to the wild-type clone. The levels of ATB-BMPA labelling in the Tyr292-Ile, Tyr293-Ile, Tyr292-Phe and Tyr293-Phe mutants were 118.7 ± 15.8 % (n=3), 126.2 ± 34.9 % (n=3), 147.6 ± 60.7 % (n=3) and 105.8 ± 27.1 % (n=3) of that of the wild-type clone, respectively.

Therefore, substitution of tyrosine 293 with another aromatic residue,

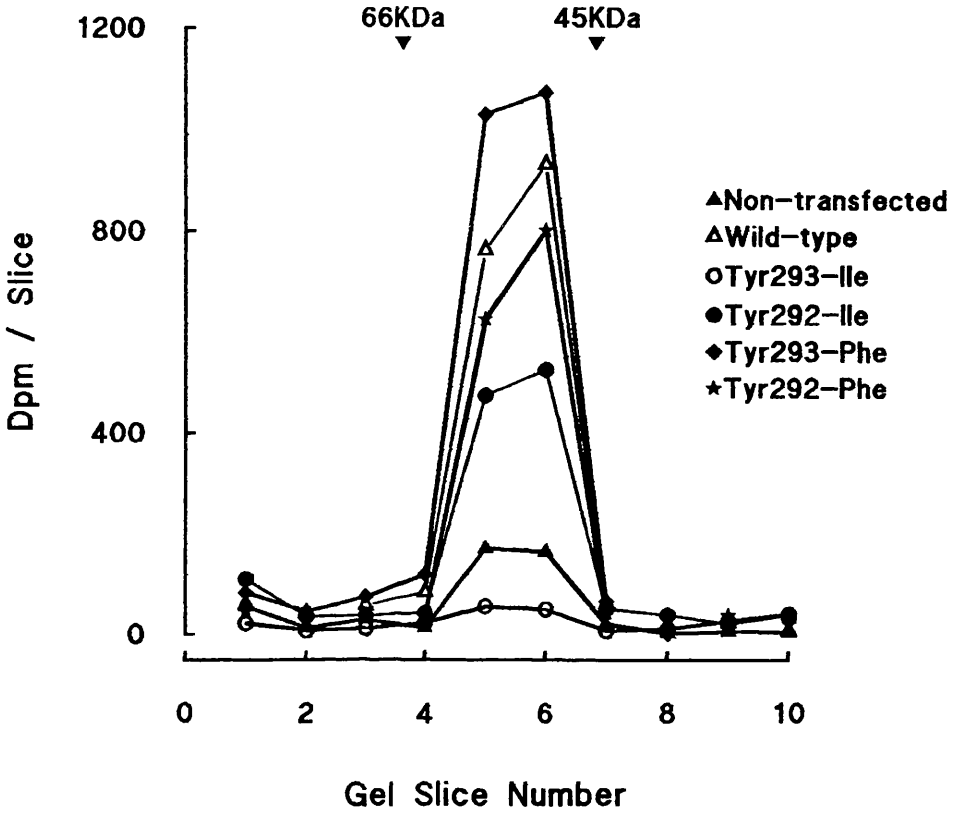

Fig. 31. Cytochalasin B labelling of GLUT1 in non-transfected, wild-type and mutant CHO-K1 clones. Cells of the wild-type (△), Tyr293-Ile (○), Tyr292-Ile (●), Tyr293-Phe (◆), Tyr292-Phe (★) and non-transfected CHO-K1 (▲) clones were grown to confluence in 90 mm culture dishes and then fractionated to yield a crude plasma membrane fraction. 100 μg of plasma membranes in 400 μl of TES and 100 μM cytochalasin E were labelled with 1.4 μCi of [4-^{3}H]cytochalasin B by irradiation. The membranes were washed twice and then analysed by electrophoresis on a 10 % acrylamide gel.

phenylalanine, can be tolerated by GLUT1. Whereas, when it is substituted with the aliphatic residue, isoleucine, 2-deoxy-D-glucose transport activity is markedly decreased and internal ligand binding is perturbed.

3.3.3. Mutation of Proline 385 in Transmembrane Segment 10

Molecular modelling studies suggest that the putative transmembrane segment 10 can undergo remarkably large conformational changes that may alternately expose the hexose binding site to the external and internal solutions (Hodgson, Osguthorpe & Holman, manuscript in preparation). Molecular dynamic simulations suggest that proline 385 in GLUT1 is particularly important in producing a pivotal point for this conformational change (Hodgson, Osguthorpe & Holman, manuscript in preparation). The amino acid motif F^{378}FEVGPGPIPW^{388}, predicted to occur in TM10 (Fig. 25), is present in all mammalian glucose transporters (GLUT's 1, 2, 3, 4 & 7) with some conservative changes in GLUT5. Proline 385 is conserved in all but the SNF3 galactose transporter from *Saccharomyces cerevisiae*, where glycine is present at this position (Celenza *et al*, 1988). The effect of replacing proline 385 in GLUT1 with glycine and isoleucine, on glucose transport activity and external and internal ligand binding was investigated.

The results are shown in table 6. Both the Pro385-Gly and Pro385-Ile GLUT1 mutants were found to be expressed at the cell surface to a level comparable to that of wild-type GLUT1. The amount of borohydride-labelled Pro385-Gly and Pro385-Ile mutant GLUT1 was 82.1 ± 9.4 % (n=4) and 92.6 ± 9.1 % (n=4) of the wild-type level, respectively (Fig. 32).

Experiment	Non-transfected	Wild-type	Pro385-Ile	Pro385-Gly
Transport Activity	25.7 ± 5.3 (n=4)	100	39.5 ± 3.6 (n=4)	121.8 ± 7.6 (n=4)
Borohydride Labelling	9.5 ± 0.3 (n=4)	100	92.6 ± 9.1 (n=4)	82.1 ± 9.4 (n=4)
Cytochalasin B Labelling	19.7 ± 2.9 (n=6)	100	106.2 ± 4.2 (n=6)	146 ± 13.6 (n=6)
ATB-BMPA Labelling	5.8 ± 0.3 (n=4)	100	3.4 ± 0.8 (n=4)	53.5 ± 1.8 (n=4)

Table 6. Transport activity and labelling levels in non-transfected, wild-type and Proline mutant clones. All values are expressed as the percentage of the level in the wild-type clone. The results are the mean ± S.E.M. from 4-6 experiments.

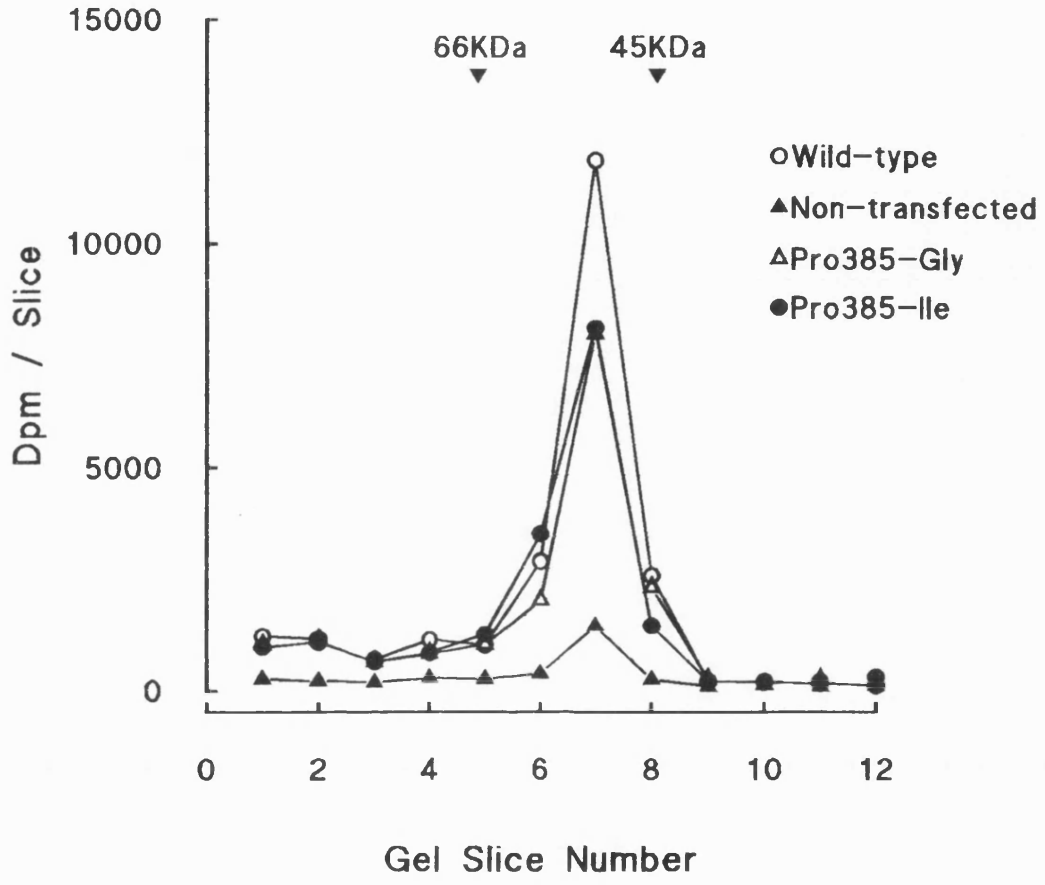

Fig. 32. Immunoprecipitation of borohydride-labelled GLUT1 in non-transfected, wild-type and proline mutant CHO-K1 clones. Cells of the wild-type (○), Pro385-Gly (△), Pro385-Ile (●) and non-transfected CHO-K1 (▲) clones were grown to confluence in 35 mm culture dishes. Cells were treated with 10 units of galactose oxidase and 1 unit of neuraminidase in 1 ml of PBS for 30 min at 18 °C. After washing in PBS, the cells were incubated with 1 mCi of tritiated sodium borohydride in 1 ml PBS for 10 min. After washing in PBS, the cells were solubilized in 2 % Thesit detergent buffer and immunoprecipitated with anti-GLUT1 antibody. The immunoprecipitates were then analysed by electrophoresis on a 10 % acrylamide gel.

The uptake of 2-deoxy-D-glucose was measured in these proline mutants. The Pro385-Gly mutant retained a high level of transport activity which was 121.8 ± 7.6 % (n=4) of the wild-type activity. However, substitution of proline 385 for isoleucine resulted in a markedly decreased transport activity which was only 39.5 ± 3.6 % (n=4) of that observed in the wild-type clone and was similar to the transport activity seen in non-transfected CHO-K1 cells (25.7 ± 5.3 % (n=4) of the wild-type clone).

Next, we determined whether this decreased transport activity in the Pro385-Ile clone was accompanied by a decrease in binding of the internal and/or the external ligands cytochalasin B and ATB-BMPA. The Pro385-Gly mutant was labelled with both cytochalasin B and ATB-BMPA to a level comparable to that of the wild-type clone (Fig. 33,34). Cytochalasin B and ATB-BMPA labelling was 146 ± 13.6 % (n=6) and 53.5 ± 1.8 % (n=4) of wild-type levels, respectively.

The Pro385-Ile mutant was also labelled with cytochalasin B to a level that was 106.2 ± 4.2 % of that of the wild-type clone. However, substitution of proline 385 for isoleucine, completely prevented labelling by the external ligand ATB-BMPA, giving labelling that was only 3.4 ± 0.8 % of the wild-type level and similar to the labelling in non-transfected CHO-K1 cells (5.8 ± 0.3 % (n=4) of the level in the wild-type clone) (Fig. 34).

Therefore, substitution of glycine for proline 385 can be tolerated by GLUT1 and causes only small changes in ligand binding and transport activity. However if proline 385 is substituted for the bulkier residue isoleucine, external ligand binding is perturbed and the mutant's ability to transport 2-deoxy-D-glucose is markedly reduced.

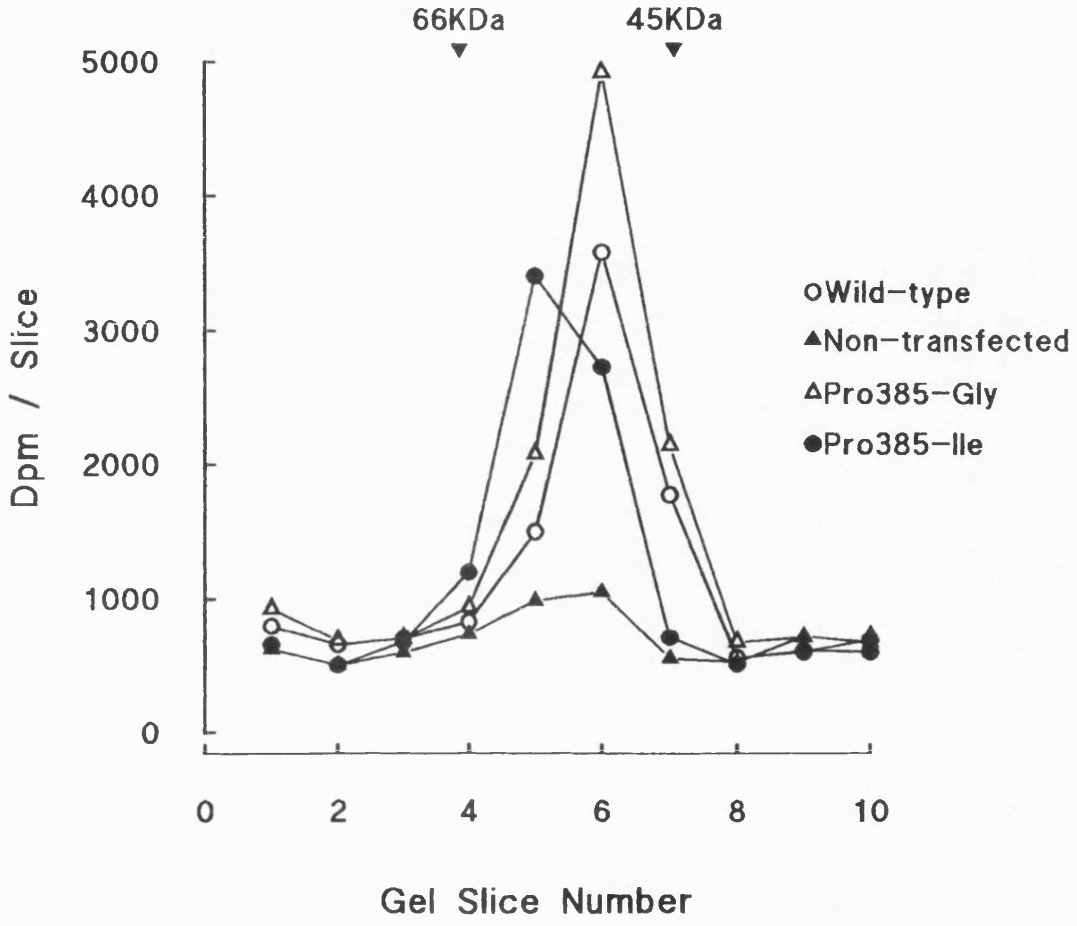

Fig. 33. Cytochalasin B labelling of GLUT1 in non-transfected, wild-type and proline mutant CHO-K1 clones. Cells of the wild-type (○), Pro385-Gly (△), Pro385-Ile (●) and non-transfected CHO-K1 (▲) clones were grown to confluence in 90 mm culture dishes and then fractionated to yield a crude plasma membrane fraction. 200 μg of plasma membranes in 400 μl of TES and 100 μM cytochalasin E were labelled with 1.4 μCi of [4-^{3}H]cytochalasin B by irradiation. The membranes were washed twice and then analysed by electrophoresis on a 10 % acrylamide gel.

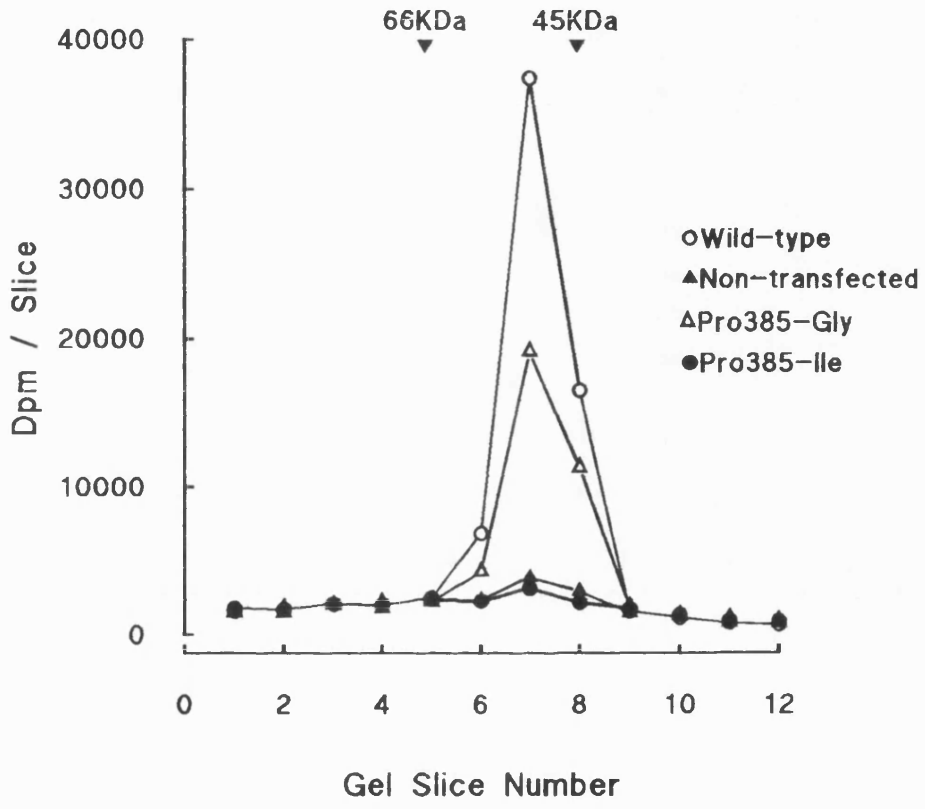

Fig. 34. ATB-BMPA labelling of GLUT1 in non-transfected, wild-type and proline mutant CHO-K1 clones. Cells of the wild-type (○), Pro385-Gly (Δ), Pro385-Ile (●) and non-transfected CHO-K1 (▲) clones were grown to confluence in 35 mm culture dishes. Cells were labelled with 100 μCi of ATB-[2-^{3}H]BMPA in 250 μl of PBS at 18 $^\circ$C by irradiation. After washing five times in PBS, the cells were solubilized directly in electrophoresis sample buffer and analysed by electrophoresis on a 10 % acrylamide gel.

3.3.4. C-Terminal Deletion Mutants of GLUT1

Upon removal of the C-terminal 37 amino acids, GLUT1 loses the ability to transport glucose and to bind the external ligand ATB-BMPA, although it can still bind the internal ligand cytochalasin B (Oka *et al*, 1990). However, GLUT1 is still fully functional after removal of the C-terminal 12 amino acids (Lin *et al*, 1992). In order to determine how many of the GLUT1 C-terminal amino acids had to be retained for exofacial ligand binding, a number of C-terminal deletion mutants were produced and assayed for their ability to bind ATB-BMPA and cytochalasin B.

The results are shown in table 7. The ability to bind the external ligand ATB-BMPA was lost after deletion of the C-terminal 25 amino acids (CD25). The CD24 mutant showed a level of ATB-BMPA labelling that was 50.67 ± 2.4 % (n=4) of the wild-type level but on deletion of the 25th residue the level of labelling decreased to 6.0 ± 1.73 % (n=3) which was comparable to labelling in non-transfected CHO-K1 cells (4.0 ± 0.58 % (n=3) of the wild-type level).

The CD24 and CD25 mutants could both still bind cytochalasin B to a level comparable to that of the wild-type clone (78.4 ± 11.1 % and 77.8 ± 13.5 % (n=5) of wild-type levels respectively).

Experiment	Non-transfected	Wild-type	CD24	CD25
Borohydride Labelling	9.25±2.4 (n=4)	100	107±30 (n=4)	48.8±3.0 (n=4)
Cytochalasin B Labelling	29.8±9.7 (n=5)	100	78.4±11.1 (n=5)	77.8±13.5 (n=5)
ATB-BMPA Labelling	4.0±0.58 (n=3)	100	50.7±2.4 (n=4)	6.0±1.7 (n=3)

Table 7. Transport activity and labelling levels in non-transfected, wild-type and C-terminal deletion mutant clones. All values are expressed as the percentage of the level in the wild-type clone. The results are the mean ± S.E.M. from 3-5 experiments.

3.4. Studies on the Regulation of Glucose Transport in the Rat Adipocyte

3.4.1. Preparation of Isolated Rat Adipocytes

Great care was taken when isolating rat adipocytes. Each new batch of insulin, collagenase and BSA was thoroughly tested to ensure that they produced viable, non-leaky cells which exhibited a low basal transport and a good insulin stimulation of transport. To avoid mechanical effects which increase the basal transport activity, the cells were maintained at 37 °C and were not centrifuged until after transport measurement or ATB-BMPA labelling.

3.4.2. Basal and Insulin-Stimulated Glucose Transport

Basal and insulin-stimulated 3-O-methyl-D-glucose transport was determined for each rat adipose cell preparation. The rate constant for influx of 3-O-[^{14}C]methyl-D-glucose into basal cells was 0.0061 ± 0.0013 s^{-1} (n=12), and into insulin-stimulated cells was 0.213 ± 0.020 s^{-1} (n=12) giving an average insulin stimulation of 35 fold.

3.4.3. Photolabelling of Rat adipocytes with ATB-BMPA

If ATB-BMPA could be used to label glucose transporters in the plasma membrane of isolated rat adipocytes without any labelling of the internal pool of

transporters, this would be an important technique for estimating levels of the separate pool of cell-surface transporters. Isolated rat adipocytes at a 40 % cytocrit were irradiated for 60 sec with ATB-[2-^{3}H]BMPA to allow total activation of the diazirine group and to get maximum incorporation. Initially the adipocytes were resuspended after 30 sec irradiation and before being irradiated for a second 30 sec but this was later found to be unnecessary and so a single 60 sec irradiation was used.

Fig. 35 shows the gel profile when insulin stimulated isolated rat adipocytes were irradiated in the presence of ATB-BMPA and the resulting plasma membranes run on a 10 % SDS-polyacrylamide gel. A peak corresponding to the glucose transporter runs between the 45 and 66 kDa markers at approximately 50 kDa. A second non-specific peak runs at approximately 75 kDa. The non-specific peak was 2.2 ± 0.1 (n=8) times the size of the specific glucose transporter peak. The exact nature of this non-specifically labelled protein is not known. Labelling of the 50 kDa protein but not the 75 kDa protein was fully displaced when the rat adipose cells were labelled in the presence of 300 mM D-glucose or 50 μM cytochalasin B (Fig. 36).

It was important that the ATB-BMPA was impermeant and could not label intracellular transporters. After labelling of insulin-stimulated cells with ATB-BMPA the low density microsome fraction was isolated and analysed by SDS-PAGE. Virtually no labelled glucose transporters were found in the low density microsome fraction (≈ 4 % of the plasma membrane level).

The effect of a 60 sec irradiation on the cells was checked to ensure that they were not being damaged by the UV light. Cells were irradiated and then transport activity was measured. Irradiation did not affect basal and insulin-stimulated glucose transport activity.

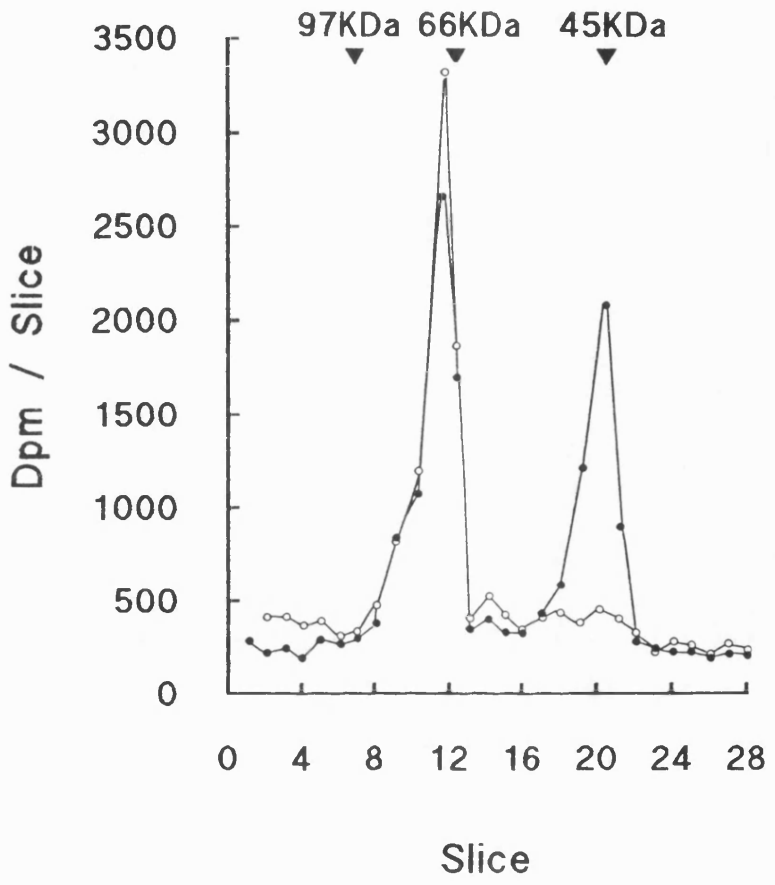

Fig. 35. ATB-BMPA labelling of basal and insulin-stimulated rat adipose cells. Isolated rat adipose cells (1 ml of 40 % cytocrit) were incubated with (●) or without (○) 10 nM insulin for 20 min at 37 °C in 1 % albumin/Hepes buffer. They were then mixed with 333 μCi of ATB-[2-^{3}H]BMPA in 35 mm polystyrene dishes and irradiated for 2 x 30 sec. The cells were fractionated to obtain a crude plasma membrane fraction which was subjected to electrophoresis on a 10 % acrylamide gel.

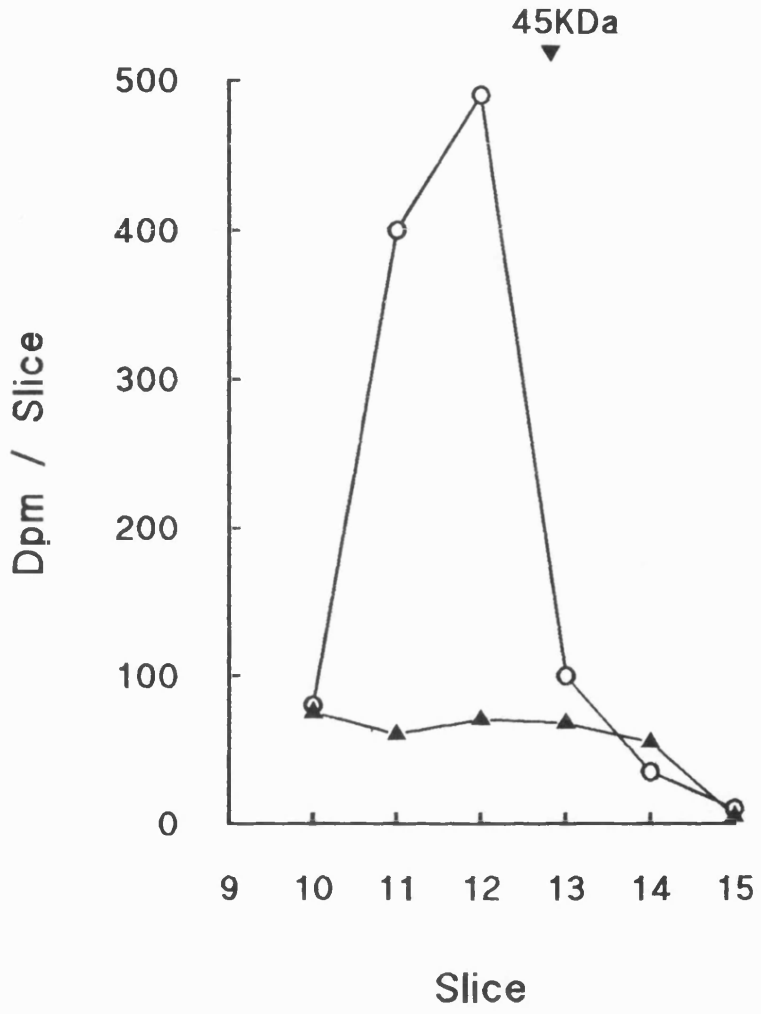

Fig. 36. Displacement of ATB-BMPA labelling of the adipocyte glucose transporter by cytochalasin B. Isolated adipose cells (1 ml of a 40 % cytocrit) were treated with 10 nM insulin for 20 min at 37 °C then photolabelled with 250 μCi of ATB-[2-^{3}H]BMPA for 2 x 30 sec with (▲) or without (○) 50 μM cytochalasin B. Plasma membranes were isolated and analysed by electrophoresis. Only the peak corresponding to the glucose transporter is shown. Cytochalasin B does not reduce the non-specific 75 kDa peak area.

3.4.4. Photolabelling of Basal and Insulin-Stimulated Rat Adipocytes

When basal and insulin-stimulated cells were photolabelled with ATB-BMPA and the plasma membranes isolated, a large (>7 fold) difference in the number of glucose transporters in the plasma membrane of basal and insulin-stimulated cells was observed (Fig. 35). The size of the non-specific peak remains the same in basal and insulin-stimulated cells suggesting that the large increase in the glucose transporter peak in insulin-stimulated cells is specific and not due to inaccurate loading of protein onto the gel.

3.4.5. Immunoprecipitation of GLUT1 and GLUT4 from Basal and Insulin-Stimulated Rat Adipocytes

Anti-GLUT1 and anti-GLUT4 antibodies (section 2.2.) were used together with ATB-BMPA to investigate cell-surface levels of the two transporter isoforms in basal and insulin-stimulated rat adipocytes. A 0.5%Mega 10 detergent buffer had been used to solubilize proteins from erythrocyte membranes. This proved to be unsuccessful with rat adipocytes so alternative detergents were tried. A detergent buffer composed of 2 % Thesit ($C_{12}E_9$) and proteinase inhibitors in phosphate buffer was found to solubilize the proteins in rat adipose cells and did not interfere with antibody-glucose transporter binding.

After incubation of the adipocytes with Thesit solubilization buffer for 20 min at room temperature, the unsolubilized material was spun down and found to contain virtually no labelled glucose transporter (Fig. 37a). The solubilized fraction was

incubated with anti-GLUT1 and anti-GLUT4 antibodies to remove the glucose transporters and chloroform/methanol precipitation of the supernatant showed that virtually all the labelled 50 kDa peak had been removed leaving the non-specific peak in the supernatant (Fig. 37b).

No peak is observed on SDS-PAGE if insulin-stimulated rat adipocytes are photolabelled with ATB-BMPA in the presence of cytochalasin B, then immunoprecipitated with anti-GLUT1 and anti-GLUT4 antibodies (results not shown). Therefore, only protein that is labelled by ATB-BMPA in a cytochalasin B inhibitable fashion is immunoprecipitated by the antibodies.

The solubilized fraction was immunoprecipitated successively with anti-GLUT1 then anti-GLUT4 antibodies or anti-GLUT4 then anti-GLUT1 antibodies. As Fig. 38 shows, the amount of a particular isoform was not dependant on the order of immunoprecipitation. The GLUT4 isoform was shown to be the most abundant isoform in the plasma membrane of both basal and insulin-stimulated cells. After insulin treatment GLUT4 accounted for 89.8 ± 1.2 % (n=4) of the total plasma membrane glucose transporters. The amount of GLUT1 in basal cells was approximately 5 fold (19.9 ± 2.4 %, n=4) less than in insulin-stimulated cells. Insulin increased the amount of plasma membrane GLUT4 approximately 20 fold (basal cells contained 4.9 ± 0.39 %, n=6 compared to insulin-treated cells). This corresponded to an average transport stimulation with insulin of 35 fold (section 3.4.2.). Therefore there was still an approximate 1.5-2 -fold discrepancy between transport stimulation and increase in plasma membrane glucose transporters as assessed by photolabelling.

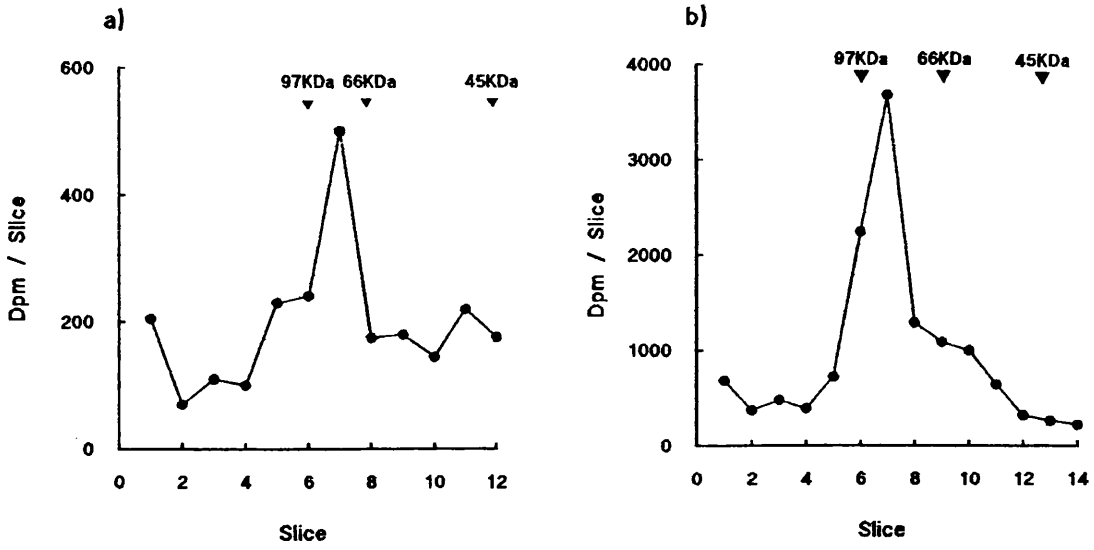

Fig. 37. Immunoprecipitation of glucose transporters from Thesit-solubilized rat adipocytes. Isolated rat adipocytes (1 ml of a 40 % cytocrit) were stimulated with 10 nM insulin and then photolabelled with ATB-BMPA. The unbound label was removed by washing in 1 % albumin/Hepes buffer. The cells were then directly solubilized in 2 % Thesit detergent buffer for 20 min at 18 °C. The unsolubilized material was then removed by centrifugation at 20,000 g for 10 min and was found to contain virtually no labelled glucose transporter (Fig. 37a). The solubilized material was incubated with anti-GLUT1 and anti-GLUT4 antibodies attached to protein A-Sepharose (GLUT4 peak = 3500 Dpm, GLUT1 peak = 400 Dpm). The supernatant after immunoprecipitation was chloroform/methanol precipitated and the labelled protein content was analysed. Virtually all the labelled glucose transporter peak had been removed leaving the labelled 75 kDa peak in the supernatant (Fig. 37b).

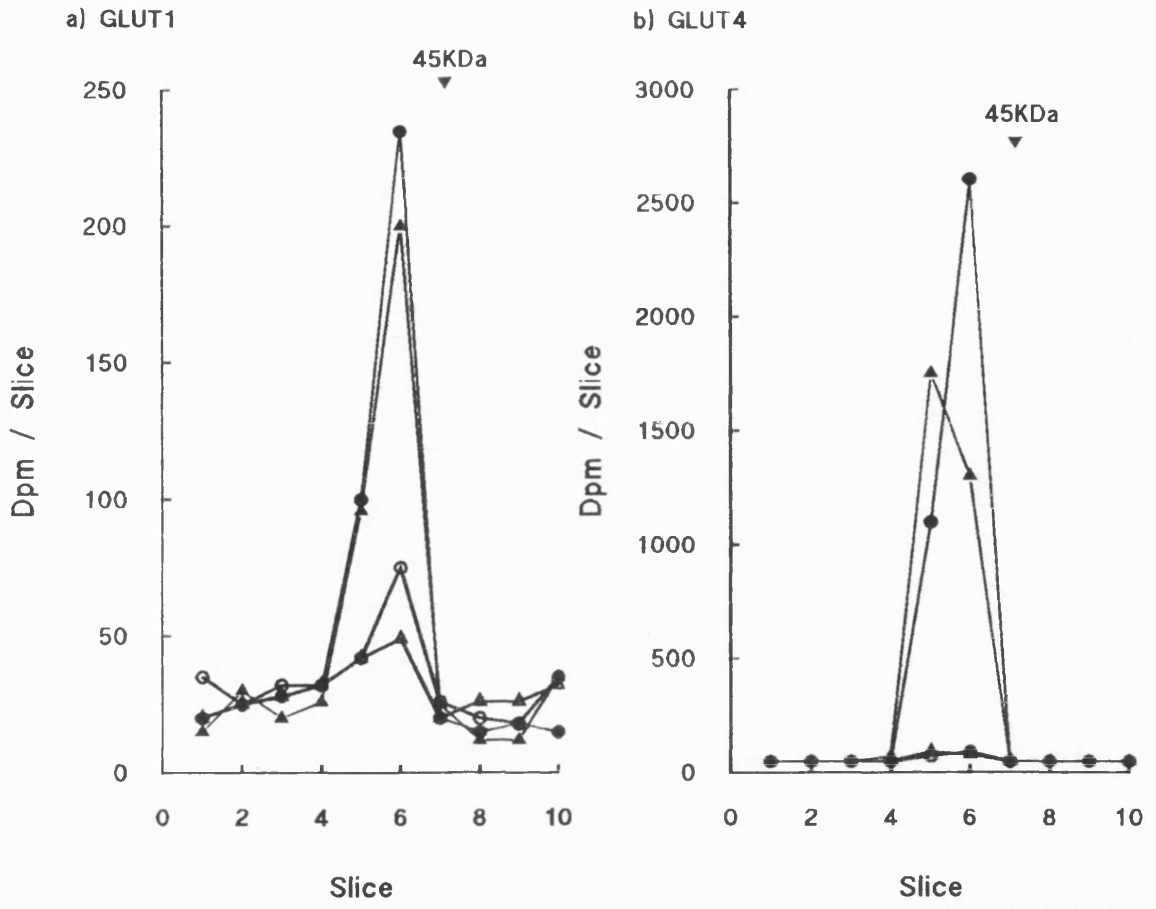

Fig. 38. Immunoprecipitation of GLUT1 and GLUT4 from ATB-BMPA labelled rat adipose cells. Isolated rat adipose cells (1 ml of a 40 % cytocrit) were incubated with (●,▲) or without (○,△) 10 nM insulin for 20 min then photolabelled with 1 mCi ATB-[2-^{3}H]BMPA (2 x 30 sec irradiation). A crude plasma membrane fraction was prepared and divided in half, then solubilized in 2 % Thesit detergent buffer. Each half was then subjected to successive immunoprecipitation with anti-GLUT1 and anti-GLUT4 antibodies and analysed by electrophoresis. In a, GLUT1 was immunoprecipitated before GLUT4 (▲,△); 340 dpm with insulin, 96 dpm basal or after GLUT4 (●,○); 300 dpm with insulin, 48 dpm basal. In b, GLUT4 was immunoprecipitated before GLUT1 (▲,△); 3764 dpm with insulin, 136 dpm basal or after GLUT1 (●,○); 3080 dpm with insulin, 136 dpm basal.

3.4.6. Trypsin-Treatment of Immunoprecipitated GLUT4

GLUT1 has a number of possible trypsin cleavage sites, but under native conditions GLUT1 is only cleaved within its cytoplasmic central loop and C-termini to give an 18 kDa ATB-BMPA-labelled fragment (section 3.2.6.). Comparison of the GLUT1 and GLUT4 amino acid sequences shows that GLUT4 has a similar pattern of possible cleavage sites to GLUT1, but GLUT4 also has an arginine in the exofacial loop between TM9 and TM10, which is not found in GLUT1. To examine the susceptibility of the GLUT4 isoform to trypsin cleavage, we first immunoprecipitated GLUT4 from ATB-BMPA-labelled rat adipocyte membrane fractions, then treated the immobilized GLUT4 with trypsin. This allowed removal of the non-specifically labelled 75 kDa protein that could also be trypsin-susceptible and so complicate the results.

Fig. 39 shows that when GLUT4 from plasma membranes and low density microsomes were treated with trypsin, a labelled 18 kDa fragment was produced from both fractions. The fact that labelled 18 and 50 kDa peaks were visible after trypsin cleavage shows that the GLUT4 is not in a denatured form after 2 % Thesit solubilization and immunoprecipitation as all the other possible cleavage sites have not become accessible.

When immunoprecipitated GLUT4 was treated with trypsin and the immunopellet and supernatant analysed separately, all the 18 kDa trypsin fragment was found in the supernatant (Fig. 40). The majority of the remaining 50 kDa glucose transporter was still attached to the immunopellet, but a small amount was found in the supernatant, suggesting that it may lack its C-terminal-antibody binding fragment.

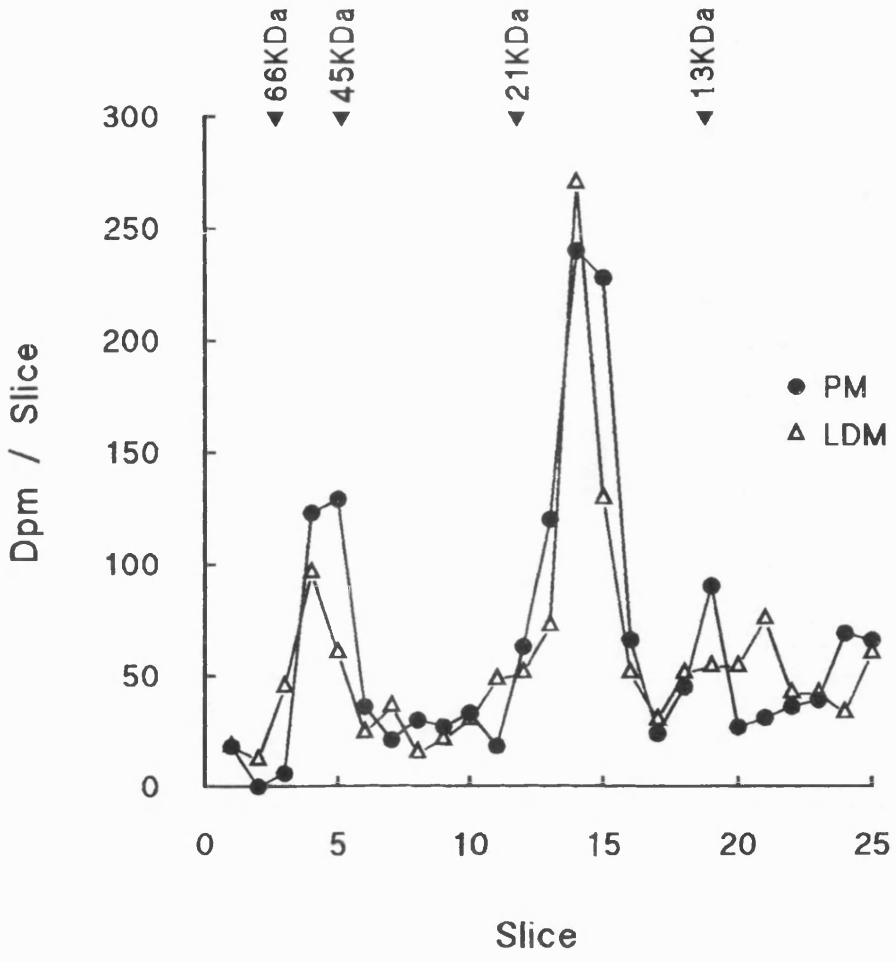

Fig. 39. Trypsin treatment of plasma membrane and low density microsome GLUT4. Plasma membrane (●, PM) and low density microsome (△, LDM) fractions were prepared from insulin-stimulated rat adipocytes as described in section 2.5.7.. 150 μg of membrane was labelled with 250 μCi ATB-[2-^{3}H]BMPA then solubilized in 2 % Thesit detergent buffer. The solubilized membrane was then incubated overnight with 5 μg purified anti-GLUT4 antibody attached to 12 μl protein A-Sepharose. The immunoprecipitates were washed then treated with 10 units of trypsin for 45 min. Electrophoresis sample buffer was then added and the released protein was analysed by electrophoresis using the Tricine gel system.

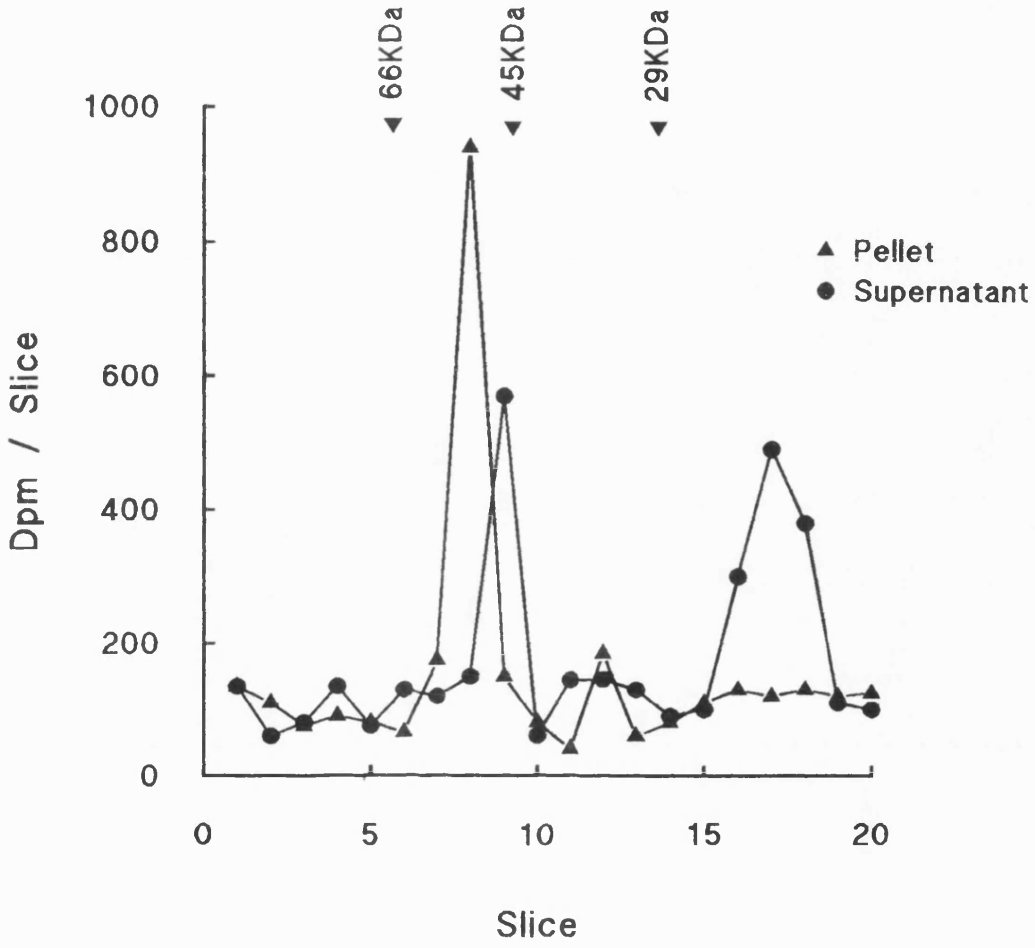

Fig. 40. Trypsin treatment of immunoprecipitated rat adipocyte GLUT4. Insulin-stimulated isolated rat adipocytes (1 ml of a 40 % cytocrit) were labelled with 250 μCi of ATB-[2-^{3}H]BMPA then washed and directly solubilized in 2 % Thesit detergent buffer. After immunoprecipitation of the GLUT4, trypsin (100 units/ml) was added for 30 min then the immunopellet (▲) and the supernatant (●) were analysed by electrophoresis on a 12 % acrylamide gel.

3.4.7. Localisation of GLUT4 in Basal and Insulin-Stimulated Cells by ATB-BMPA Labelling of Subcellular Fractions

In order to determine where GLUT4 is localised in basal and insulin-stimulated cells, plasma membrane and low density microsome fractions were isolated as described (section 2.5.7.), then photolabelled with ATB-[2-^{3}H]BMPA and immunoprecipitated with anti-GLUT4 antibodies. The results were calculated as a percentage of the radioactivity in the insulin-treated plasma membrane sample (Fig. 41). The increase in plasma membrane GLUT4 after insulin-stimulation was determined by this method to be only approximately 3-fold, compared to an average transport stimulation of 35-fold. The increase in GLUT4 in the plasma membrane in the insulin-stimulated state was accompanied by a decrease in the low density microsomes, the total being similar in basal and insulin-stimulated cells. The difficulties in fractionating rat adipocytes reproducibly resulted in large standard errors. The amount of the GLUT4 isoform in the basal plasma membrane was only approximately 10 % of the total in basal cells. Therefore even a small contamination of the plasma membrane fraction by low density microsomes would increase the apparent number of basal plasma membrane glucose transporters and so underestimate the stimulation due to insulin.

3.4.8. GLUT4 Distribution in Basal and Insulin-Stimulated Cells by Western Blotting

Basal and insulin-stimulated cells were subfractionated into mitochondria/nuclei, plasma membrane, high-density microsome and low-density

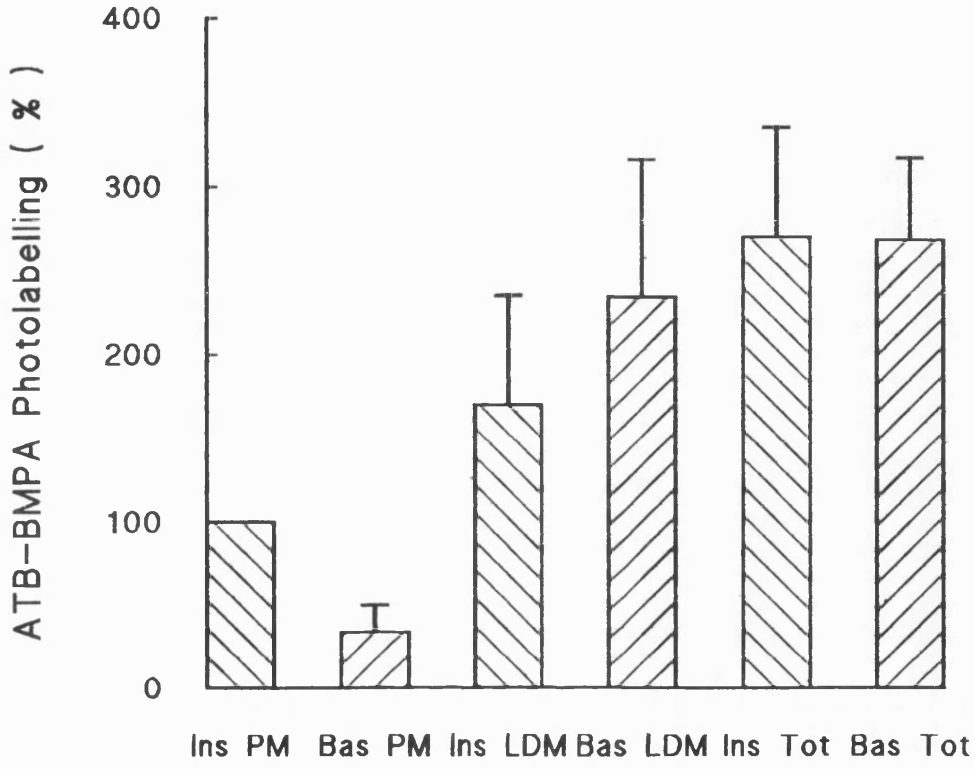

Fig. 41. Immunoprecipitation of GLUT4 from ATB-BMPA-labelled membrane fractions isolated from rat adipose cells. Basal and insulin-treated isolated rat adipocytes were fractionated and plasma membrane and low density microsome fractions (200 μg) were labelled with 200 μCi of ATB-[2-^{3}H]BMPA. The membranes were solubilized in 2 % Thesit detergent buffer and immunoprecipitated with anti-GLUT4 antibody attached to protein A-Sepharose. The immunoprecipitated material was subjected to electrophoresis. The total radioactivity per sample was calculated as a percentage of the radioactivity in the insulin-treated plasma membrane sample. The results are the means $\pm$ S.E.M. from three experiments.

microsome fractions. 10 μg of each fraction was run on SDS-PAGE then transferred to nitrocellulose and probed with anti-GLUT4 antibody then ^{125}I-protein A. The ^{125}I band corresponding to the glucose transporter was excised and counted and the counts (after a nonspecific background was removed) were multiplied by the total protein to give the amount of GLUT4 in each fraction. An approximate 5 fold increase in plasma membrane GLUT4 after insulin-stimulation was measured by this method and there was a corresponding decrease of GLUT4 from the low-density microsome fraction (Fig. 42). In insulin-stimulated cells approximately 45 % of the GLUT4 was found to be at the plasma membrane. The 5 fold increase observed with this method is still small compared to the approximate 20 fold increase seen with immunoprecipitation of ATB-BMPA labelled glucose transporters from isolated adipocytes (section 3.4.5) and compared to the average 35-fold transport stimulation. As with ATB-BMPA labelling of membrane fractions (section 3.4.7.), the main reason for this small increase in GLUT4 is likely to be an artificially high basal due to contamination of plasma membrane with high and low-density microsomes. 85 % of the GLUT4 in the basal state was located in the microsomal fraction, so even a small contamination of the plasma membrane with this fraction would increase the basal considerably. A small amount of GLUT4 was detected in the HDM fraction and the mitochondria/nuclei fraction, which is probably in part due to a contamination with low density microsomes and plasma membrane.

3.4.9. Inhibition of Glucose Transporter Translocation by Potassium Cyanide

Insulin-stimulation of glucose transport has been shown to be energy-dependant

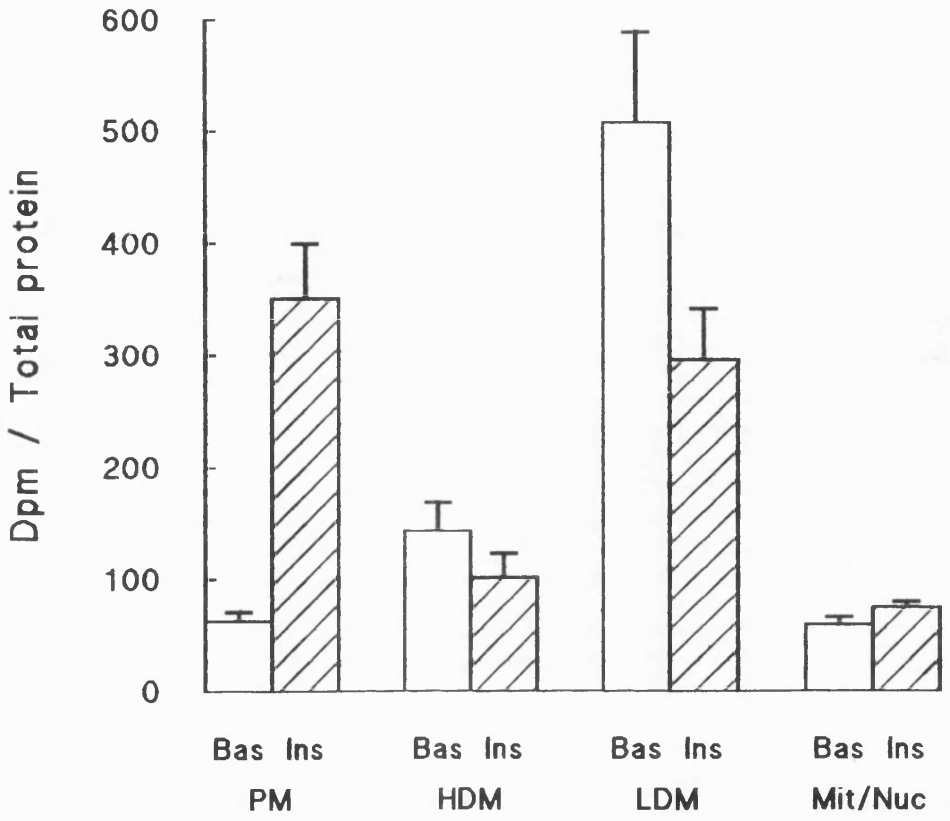

Fig. 42. **Western blotting of basal and insulin-stimulated rat adipocyte membrane fractions with anti-GLUT4 antibody.** Isolated rat adipocytes (2 ml of a 40 % cytocrit) were incubated with or without insulin (10 nM, 20 min) then fractionated into plasma membrane (PM), mitochondria/nuclei (Mit/Nuc), high density microsomes (HDM) and low density microsomes (LDM) as described (section 2.5.7.). 10 μg of each fraction was separated on a 1.5 mm, 10 % acrylamide gel and then transferred to nitrocellulose. The nitrocellulose was blotted with anti-GLUT4 antibody then 0.1 μCi/ml ^{125}I-protein A. It was then exposed to film and cut and counted. The counts obtained for 10 μg were multiplied by the total protein per fraction, which did not vary significantly between basal and insulin-stimulated samples. The results are expressed as the mean and standard error (n=4) of Dpm/total protein.

and can be inhibited by KCN (Kono *et al*, 1981). The effect of KCN on glucose transporter translocation in isolated rat adipocytes upon addition and removal of insulin was investigated.

Cells were stimulated with insulin in the presence or absence of 2 mM potassium cyanide, then assayed for 3-O-methyl-D-glucose transport activity and labelled with ATB-BMPA to determine plasma membrane glucose transporter levels. KCN added 2 min prior to the addition of insulin blocked the insulin-stimulation of glucose transport activity keeping the activity close to basal levels. The rate constants for 3-O-methyl-D-glucose transport were: in basal cells $k = 0.0021\ s^{-1}$, in KCN and insulin-treated cells $k = 0.0021\ s^{-1}$ and in insulin-treated cells $k = 0.198\ s^{-1}$.

The addition of KCN before insulin also appeared to totally block translocation of the glucose transporter as cell surface glucose transporter levels were found to be similar to basal levels (Fig. 43a). To check that cyanide did not interfere with ATB-BMPA labelling of the glucose transporter, rat adipose cells were fully stimulated with insulin then incubated with or without 2 mM cyanide for 2 min before being labelled with ATB-BMPA. Fig. 43b shows that the addition of cyanide does not affect labelling of insulin-stimulated cells by ATB-BMPA. Addition of cyanide after full insulin stimulation also had no effect on glucose transport activity.

It has been reported that cyanide also blocks fully the effects of removing insulin from fully stimulated cells (Kono *et al*, 1981). The effect of cyanide on the reversal of insulin-stimulated glucose transport activity in isolated rat adipocytes was investigated. It was found that 2 mM KCN only partially blocked the decrease in glucose transport activity due to removal of insulin. Transport activity in KCN-treated cells was still approximately 50 % of the fully insulin-stimulated level. KCN was also found to be ineffective in blocking the reversal of glucose transport activity in 3T3-L1

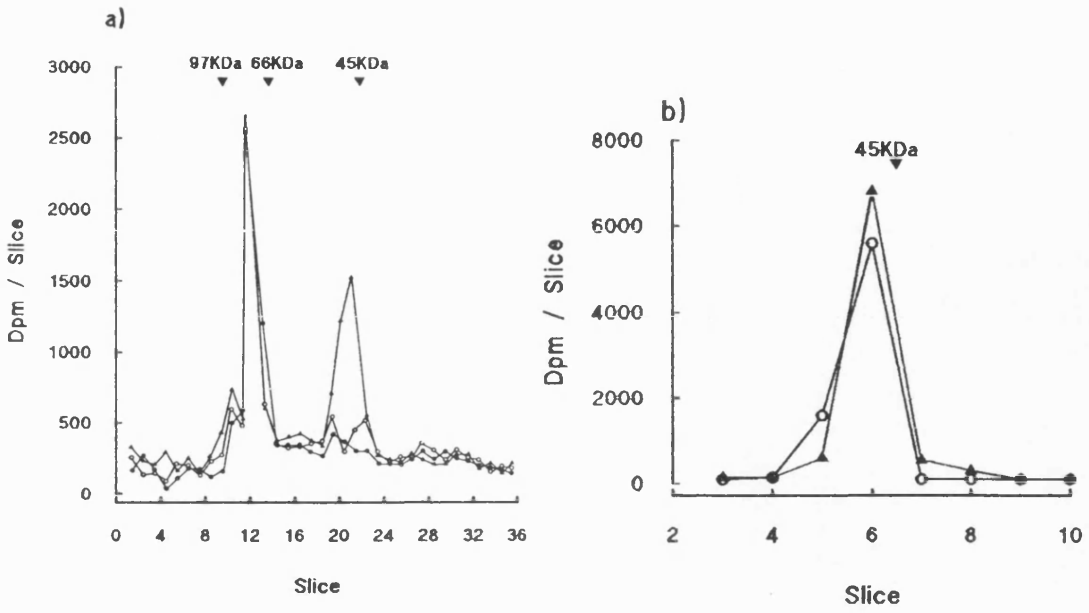

Fig. 43. Effect of KCN on glucose transporter translocation and ATB-BMPA labelling. The effect of KCN when added before and after insulin treatment was investigated. a) Isolated rat adipose cells (1 ml of a 40 % cytocrit) were untreated (●) or treated with 10 nM insulin alone (▲) or with 2 mM KCN for 2 min then 10 nM insulin for 20 min (○). After labelling with 333 μCi ATB-BMPA a crude plasma membrane fraction was isolated and analysed by electrophoresis. b) Insulin-stimulated isolated rat adipocytes (1 ml of a 40 % cytocrit) were incubated with (○) or without (▲) 2 mM KCN for 2 min before labelling with 500 μCi ATB-BMPA. Cells were then washed, solubilized in 2 % Thesit detergent buffer and immunoprecipitated with anti-GLUT4 antibody. The immunoprecipitated protein was then analysed by electrophoresis and cutting and counting gel slices.

adipocytes (Kozka *et al*, 1991).

3.4.10. The Time Course For Activation of Insulin-stimulated Glucose Transport

The time course for insulin-stimulated glucose transport activity in rat adipocytes was compared with the time course of appearance of the GLUT1 and GLUT4 isoforms at the plasma membrane (as determined by their ability to bind ATB-BMPA). Rat adipose cells were stimulated with insulin and then at various times KCN was added to stop further translocation and photolabelling was carried out immediately.

Stimulation of 3-O-methyl-D-glucose transport with 2 nM insulin was rapid at 37 °C, giving a maximum stimulation after only approximately 10 min (Fig. 44a). A log plot of the data (Fig. 44b) had a positive intercept on the time axis suggesting there was a lag time for activation. The lag time, calculated as the intercept on the time axis, was 47.1 ± 9.5 sec (n=5). As the intercept on the time axis was positive, the t½ was not calculated from the slope of this plot in the normal way, but was calculated as $t = (\ln 2 - c)/m$, where c is the intercept on the y axis and m is the slope. This gave a t½ of 3.2 ± 0.2 min (n=5).

Fig. 44a also shows the time course of appearance of the glucose transporter isoforms, GLUT1 and GLUT4 at the plasma membrane. Like transport, the appearance at the cell surface was very rapid with maximum levels by 10 min. The log plot of this data (Fig. 44b) showed no detectable lag and the half-times for the appearance of GLUT1 and GLUT4 at the plasma membrane were calculated from the slope to be 2.32 ± 0.30 min and 2.17 ± 0.18 min respectively, (n=3). Therefore

Fig. 44. Time course for the insulin-stimulation of glucose transport and for the appearance of cell-surface transporters. Isolated rat adipocytes were treated with 2 nM insulin for the indicated times. After addition of 2 mM KCN, 3-O-methyl-D-glucose transport (●) was measured and cell-surface glucose transporters were photolabelled with ATB-BMPA. Following labelling, the cells were washed and directly solubilized in 2 % Thesit detergent buffer, then immunoprecipitated with antibodies to GLUT1 (■) and to GLUT4 (□). The immunoprecipitates were then analysed by electrophoresis. The results in a) were calculated as a fraction of the fully stimulated level of transport or labelling, with subtraction of the levels found in basal cells, and are the mean ± S.E.M. from three to five experiments. In b) the lines were derived from regression (weighted for relative error) of the combined GLUT1 and GLUT4 labelling or transport. Insulin-stimulation of glucose transport (●) showed a lag time of 47.1 ± 9.5 sec (n=5) and a half time of 3.2 ± 0.2 min (n=5). The appearance of GLUT1 (■) and GLUT4 (□) at the cell surface occurred with half times of 2.32 ± 0.30 min and 2.17 ± 0.18 min respectively (n=3).

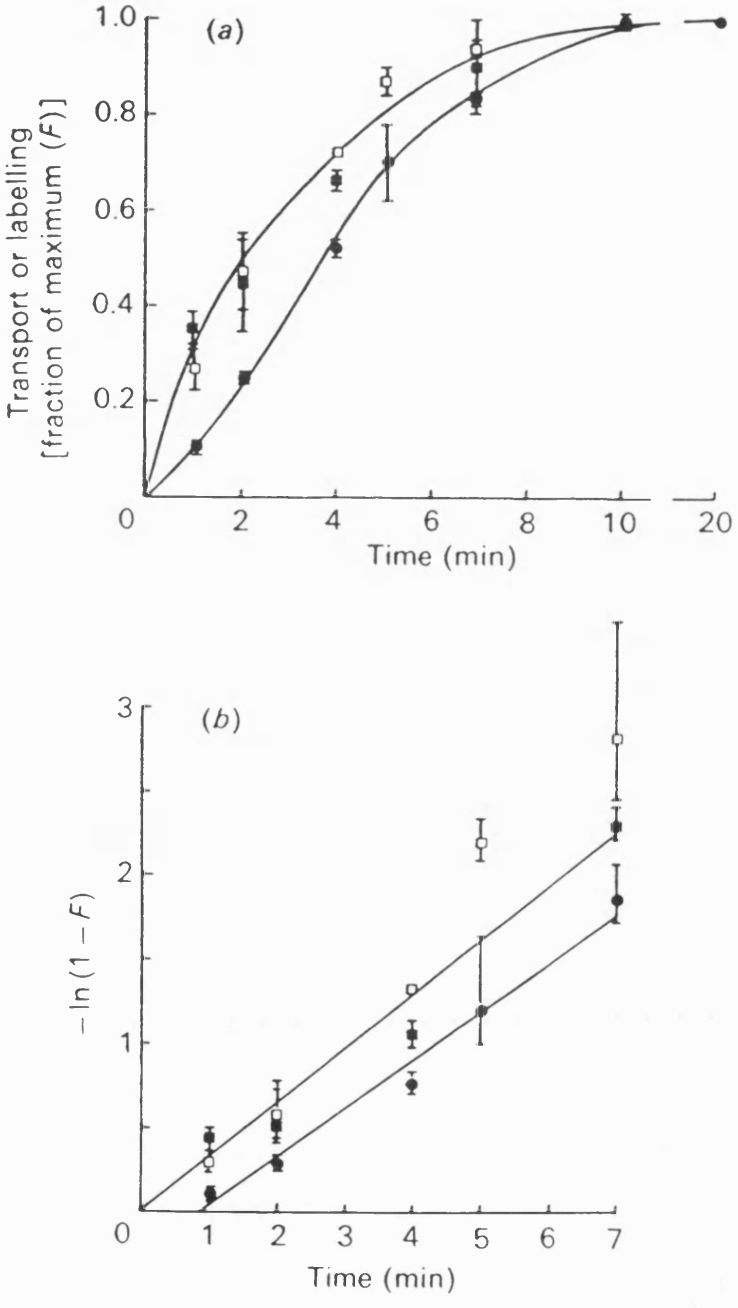
(a)
Transport or labelling
[fraction of maximum (F)]
1.0
0.8
0.6
0.4
0.2
0
2
4
6
8
10
20
Time (min)
(b)
$-\ln(1-F)$
3
2
1
0
1
2
3
4
5
6
7
Time (min)

the transporters appeared at the plasma membrane with no significant lag and their appearance slightly preceded the full transport stimulation.

The experimental errors involved in the determination of cell-surface transporters were found to be greater than those involved in the determination of transport activity. Although the mean values (from 3-5 experiments) for the transporter levels and the transport rate were different, at some points the S.E.M. values for these estimates overlapped. The maximum difference between transporter appearance and transport stimulation (which was only approximately 2 fold) occurred only at short times after insulin addition. This small difference was less evident when insulin concentrations higher than 2 nm were used. This result, along with the two-fold discrepancy observed between transport stimulation and transporter appearance may be due to insulin also producing a small change in the intrinsic activity of the glucose transporters as well as its major effect on their translocation to the plasma membrane.

3.4.11. Reversal of Insulin-Stimulated Glucose Transport

Cells were fully stimulated with insulin and then either the cells were washed at least 4 times to remove the insulin or alternatively, the insulin was removed by digestion with a low concentration (0.25 mg/ml) of collagenase. At each time point, translocation was stopped by the addition of 2 mM potassium cyanide, and this was followed quickly by transport and ATB-BMPA photolabelling assays. Fig. 45a shows that reversal of insulin-stimulated glucose transport was less rapid than activation. Removal of insulin caused an approximate 90 % decrease in transport, the transport

level returning to near basal levels. The t½ for the reversal of transport (t½ = 10.9 ± 1.4 min, n=3) was similar to the half-time for the decrease in cell-surface GLUT1 and GLUT4 levels, t½ = 11.7 ± 2.7 min (n=3) for GLUT1 and t½ = 12.3 ± 3.0 min (n=2) for GLUT4 (Fig. 45b). Therefore there was no detectable lag between loss of transport activity and removal of the transporters from the cell surface.

Fig. 45. Time course for the decrease in glucose transport activity and cell-surface transporters upon removal of insulin. Isolated rat adipocytes were fully stimulated with 1 nM insulin for 30 min then the insulin was removed by washing or by the addition of collagenase (0.25 mg/ml). At the indicated times after insulin removal, 2 mM KCN was added and 3-O-methyl-D-glucose transport (●) was measured and the remaining cell-surface transporters were labelled with ATB-BMPA. Following labelling, the cells were washed and directly solubilized in 2 % Thesit detergent buffer, then immunoprecipitated with antibodies to GLUT1 (○) and GLUT4 (●). The immunoprecipitates were then analysed by electrophoresis. The results were calculated as a fraction of the fully stimulated level of transport or labelling, with subtraction of the levels found in basal cells, and are the mean ± S.E.M. from two to three experiments. Half times were calculated from semi-log plots of these data. The half times for reversal of transport and cell-surface GLUT1 and GLUT4 were 10.9 ± 1.4 min (n=3), 11.7 ± 2.7 min (n=3) and 12.3 ± 3.0 min (n=2) respectively.

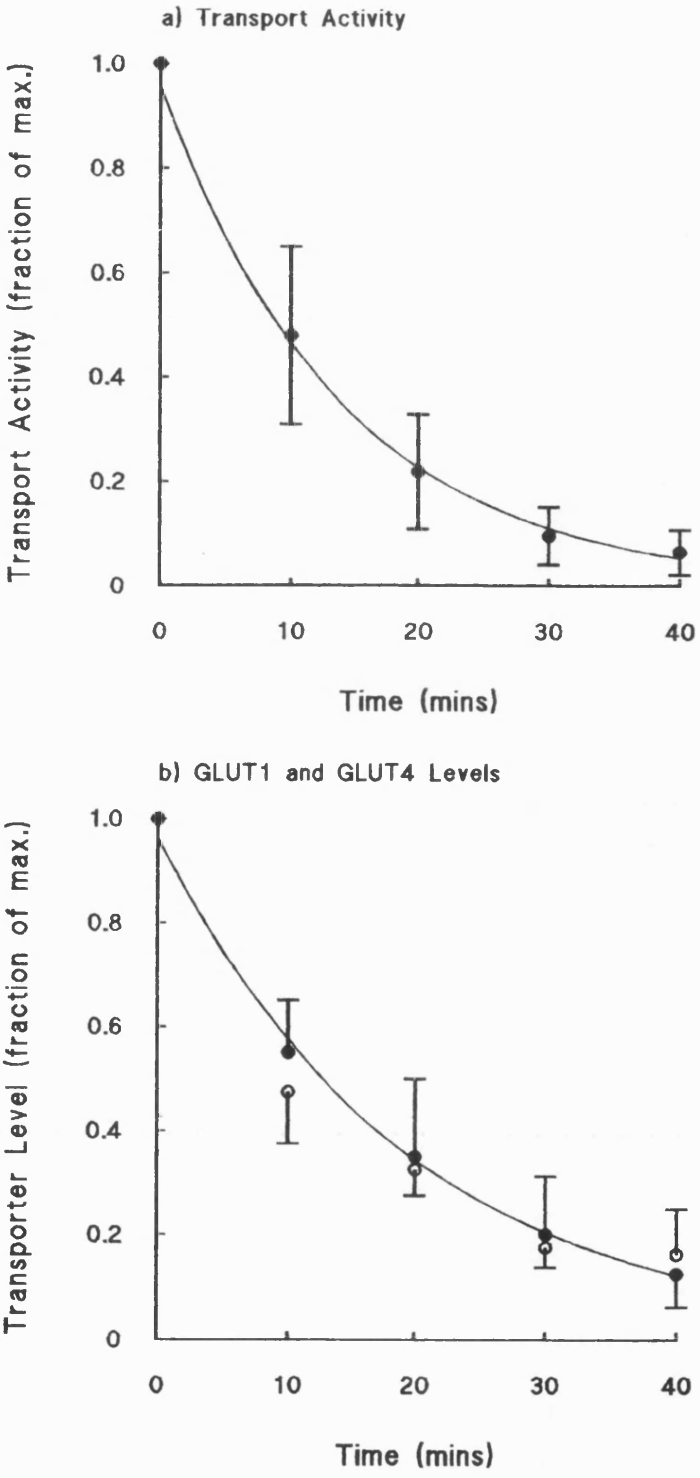
a) Transport Activity
Transport Activity (fraction of max.)
1.0
0.8
0.6
0.4
0.2
0
0
10
20
30
40
Time (mins)
b) GLUT1 and GLUT4 Levels
Transporter Level (fraction of max.)
1.0
0.8
0.6
0.4
0.2
0
0
10
20
30
40
Time (mins)

CHAPTER 4 : DISCUSSION

4.1. Photolabelling the Erythrocyte Glucose Transporter with ATB-BMPA

ASA-BMPA, a 4-azidosalicylate derivative of the bis-mannose compound (1,3-bis-(D-mannos-4-yloxy)-2-propylamine, BMPA) has been used by Holman *et al* (1986) to label the erythrocyte glucose transporter. Holman *et al*, (1986) found that ASA-BMPA specifically labels this glucose transporter protein when labelling is carried out on intact erythrocytes. However, when labelling of the glucose transporter with ASA-BMPA is carried out on erythrocyte membranes, ASA-BMPA also labels other proteins that are unrelated to the glucose transporter (Holman, G. D., Parkar, B. A. & Midgley, P. J. W. unpublished data). The diazirine derivative of BMPA (2-N-(1-azi-2,2,2-trifluoroethyl)benzoyl-1,3-bis-(D-mannos-4-yloxy)-2-propylamine, ATB-BMPA) is used in this study to label the erythrocyte glucose transporter. Diazirines are photoactivated to give reactive carbenes. Nitrenes undergo similar reactions to those of carbenes but the reactivity of nitrenes is considerably lower (Bayley & Knowles, 1977). The results described in this thesis show that ATB-BMPA labels the erythrocyte glucose transporter to give a single broad peak on SDS-PAGE at $\approx$ 50 kDa. ATB-BMPA is also shown to label only the glucose transporter protein, but no other proteins, when labelling is carried out on erythrocyte membranes. The labelling of the glucose transporter by ATB-BMPA is displaceable by D-glucose. The displacement of ATB-BMPA-labelling by a transported substrate of the glucose transporter, suggests that ATB-BMPA may bind to the transporter at or near the external ligand-binding site. ATB-BMPA labelling of the glucose transporter is also displaced by cytochalasin B. Davies *et al*, (1992) have localised the site of

cytochalasin B labelling in the erythrocyte glucose transporter to the region phenylalanine 389 to tryptophan 412 at the bottom of TM10 and TM11. The finding that cytochalasin B binding to the internal surface of the transporter inhibits the binding of ATB-BMPA to the external surface suggests that the transporter can not bind internal and external ligands simultaneously.

Results described in this thesis show that GLUT1 is the major isoform in erythrocytes. An antibody has been produced against a peptide corresponding to the C-terminal 13 amino acids of the HepG2/GLUT1 sequence reported by Mueckler *et al* (1985). The anti-GLUT1 antibody immunoprecipitates over 80 % of the ATB-BMPA-labelled glucose transporter protein from solubilized erythrocyte membranes.

The efficiency of ATB-BMPA-labelling of erythrocyte GLUT1 is calculated to be ≈ 100 %. This is calculated assuming the concentration of glucose transporter protein in the erythrocyte plasma membrane to be 600 pmol/mg of membrane protein (Allard & Lienhard, 1985). 90 pmol of transporter incorporates 5.7 pmol of ATB-BMPA. Therefore 6.3 % of the glucose transporter sites are labelled with ATB-BMPA. The affinity constant (or half maximal inhibition constant, K_i) of erythrocyte GLUT1 for ATB-BMPA is calculated to be ≈ 350 μM. Therefore, at the ATB-BMPA concentration used (20 μM) the sites will be 5.4 % saturated. The efficiency of labelling is therefore calculated as 117 %. Similar studies in 3T3-L1 adipocytes and rat adipocytes also suggest the labelling by ATB-BMPA is approximately 100 % efficient (Palfreyman *et al*, 1992, Nishimura *et al*, 1993). Therefore, if all the sites are occupied by ligand, then all the sites would covalently cross-link with the ATB-BMPA.

The affinity of the erythrocyte glucose transporter for ATB-BMPA has been determined in two ways: either from the inhibition of the uptake of 100 μM D-

galactose by ATB-BMPA or from the inhibition of the reversible binding of the exofacial label ASA-BMPA. The affinity constant (K_i) is determined from transport inhibition experiments to be ≈ 297 μM at 20 °C. The K_i is determined from the binding experiments to be ≈ 368 μM at 0 °C and ≈ 338 μM at 20 °C. Therefore, the two methods give similar K_i values for the affinity of GLUT1 for ATB-BMPA. ATB-BMPA binding to GLUT1 does not show any marked temperature dependence. The K_i obtained for GLUT1 binding of ATB-BMPA is similar to the value obtained by Jordan & Holman (1992) for the affinity of the liver transporter for ATB-BMPA (K_i ≈ 250 μM), where GLUT2 is the major glucose transporter isoform. Also Holman *et al* (1990) reported a K_i of ≈ 247 μM for ATB-BMPA binding in basal and insulin-stimulated rat adipocytes where GLUT4 is the major isoform. Therefore GLUT1, GLUT2 and GLUT4 appear to have a similar affinity for the external ligand ATB-BMPA. By contrast, Hellwig & Joost (1991) have reported that GLUT1, GLUT2 and GLUT4 vary markedly in their affinities for transported substrates and for inside-specific ligands, cytochalasin B and forskolin.

A lack of temperature dependence for ATB-BMPA binding to erythrocyte GLUT1 is described in this thesis. Midgley *et al*, (1985b) have reported a similar lack of temperature-dependence for the bis-mannose derivative nitroazidophenyl-BMPA binding to the erythrocyte glucose transporter. The K_i is dependent on the equilibrium dissociation constant:

$$K_i = K_{diss.} \cdot (1+A)$$

(where A is the asymmetry in the unloaded carrier distribution; that is, the rate constant for empty carrier movement from outside to inside over the rate constant for empty carrier movement from inside to outside). Lowe and Walmsley, (1986) have studied the temperature-dependence of erythrocyte glucose transporter kinetics. Their

results show a large decrease in the V_{max} of the transporter as the temperature decreases from 20 °C to 0 °C. Little temperature-dependence of K_m was observed. Lowe & Walmsley (1986) reported a large decrease in the proportion of both unloaded- and loaded-outward-facing carriers as the temperature was decreased from 50 °C to 0 °C. Therefore a lowering of temperature, which apparently increases A, would have to produce a corresponding decrease in $K_{diss.}$ so that there is no overall effect on the K_i. There is no evidence presently available to suggest that the dissociation constant $K_{diss.}$ is temperature-dependent. This apparent discrepancy between the observed lack of temperature effects on ligand binding and the marked temperature effect on glucose transport activity requires further investigation.

Erythrocyte GLUT1 has six cysteine residues at positions 133, 201, 207, 347, 421 and 429 (Mueckler *et al*, 1985). Fragmentation of the ATB-BMPA-labelled purified erythrocyte glucose transporter at cysteine residues, by NTCB, is shown in this thesis to produce ATB-BMPA-labelled fragments on SDS-PAGE of approximate molecular weight 6 kDa, 14 kDa, 23 kDa, 29 kDa and 50 kDa. The labelled fragments have been further identified by using antibodies to the C-terminal and to the central cytoplasmic loop of GLUT1. The immunoprecipitation of a 14 kDa labelled fragment by the antibody to the central loop of GLUT1 suggests that ATB-BMPA must label the region between cysteines 201 or 207 and cysteine 347. The C-terminal antibody also immunoprecipitates a 14 kDa fragment suggesting that ATB-BMPA labels between cysteine 347 and the C-terminal of GLUT1. Therefore, these results suggest that ATB-BMPA may label more than one site in the C-terminal region of GLUT1. A subsequent study in collaboration with Baldwin's group has used anti-peptide antibodies, generated against all the cytoplasmic loop regions of GLUT1, to

more accurately identify ATB-BMPA-labelled fragments produced after chemical and proteolytic cleavage of the glucose transporter (Davies *et al*, 1992). The results of this study suggest that the major site of labelling of GLUT1 by ATB-BMPA is around TM8 between alanine 301 and arginine 330. Holman & Rees, (1987) have identified TM9 in GLUT1 as the site of labelling of ASA-BMPA. The identification of the labelled fragments in their study was based solely on the molecular weight of the fragments as seen on SDS-PAGE. The differences observed between the sites of labelling of ATB-BMPA and ASA-BMPA may be due to inaccuracies in identifying the labelled fragments in the various methods used. However, the differences in the structures of the photoactivatable groups (ATB and ASA) on the bis-mannose ligands may result in the compounds fitting into the GLUT1 substrate binding site in slightly different orientations. Upon activation of the ligands, the reactive carbene and nitrene groups may be facing different regions of the binding site and so label different transmembrane segments. In addition, it is known that azides and diazirines show reactivity towards different types of amino acid side chains (Bayley & Knowles, 1977).

4.2. Investigation of Glucose Transporter Conformational Changes Using Proteinases

ATB-BMPA is shown in this thesis to bind to the C-terminal half of GLUT1. Photolabelling of erythrocyte GLUT1 with ATB-BMPA, followed by trypsin- or thermolysin-treatment of the transporter, produces a labelled fragment on SDS-PAGE of $\approx$ 18 kDa. The 18 kDa fragment is derived from the C-terminal half of GLUT1 as the fragment can be immunoprecipitated by an anti-GLUT1 C-terminal peptide

antibody. The effect of binding of the external ligand (ATB-BMPA) and the internal ligand (cytochalasin B) on the susceptibility of the glucose transporter to proteolysis is reported in this thesis. When ATB-BMPA-labelled-GLUT1 is treated with trypsin ≈ 50 % of the native transporter is converted to an 18 kDa tryptic fragment. Some of the 18 kDa tryptic fragment is still immunoprecipitatable with the GLUT1 anti-C-terminal peptide antibody. Therefore, some of the ATB-BMPA-labelled tryptic fragment must still retain its C-terminal antibody-binding fragment. By contrast, when unlabelled GLUT1 is treated with trypsin, almost complete conversion of the native transporter to an 18 kDa fragment is observed. Therefore, ATB-BMPA stabilizes a conformation of GLUT1 that is more resistant to proteolysis by trypsin than the unlabelled transporter. The protection from thermolysin-cleavage by ATB-BMPA binding to GLUT1 is even more pronounced. Thermolysin-treated ATB-BMPA-labelled GLUT1 is fully immunoprecipitated as a 50 kDa protein, demonstrating that neither the central loop nor the C-terminal regions of GLUT1 have been cleaved. Cairns *et al*, (1987) showed that trypsin and thermolysin cleaved the native glucose transporter solely at the cytoplasmic face. Therefore, this protection from proteolysis of GLUT1 by the outside-binding ligand can not be due to steric hindrance. The outside-specific ligand is thought to stabilize an outward-facing conformation in which the proteolytic cleavage sites are not accessible. These results support those of a number of other investigators. Holman & Rees, (1987) found that thermolysin cleaved the cytochalasin B-labelled transporter and not the ASA-BMPA-labelled transporter. The rate of tryptic cleavage of the erythrocyte glucose transporter was shown by Gibbs *et al* (1988) to be slower in the presence of the outside ligands, phloretin or 4,6-O-ethylidene-D-glucose.

At a concentration of thermolysin that is 6 times lower than that which

produces no cleavage of the ATB-BMPA-labelled transporter, virtually complete cleavage of cytochalasin B-labelled GLUT1 is observed. Therefore, cytochalasin B appears to stabilize a conformation that is more susceptible to proteolysis than the conformation stabilized by the outside binding ligand, ATB-BMPA. This is consistent with the comparison of the ASA-BMPA- and cytochalasin B-labelled glucose transporters (Holman & Rees, 1987). King *et al*, (1991) have also reported that the non-covalent binding of the inside-specific hexose, propyl glucoside, to GLUT1 renders the transporter more susceptible to proteolysis.

The results described in this thesis show that the native erythrocyte glucose transporter (GLUT1) and the tryptic fragment differ markedly in their affinities for the external ligand ATB-BMPA and for the transported substrate D-glucose. Trypsin-treated erythrocyte membranes show 10-12-fold less ATB-BMPA-labelling than the native transporter. This suggests that the affinity for ATB-BMPA is markedly reduced in the trypsin fragment. By contrast, the D-glucose affinity is increased ≈ 6-fold. Results presented here are therefore consistent with those of Cairns *et al* (1987) who have shown that the K_i for D-glucose inhibition of cytochalasin B-binding to the tryptic fragment is reduced by approximately 10-fold compared to the K_i for D-glucose inhibition of cytochalasin B-binding to the unproteolysed transporter. Binding of the inside-specific ligand, cytochalasin B, to the trypsin fragment has been shown to be only slightly less efficient than binding of cytochalasin B to the native glucose transporter (Karim *et al*, 1987, Cairns *et al*, 1987).

Oka *et al*, (1990) have shown that deletion of the C-terminal 37 amino acids of GLUT1 produces a mutant transporter that still binds cytochalasin B efficiently, shows poor binding of the exofacial ligand ATB-BMPA, and loss of the ability to

transport glucose. Lin *et al*, (1992) have shown that deletion of the C-terminal 12 amino acids of GLUT1 produces a mutant glucose transporter which retains its ability to bind the external and internal ligands and its ability to transport glucose. To further explore the region of the C-terminal that is required for ligand binding, additional C-terminal deletion mutants have been investigated here. The results described in this thesis show that the ability of GLUT1 to bind ATB-BMPA is lost upon deletion of the 25th residue at the C-terminal of the protein. A mutant GLUT1 lacking the C-terminal 24 amino acid residues still binds ATB-BMPA efficiently. The ability to bind cytochalasin B is retained when 24 or 25 amino acids are deleted from the C-terminal of GLUT1. Therefore, upon deletion of 25 amino acids from the C-terminal of GLUT1, the transporter may adopt a similar conformation to that adopted by the GLUT1 tryptic fragment as they both have a reduced affinity for the external ligand, ATB-BMPA. In addition, it has been reported that both the GLUT1 tryptic fragment (Baldwin *et al*, 1980) and a GLUT1 deletion mutant lacking the 37 C-terminal amino acids (Oka *et al*, 1990) lose the ability to transport glucose.

The truncated mutant and the GLUT1 tryptic fragment may be adopting an inward-facing conformation. This inward-facing conformation could expose the inside binding site and so enable the mutant GLUT1 to bind cytochalasin B. The alternating conformational change that exposes the external site may involve TM12 moving up in the membrane. The truncation of the C-terminal segment of TM12 may prevent this upward movement. May, (1989) has shown that the binding of cytochalasin B to GLUT1 results in a decrease in the cell-surface accessibility, to permeable thiol reagents, of the top of TM12. This observation is consistent with the possibility that this segment moves down in the membrane when cytochalasin B is bound. The binding of exofacial ligands such as maltose increase the accessibility to the treatment

with the thiol reagent, which is consistent with TM12 moving up in the membrane (May, 1989).

The susceptibility of the GLUT4 glucose transporter isoform to proteolysis is also shown here to be dependant on the liganded state of the transporter protein. Oka *et al* (1988) and Yano & May (1993) have reported that no low molecular weight fragments are detected on SDS-PAGE after trypsin-treatment of cytochalasin B-labelled GLUT4. These authors suggest that trypsin cleaves GLUT4 more extensively than is observed with GLUT1. Additional cleavage of GLUT4 within the C-terminal half of the transporter would reduce the 18 kDa fragment normally observed with GLUT1 cleavage to smaller fragments that are not detectable on SDS-PAGE. The results in this thesis show that trypsin-treatment of ATB-BMPA-labelled GLUT4 from rat adipocytes produces a labelled 18 kDa fragment. ATB-BMPA-labelled GLUT4 has been immunoprecipitated from Thesit-solubilized adipocyte membranes with anti-GLUT4 antibody and subsequently treated with trypsin. The trypsin-treatment of GLUT4 results in complete removal of the C-terminal antibody-binding fragment of the transporter. The ATB-BMPA-labelled 18 kDa GLUT4 fragment no longer precipitates with the antibody-protein A-Sepharose conjugate. The finding that cleavage of ATB-BMPA-labelled GLUT4 by trypsin produces a significant amount of an 18 kDa fragment suggests that the ATB-BMPA-labelled GLUT4 is cleaved less extensively than cytochalasin B-labelled GLUT4. Yano & May, (1993) have reported that cleavage of GLUT4 by thermolysin is retarded by the exofacial ligand, 4,6-O-ethylidene-D-glucose. Therefore ATB-BMPA, and other external ligands, may be stabilizing a conformation in which a number of sites in the C-terminal half of GLUT4 are protected from proteolysis. Cytochalasin B binding to GLUT4 may

expose these cleavage sites. The structure of the GLUT4 glucose transporter could be further investigated using a number of other proteinases and chemical cleavage reagents. The GLUT1 and GLUT4 isoforms may differ in their susceptibility to various proteinases and chemical cleavage reagents and produce different proteolytic fragments. A difference between GLUT1 and GLUT4 cleavage by trypsin has already been observed. These different proteolytic patterns may help to identify differences in the conformations of GLUT1 and GLUT4. A difference between the conformations of the glucose transporters in the basal and insulin-stimulated states may be identified.

4.3. The Structure-Function Relationship of GLUT1

There are presently known to be six different mammalian glucose transporter isoforms (GLUT's 1-5 & 7, this is reviewed in section 1.1.). These glucose transporter isoforms have now been sequenced from a number of different species including human, rat, mouse, pig and rabbit. A number of other sugar transporters have been sequenced and display some sequence identity with the mammalian glucose transporter family. These include sugar transporters from bacteria, yeast, cyanobacteria and protozoa. Some of the sugar transporters in this superfamily cotransport protons or possibly other ions during the sugar transport process. All these sugar transporters are thought to have a similar structure to that proposed for GLUT1 (Mueckler *et al*, 1985). Sequence alignment of the members of the glucose transporter family identifies residues that are highly conserved in all or most of the transporters.

This should provide information on which residues may be important or essential for maintenance of the common structure and function. The residues that are predicted to be important can then be studied using site-directed mutagenesis, followed by expression of these mutated glucose transporters in cells such as CHO cells or *Xenopus* oocytes.

29 sequences of members of the sugar transporter superfamily have been sequenced aligned by Dr. P Hodgson (University of Bath). The alignment is shown in Table 8. The sequence alignment shows that asparagine (N) and glutamine (Q) residues are highly conserved especially around the top of TM's 7 and 8. Asparagine (Asn) and glutamine (Gln) residues can participate in hydrogen bonding, both as hydrogen donors and as hydrogen acceptors. Therefore, these residues may be involved in hydrogen bonding to a sugar molecule in the external or internal binding sites or they may be involved in the transport of the sugar through the glucose transporter protein. Studies described in this thesis examine the importance of Gln282 and Asn288 in TM7 and Asp317 in TM8 of GLUT1 in the ability of GLUT1 to bind ligands and to transport 2-deoxy-D-glucose. The amide residues are substituted with the aliphatic residues leucine (Leu) and isoleucine (Ile), residues which can not participate in hydrogen bonding. The GLUT1 mutants are expressed at the cell-surface of CHO-K1 cells as detected by Western blotting or by borohydride-labelling of cell-surface carbohydrate followed by specific immunoprecipitation of labelled GLUT1. None of the Asn or Gln mutants lose the ability to transport 2-deoxy-D-glucose or to bind the internal ligand, cytochalasin B. Therefore, none of these residues are an absolute requirement for transport or for binding of cytochalasin B. This may seem surprising considering the degree of conservation of these residues. A number of these residues may be involved in the transport of sugars through the

HUMGLUT1 (282-294)	**Q**	Q	L	S	G	I	N	A	V	F	Y	**Y**	S
RATGLUT1 (282-294)	**Q**	Q	L	S	G	I	N	A	V	F	Y	**Y**	S
MUSGLUT1 (282-294)	**Q**	Q	L	S	G	I	N	A	V	F	Y	**Y**	S
RABGLUT1 (282-294)	**Q**	Q	L	S	G	I	N	A	V	F	Y	**Y**	S
PIGGLUT1 (241-253)	**Q**	Q	L	S	G	I	N	A	V	F	Y	**Y**	S
HUMGLUT2 (314-326)	**Q**	Q	F	S	G	I	N	G	I	F	Y	**Y**	S
RATGLUT2 (312-324)	**Q**	Q	F	S	G	I	N	G	I	F	Y	**Y**	S
MUSGLUT2 (313-325)	**Q**	Q	F	S	G	I	N	G	I	F	Y	**Y**	S
HUMGLUT3 (280-292)	**Q**	Q	L	S	G	I	N	A	V	F	Y	**Y**	S
HUMGLUT4 (298-310)	**Q**	Q	L	S	G	I	N	A	V	F	Y	**Y**	S
RATGLUT4 (298-310)	**Q**	Q	L	S	G	I	N	A	V	F	Y	**Y**	S
MUSGLUT4 (300-312)	**Q**	Q	L	S	G	I	N	A	V	F	Y	**Y**	S
HUMGLUT5 (288-300)	**Q**	Q	L	S	G	V	N	A	I	Y	Y	**Y**	A
HUMGLUT7 (312-324)	**Q**	Q	T	S	G	V	N	G	I	F	Y	**Y**	H

HUMGLUT1 (378-389)	F	F	E	V	G	P	G	**P**	I	P	W	F
RATGLUT1 (378-389)	F	F	E	V	G	P	G	**P**	I	P	W	F
MUSGLUT1 (378-389)	F	F	E	V	G	P	G	**P**	I	P	W	F
RABGLUT1 (378-389)	F	F	E	V	G	P	G	**P**	I	P	W	F
PIGGLUT1 (337-348)	F	F	E	V	G	P	G	**P**	I	P	W	F
HUMGLUT2 (410-421)	F	F	E	I	G	P	G	**P**	I	P	W	F
RATGLUT2 (408-419)	F	F	E	I	G	P	G	**P**	I	P	W	F
MUSGLUT2 (409-420)	F	F	E	I	G	P	G	**P**	I	P	W	F
HUMGLUT3 (376-387)	F	F	E	I	G	P	G	**P**	I	P	W	F
HUMGLUT4 (394-405)	F	F	E	I	G	P	G	**P**	I	P	W	F
RATGLUT4 (394-405)	F	F	E	I	G	P	G	**P**	I	P	W	F
MUSGLUT4 (396-407)	F	F	E	I	G	P	G	**P**	I	P	W	F
HUMGLUT5 (386-397)	G	H	A	L	G	P	S	**P**	I	P	A	L
HUMGLUT7 (408-419)	F	F	E	I	G	P	I	**P**	I	P	F	F

Table 8. Sequence alignment of GLUT's 1-7 around transmembrane segments 7 and 10. Sequences of GLUT's 1-7 were sequence aligned by Dr P. Hodgson. The sequence alignments around transmembrane segments 7 and 10 are shown. Mutation of the residues Gln282, Tyr293 and Pro385 (from GLUT1) resulted in perturbation of GLUT1 function.

protein and the mutation of just one residue may be compensated for by the presence of the other residues. Although no change in transport or internal ligand binding is observed with these mutants, substitution of Gln282 with a leucine residue selectively perturbs binding of the external ligand, ATB-BMPA. In the predicted 2-dimensional model for GLUT1 (Mueckler *et al*, 1985) Gln282 is located towards the centre of TM7. Therefore, TM7 may move up in the membrane to accept exofacial ligands. The mutagenesis results are consistent with the studies using proteases described above. The upward-movement of TM7 may move a region at the bottom of TM7, possibly including a proteolytic cleavage site, further into the membrane. This could be investigated further by studying the extent of proteolysis of the wild-type GLUT1 and the Gln282-Leu mutant. If the Gln282-Leu is locked in an inward-facing conformation, the Gln282-Leu mutant might be expected to be more extensively cleaved than the wild-type GLUT1 if the proteolysis is carried out in the absence of internal or external ligands. If the Gln282-Leu mutant can adopt an outward-facing conformation but this conformation can not be stabilized by binding of the external ligand ATB-BMPA, the ATB-BMPA-bound wild-type GLUT1 may be less susceptible to trypsin-cleavage than the Gln282-Leu mutant.

Maiden *et al* (1987) have suggested that the two halves of the glucose transporter protein may be arranged in a similar manner as there is a high degree of duplication of sequences in the N- and C-terminal halves of the protein. Mueckler *et al* (1985) have suggested that as transmembrane segments 7, 8 and 11 are predicted to be amphipathic, they may form part of a hydrophilic channel. The results described here suggest that both TM7 and TM12 may move up in the membrane to accept exofacial ligands. The six transmembrane segments of the C-terminal half of GLUT1 may be arranged concentrically, with TM7 next to TM12, to form a channel. The

outside site would be occupied by upward movement of TM7 and TM12. In this conformation of the protein, the binding of a nontransported ligand may be very dependent on glutamine 282. However, a transported substrate such as 2-deoxy-D-glucose would be rapidly relayed from the exofacial site to the inside site by a cluster of hydrogen-bonding residues in the centre of the protein. In this position in the centre of the protein, a single amino acid substitution might be less critical. Therefore, 2-deoxy-D-glucose binding and transport would be less dependent on glutamine 282. However, as substitution of glutamine 282 alters the specificity of the exofacial site, the transport of hexoses other than 2-deoxy-D-glucose may be perturbed. Therefore, the transport properties of other glucose analogues in the glutamine 282 mutant clone may provide important information regarding the interactions involved in the transport of sugars through the glucose transporter. Further investigation of the importance of these Gln and Asn residues could involve the study of a mutant in which two or three of these residues has been substituted.

To investigate further the role of TM7 in the transport of hexoses by GLUT1, the tyrosine (Tyr) residues 292 and 293, which are predicted to be at the top of TM7 (Mueckler *et al*, 1985), have been studied. The motif Q^{282}QXSGXNXXXYY^{293} is present in all mammalian glucose transporters and is widely conserved in members of the wider glucose transporter superfamily (Dr. P Hodgson, University of Bath, Table 8). Barnett *et al*, (1973a,b) have studied the binding of D-glucose analogues to the inside and outside binding sites of the erythrocyte GLUT1 transporter. Studies with C6 analogues of D-glucose led Barnett *et al* (1973a) to propose that hydrogen bonding and hydrophobic binding may contribute to the binding of glucose analogues to the external binding site. The authors suggested that either a tryptophan or a tyrosine

residue suitably placed with respect to the C6 position of the sugar could fulfil both of these functions. Tyrosine's 292 and 293 at the top of TM7 may form part of the proposed hydrophobic region at the exofacial substrate binding site. The effects of substituting Tyr292 and Tyr293 by phenylalanine (Phe) and isoleucine (Ile) on GLUT1 transport activity and ligand-binding properties are reported here. Phenylalanine has a similar aromatic side chain to that of tyrosine but it lacks a hydroxyl and is unable to participate in hydrogen bonding. Isoleucine is a smaller, less bulky residue than tyrosine and is unable to participate in hydrogen bonding. Substitutions of Tyr292 by either phenylalanine or isoleucine are tolerated by GLUT1 and the mutant glucose transporters show no reduction in glucose transport activity or in external or internal ligand binding. The mutant Tyr293-Phe is also fully functional as a glucose transporter. However, when tyrosine 293 is substituted by isoleucine the ability of the mutant GLUT1 to transport glucose and to bind the internal ligand cytochalasin B is lost. By contrast, the ability of the Tyr293-Ile mutant to bind ATB-BMPA is retained. These results suggest that the hydrogen bonding properties of tyrosines 292 and 293 are not essential for glucose transporter function. However, the size of tyrosine residue must be important as well as its hydrophobicity as the relatively small but hydrophobic residue, isoleucine, affects the functioning of the transporter whereas the large hydrophobic residue, phenylalanine does not. The Tyr293-Ile mutant may be unable to undergo the conformational change that transports the sugar from outside to inside and that subsequently exposes the inside site and possibly a proteolytic cleavage site.

This could be investigated further by examining the susceptibility to proteolysis of the wild-type and the Tyr293-Ile mutant. If the Tyr293-Ile mutant is locked in an outward-facing conformation it may be less susceptible to cleavage by

trypsin than the unliganded wild-type GLUT1.

The conformational changes involved in external and internal ligand binding and transport by GLUT1 are likely to involve other transmembrane segments as well as TM7 and TM12. Molecular modelling studies (Hodgson, Osguthorpe & Holman, manuscript in preparation) suggest that the putative TM10 can undergo remarkably large conformational changes that may alternately expose the hexose binding site to the external and internal solution. These authors (Hodgson, Osguthorpe & Holman, manuscript in preparation) suggest that proline 385 in GLUT1 is particularly important in producing a pivotal point for these conformational changes. Proline 385 is situated in a proline rich region. The amino acid motif $F^{378}FEVGPGPIPW^{388}$ which is predicted to occur in TM10 (Mueckler *et al*, 1985) is widely conserved in all mammalian glucose transporters (Dr. P Hodgson, University of Bath, Table 8). Mutagenesis of tryptophan 388 in GLUT1 has been shown to result in reduced binding of cytochalasin B (Katagiri *et al*, 1991, Garcia *et al*, 1992). The authors suggest that tryptophan 388 may comprise part of the inside binding site. Davies *et al*, (1992) have localised the site of labelling of cytochalasin B to the region phenylalanine 389 to tryptophan 412 at the bottom of TM10 and TM11. Proline (Pro) is the only mammalian imino acid. As such, its side chain is bonded to the tertiary nitrogen in a cyclic pyrrolidine ring. Prolines may have both structural and dynamic roles in membrane proteins (this topic is reviewed by Williams & Deber, 1991). Structural roles include purely static effects such as those arising from a kinked helix, as well as electronic effects that stem from increased local polarity. Evidence for a more dynamic, transport catalysis role has come from mutagenesis studies on membrane proteins in which perturbations of transport occur as a result of proline mutation

(Williams & Deber, 1991).

The results of the substitution of proline 385 by isoleucine (Ile) and glycine (Gly) on the transport and ligand-binding abilities of GLUT1 are described here. Isoleucine is a large aliphatic residue, whereas glycine is smaller with only a single hydrogen on its side chain. Substitution of Pro385 by Ile produces a mutant GLUT1 with greatly reduced transport activity and with no ability to bind the external ligand ATB-BMPA. Binding of the internal ligand cytochalasin B is unaffected by the mutation of Pro385 to Ile. By contrast, substitution of Pro385 by the less bulky residue Gly is tolerated and the mutant GLUT1 retains the ability to bind both the external and internal ligands and to transport 2-deoxy-D-glucose. Interestingly, proline 385 is conserved in all members of the wider glucose transporter family other than in the SNF3 galactose transporter from *Saccharomyces cerevisiae*, where glycine is present at this position (Celenza *et al*, 1988).

Therefore, conformational changes of the GLUT1 protein may require the flexibility of the proline-rich region around TM10. The effect of the glycine substitution, which maintains the transport function of GLUT1, may be because it provides a non-hindering atomic environment for rotation around prolines 383 and 387. The substitution of proline 385 by isoleucine clearly perturbs the transport function and the ability of GLUT1 to expose a site at the external surface. The conformation of the transporter may however be relatively stable as the cytochalasin B binding is unperturbed by the isoleucine substitution. Further work could be carried out to examine whether the proposed upward movement of TM's 7 and 12 are part of the conformational change that is prevented by the mutation of Pro385 to Ile. If the Pro385-Ile mutant is locked in an inward-facing conformation it may be more susceptible to proteolytic cleavage than wild-type GLUT1 Pro385-Ile, if this inward-

facing conformation involves the downward movement of TM's 7 and 12.

ATB-BMPA has proved to be an important tool in the study of the structure-function relationship of GLUT1. The investigation of a number of other amino acid residues in both the N- and C-terminal halves of the glucose transporter protein will provide further information about the structure of the protein and the way in which it transports sugars. When the glucose transporter protein is successfully crystallised and a 3-dimensional structure is obtained, this mutagenesis data should be useful in providing additional evidence on how these residues (which have been shown to be important by mutagenesis) are involved in transport catalysis. A similar technique would also provide information about the insulin-responsive isoform (GLUT4) and the other members of the glucose transporter family. Regions of the isoforms that are responsible for the differences in substrate specificity, kinetic parameters and regulation may then be elucidated.

4.4. Insulin-Stimulation of Glucose Transport in the Rat Adipocyte

Holman *et al*, (1988) have previously used a benzophenone derivative of BMPA to label the glucose transporter in isolated rat adipocytes. However, relatively long irradiation times were required to activate the photolabile group and so a new compound, ATB-BMPA has been developed in order to get improved labelling of the adipocyte glucose transporter using a shorter irradiation time.

The results in this thesis show that ATB-BMPA labels the glucose transporter in isolated rat adipocytes in a D-glucose- and cytochalasin B-displaceable manner.

The labelled glucose transporter runs as a band at approximately 50 kDa in our gel system which is clearly separated from a non-specific band at approximately 75 kDa. A similar non-specific peak has been reported with the exofacial labels BB-BMPA (Holman *et al*, 1988) and B3GL (Jhun *et al*, 1992). Midgley *et al*, (1985a) have previously shown that BMPA derivatives are not significantly taken up by either adipocytes or erythrocytes, neither via the transporter nor through the lipid bilayer. The results described here show that ATB-BMPA is non-permeable to the adipocyte plasma membrane. When insulin-stimulated rat adipocytes are labelled with ATB-BMPA and the plasma membrane and LDM's are analysed by SDS-PAGE, the ATB-BMPA label recovered in the LDM fraction is only $\approx$ 4 % of that found in the plasma membrane. The lack of labelling of the LDM glucose transporters is not because the intracellular transporters are unable to bind ATB-BMPA. Glucose transporters in the LDM fraction are labelled with ATB-BMPA if the labelling is carried out on membrane fractions. Therefore, ATB-BMPA can be used to selectively label those glucose transporters that are present at the cell-surface without labelling those in the intracellular pool.

The stimulation of glucose transport by insulin is known to involve the translocation of glucose transporters from an internal pool to the plasma membrane (Cushman & Wardzala, 1980, Suzuki & Kono, 1980). Large differences have been reported between the insulin-stimulated increase in glucose transport activity and the extent of transporter translocation to the cell-surface. The quantitation of the insulin-stimulated increase in cell-surface glucose transporters was initially based on measurements (either cytochalasin B binding or Western blotting) using isolated plasma membranes while the large stimulations of glucose transport activity (20-30-

fold) were measured in intact cells. In 1988, James *et al* (1988) discovered an insulin-responsive glucose transporter isoform in adipocytes. Although the existence of GLUT4 readily explains why the original Western blotting studies using anti-GLUT1 antibodies were so discrepant, a substantial disparity remains between glucose transport activity and the translocation of the GLUT4 isoform as measured by cytochalasin B binding to plasma membrane fractions.

The results described here show that labelling of adipocyte membrane fractions with ATB-BMPA, followed by immunoprecipitation of GLUT4 from the membrane fractions, only results in an approximate 3-fold increase in plasma membrane GLUT4 in insulin-stimulated cells. The amount of GLUT4 in the basal plasma membrane is only approximately 10 % of the total GLUT4 in basal cells. Therefore, even a small contamination of the plasma membrane fraction with low density microsomes will increase the apparent number of basal plasma membrane glucose transporters and so underestimate the stimulation due to insulin. When ATB-BMPA is used to label cell-surface glucose transporters in basal and insulin-stimulated adipocytes, a large ($\approx$ 7-fold) increase in plasma membrane glucose transporters is observed in the insulin-stimulated state compared to the basal state. The increase in plasma membrane glucose transporters after insulin-stimulation, as detected by the cell-surface labelling method is greater than the increases seen using methods involving labelling or Western blotting membrane fractions. Use of the exofacial label, ATB-BMPA and antibodies to GLUT1 and GLUT4 have enabled a more detailed examination of the individual effects of insulin on each glucose transporter isoform which are described here. Both the efficiency of labelling and of immunoprecipitation of GLUT4 and GLUT1 must be similar if the photolabelling technique is to give a good approximation of the relative cell-surface concentrations of GLUT1 and GLUT4. The

anti-GLUT4 antibody immunoprecipitates 70-80 % of the labelled glucose transporter peak obtained in membranes which are isolated from insulin-stimulated cells but are not subjected to immunoprecipitation. This is similar to the efficiency of immunoprecipitation of GLUT1 from erythrocyte membranes by the anti-GLUT1 antibody which is discussed above. The affinity of GLUT1 for ATB-BMPA ($K_i \approx 300$ μM) is reported here and is similar to the affinity of GLUT4 for ATB-BMPA ($K_i \approx$ 250 μM) as reported by Holman *et al* (1990).

Immunoprecipitation of GLUT1 and GLUT4 from ATB-BMPA-labelled cells shows that the GLUT4 isoform is the most abundant glucose transporter isoform at the cell-surface in basal and insulin-stimulated adipocytes. GLUT4 accounts for ≈ 90 % of the total plasma membrane glucose transporters after insulin-stimulation. This result is consistent with those of Zorzano *et al* (1989) who found that GLUT4 is the most abundant isoform at the cell-surface in insulin-stimulated cells. However, these authors suggest that GLUT1 is the major isoform in basal cells, whereas the results described here suggest that GLUT4 is the major isoform in basal cells also. Calderhead *et al*, (1990) reported that GLUT1 is the most abundant isoform at the cell-surface in basal 3T3-L1 adipocytes. This may be associated with the much greater proportion of GLUT1 in 3T3-L1 adipocytes where the ratio of GLUT1 to GLUT4 has been reported as 1:1 (Yang *et al*, 1992b). The basal level of GLUT1 in the plasma membrane of rat adipocytes may vary depending on the age and the size of the cells. The GLUT1 K_m value for 3-O-methyl-D-glucose exchange transport in erythrocytes (Barnett *et al*, 1973a) and in the oocyte expression system (Gould & Lienhard, 1989) is 5-fold higher than the GLUT4 K_m in insulin-stimulated rat adipocytes (Whitesell & Gliemann, 1979, Taylor & Holman, 1981). The finding that

the K_m in basal cells is similar to that in insulin-stimulated adipocytes (Whitesell & Gliemann, 1979, Taylor & Holman, 1981) suggests that the GLUT1 K_m makes only a very small contribution to the operational K_m in basal cells.

Kono *et al* (1981) have shown that reagents such as KCN, which deplete cellular ATP levels, block the stimulation of glucose transport by insulin. The effect of KCN on the translocation of GLUT4 has been studied and is described here. Addition of KCN prior to insulin addition prevents any increase in cell-surface GLUT4 levels as no increase in ATB-BMPA-labelling above basal levels is observed. KCN treatment does not inhibit ATB-BMPA-labelling of cell-surface glucose transporters in fully insulin-stimulated cells. Therefore, ATP must be required for the translocation of the glucose transporters to the plasma membrane. Whether ATP is also required for the proposed insulin-induced intrinsic activation of the glucose transporter still needs to be investigated. In contrast, KCN only partially blocks the decrease in glucose transport activity after insulin removal. Therefore, the activation of glucose transport by insulin appears to be more sensitive to ATP depletion than the inactivation process. Kozka *et al*, (1991) have reported a similar failure of KCN to prevent the reversal of insulin-stimulated glucose transport activity, upon insulin-removal, in 3T3-L1 adipocytes.

The time courses for the insulin-stimulation of glucose transport and for the reversal of insulin-stimulated glucose transport have been studied and are described in this thesis. The time course for activation of glucose transport by insulin shows a lag period of 47 sec and a half time of 3.2 min. A similar lag period for activation of glucose transport has been reported by others (Haring *et al*, 1978, Ciaraldi &

Olefsky, 1979). The activation of glucose transport is preceded by the appearance of both GLUT1 and GLUT4 at the cell-surface with half times of ≈ 2.3 min at 37 °C. Karnieli *et al*, (1981) have shown that the appearance of cytochalasin B binding sites at the plasma membrane precede transport stimulation. More recently, the appearance of GLUT4 at the plasma membrane, as measured by Western blotting, has been reported to precede the appearance of ATB-BMPA-accessible GLUT1 and GLUT4 when the activation by insulin is carried out at 20 °C (Satoh *et al*, 1993). This evidence suggests that insulin-stimulation of glucose transport may involve an activation process as well as translocation of the glucose transporters to the plasma membrane. This additional activation step is only likely to produce a small stimulation in the absence of translocation. It seems unlikely that all the transporters in the basal state are intrinsically inactive. Suzuki & Kono, (1980) reconstituted glucose transporters from the LDM fraction into phospholipid vesicles where they showed glucose transport activity. The results described here show that glucose transporters in the LDM fraction can be labelled at the external site by ATB-BMPA. In addition, the results described here show that the discrepancy between GLUT4 transporter abundance and the transport rate is only ≈ 1.5-2-fold in the basal state. Thus only a small proportion of the plasma membrane transporters are likely to have low intrinsic activity, and it may be these transporters that require a subsequent covalent or structural activation by insulin.

The time course for the return of glucose transport activity to basal levels after insulin-removal, is much slower than that for transport activation which decreases with a t½ of 10.9 min. This correlates closely with the time courses for the loss of cell-surface GLUT1 and GLUT4 levels which decrease with half times of ≈ 12 min. Satoh

et al, (1993) have used ATB-BMPA to tracer-tag GLUT4 in order to investigate GLUT4 recycling. The half time for the loss of cell-surface GLUT4 reported in this thesis is similar to the half times (reported by Satoh *et al*, (1993)) for the internalization of the ATB-BMPA-tagged GLUT4 both in the absence and in the continuous presence of insulin. Satoh *et al*, (1993) have found that the internalized ATB-BMPA-labelled GLUT4 equilibrates with the entire intracellular pool of glucose transporters. Upon restimulation by insulin the half times for the reappearance at the cell-surface of both non-tagged and ATB-BMPA-tagged GLUT4 are similar and are ≈ 3 min (Satoh *et al*, 1993). The fact that the internalization of GLUT4 is similar in both the continuous presence and in the absence of insulin suggests that the effect of insulin to increase cell-surface GLUT4 is not due to a significant decrease in the endocytosis of GLUT4. Therefore, the main effect of insulin to increase cell-surface GLUT4 is likely to be due mainly to an increase in the exocytosis of GLUT4. Yang & Holman, (1993) have reported that the main effect of insulin in stimulating glucose transport in 3T3-L1 adipocytes is to increase the GLUT1 and GLUT4 exocytosis rate constants.

Jhun *et al*, (1992) have used a bis-glucose derivative (B3GL) to study GLUT4 recycling in rat adipocytes. They conclude that insulin modifies both the internalization and the externalization steps of GLUT4 recycling in rat adipocytes. However, they report only an 11-fold stimulation of glucose transport by insulin compared to a typical 20-40-fold stimulation reported here and by others (Taylor & Holman, 1981, Satoh *et al*, 1993). The lower fold insulin response may be due to an increased basal rate of glucose transport activity. Also Jhun *et al*, (1992) report a t½ of 3.2 min for the internalization of B3GL-labelled GLUT4. This half time is very short compared to the half time for GLUT4 internalization reported here (t½ ≈ 12

min) and the half time reported by Satoh *et al* (1993) for the internalization of ATB-BMPA-tagged GLUT4 of ≈ 10 min. Jhun *et al*, (1992) stop the translocation of GLUT4 by cooling the cells to 10 °C. This cooling may mechanically disrupt the adipocytes and alter their fractionation properties as at zero time after labelling plasma membrane GLUT4, they already recover ≈ 25 % of the total labelled GLUT4 in the LDM fraction. By contrast, as reported in this thesis, after fractionation of ATB-BMPA labelled adipocytes, only ≈ 4 % of the labelled GLUT4 is recovered in the LDM fraction. Therefore, Jhun *et al* (1992) may be underestimating the insulin-induced exocytosis of GLUT4 and overestimating the endocytosis of GLUT4.

A possible explanation for the much slower rate of GLUT4 internalization and recycling (t½ ≈ 10 min) than the initial stimulation of translocation (t½ ≈ 2-3 min) may be that the glucose transporter is recycled through a number of intermediate states in the cytosol. Slot *et al*, (1991a) have identified 11 separate locations of immunodetectable GLUT4, eight are cytoplasmic and three are associated with the plasma membrane. Satoh *et al*, (1993) have described a hypothetical mechanism for insulin's stimulatory action on glucose transport based on the original hypothetical mechanism described by Karnieli *et al* (1981) and the histochemical data of Slot *et al* (1991a). The model suggests that the GLUT4 can be in an occluded state (in which it can be detected in the plasma membrane by Western blotting only), a partially occluded state (in which it can be detected by Western blotting and can bind the photolabel ATB-BMPA) and the fully functional state (in which it can be detected by blotting and by ATB-BMPA labelling and can also transport glucose).

ATB-BMPA has proved to be a useful tool in the study of the regulation of glucose transport in the rat adipocyte. The impermeable nature of ATB-BMPA (which

has circumvented the need for subcellular fractionation) has allowed a more accurate estimate of the effect of insulin on GLUT1 and GLUT4 translocation. Also, the ability of ATB-BMPA to label plasma membrane glucose transporters in intact cells has allowed a comparison of the time courses for the insulin-stimulation of GLUT1 and GLUT4 translocation and glucose transport activity. The results have shown that the activation of glucose transport by insulin is preceded by the appearance of GLUT1 and GLUT4 at the cell-surface.

As ATB-BMPA-tagged glucose transporters are recycled in a similar manner to non-tagged transporters, ATB-BMPA should be useful in defining the intermediate states involved in the recycling process. Further analysis of ATB-BMPA-labelled glucose transporter-containing vesicles could identify proteins involved in the movement and docking of the intracellular vesicles. The effect of inhibitors of signalling pathway intermediates from other cell types on glucose transporter translocation, could help identify those intermediates that are involved in the insulin-signalling pathway in rat adipocytes.

References

Allard, W. J. & Lienhard, G. E. (1985) *J. Biol. Chem.* **260**, 8668-8675.

Alvarez, J., Lee, D. C., Baldwin, S. A. & Chapman, D. (1987) *J. Biol. Chem.* **262**, 3502-3509.

Appleman, J. R. & Lienhard, G. E. (1989) *Biochemistry* **28**, 8221-8227.

Asano, T., Katagiri, H., Takata, K., Lin, J.-L., Ishihara, H., Inukai, K., Tsukuda, K., Kikuchi, M., Hirano, H., Yazaki, Y. & Oka, Y. (1991) *J. Biol. Chem.* **266**, 24632-24636.

Asano, T., Takata, K., Katagiri, H., Tsukuda, K., Lin, J.-L., Ishihara, H., Inukai, K., Hirano, H., Yazaki, Y. & Oka, Y. (1992a) *J. Biol. Chem.* **267**, 19636-19641.

Asano, T., Katagiri, H., Tsukuda, K., Lin, J.-L., Ishihara, H., Inukai, K., Yazaki, Y. & Oka, Y. (1992b) *FEBS Lett.* **298**, 129-132.

Asano, T., Katagiri, H., Takata, K., Tsukuda, K., Lin, J.-L., Ishihara, H., Inukai, K., Hirano, H., Yazaki, Y. & Oka, Y. (1992c) *Biochem. J.* **288**, 189-193.

Asano, T., Takata, K., Katagiri, H., Ishihara, H., Inukai, K., Anai, M., Hirano, H., Yazaki, Y. & Oka, Y. (1993) *FEBS Lett.* **324**, 258-261.

Atherton, E. & Sheppard, R. C. (1985) J. Chem. Soc. Perkin trans. **1**, no. 10, 2057-2073.

Backer, J. M., Myers Jr., M. G., Shoelson, S. E., Chin, D. J., Sun, X.-J., Miralpeix, M., Hu, P., Margolis, B., Skolnik, E. Y., Schlessinger, J. & White, M. F. (1992) *EMBO J.* **11**, 3469-3479.

Baldwin, J. M., Lienhard, G. E. & Baldwin, S. A. (1980) *Biochim. Biophys. Acta* **599**, 699-714.

Baldwin, S.A. (1993) *Biochim. Biophys. Acta* **1154**, 17-49.

Baldini, G., Hohman, R., Charron, M. J. & Lodish, H. F. (1991) *J. Biol. Chem.* **266**, 4037-4040.

Baldini, G., Hohl, T., Lin, H. Y. & Lodish, H. F. (1992) *Proc. Natl. Acad. Sci. USA* **89**, 5049-5052.

Barnett, J. E. G., Holman, G. D. & Munday, K. A. (1973a) *Biochem. J.* **131**, 211-221.

Barnett, J. E. G., Holman, G. D. & Munday, K. A. (1973b) *Biochem. J.* **135**, 539-541.

Barnett, J. E. G., Holman, G. D., Chalkley, A. & Munday, K. A. (1975) *Biochem.J.* **145**, 417-429.

Bayley, H. & Knowles, J. R. (1977) *Methods Enzymol.* **46**, 69-114.

Beck, K. A. & Keen, J. H. (1991) *J. Biol. Chem.* **266**, 4442-4447.

Begum, N. & Draznin, B. (1992) *J. Clin. Invest.* **90**, 1254-1262.

Birnbaum, M. J., Haspel, H. C. & Rosen, O. M. (1986) *Proc. Natl. Acad. Sci. USA* **83**, 5784-5788.

Birnbaum, M. J. (1989) *Cell* **57**, 305-315.

Brunner, J., Senn, H. & Richards, F. M. (1980) *J. Biol. Chem.* **255**, 3313-3318.

Brunner, J. & Richards, F. M. (1980) *J. Biol. Chem.* **255**, 3319-3329.

Burant, C. F., Takeda, J., Brot-Laroche, E., Bell, G. I. & Davidson, N. O. (1992) *J. Biol. Chem.* **267**, 14523-14526.

Burant, C. F. & Bell, G. I. (1992) *Biochemistry* **31**, 10414-10420.

Cairns, M. T., Elliot, D. A., Scudder, P. R. & Baldwin, S. A. (1984) *Biochem. J.* **221**, 179-188.

Cairns, M. T., Alvarez, J., Panico, M., Gibbs, A. F., Morris, H. R., Chapman, D. & Baldwin, S. A. (1987) *Biochim. Biophys. Acta* **905**, 295-310.

Cain, C. C., Trimble, W. S. & Lienhard, G. E. (1992) *J. Biol. Chem.* **267**, 11681-11684.

Calderhead, D. M. & Lienhard, G. E. (1988) *J. Biol. Chem.* **263**, 12171-12174.

Calderhead, D. M., Kitagawa, K., Tanner, L. I., Holman, G. D. & Lienhard, G. E. (1990) *J. Biol. Chem.* **265**, 13800-13808.

Carruthers, A. (1990) *Physiological Reviews* **70**, 1135-1176.

Celenza, J. L., Marshall-Carlson, L. & Carlson, M. (1988) *Proc. Natl. Acad. Sci. USA* **85**, 2130-2134.

Chin, J. J., Jung, E. K. Y., Chen, J. V. & Jung, C. J. (1987) *Proc. Natl. Acad. Sci. USA* **84**, 4113-4116.

Chin, J. J., Jhun, B. H. & Jung, C. Y. (1992) *Biochemistry* **31**, 1945-1951.

Ciaraldi, T. P. & Olefsky, J. M. (1979) *Arch. Biochem. Biophys.* **193**, 221-231.

Ciaraldi, T. P., Horuk, R. & Matthaei, S. (1986) *Biochem. J.* **240**, 115-123.

Clancy, B. M., Harrison, S. A., Buxton, J. M. & Czech, M. P. (1991) *J. Biol. Chem.* **266**, 10122-10130.

Clark, A. E. & Holman, G. D. (1990) *Biochem. J.* **269**, 615-622.

Clark, A. E., Holman, G. D. & Kozka, I. J. (1991) *Biochem. J.* **278**, 235-241.

Cormont, M., Tanti, J.-F., Gremeaux, T., Van Obberghen, E. & Le Marchand-Brustel, Y. (1991) *Endocrinology* **129**, 3343-3350.

Corvera, S. (1990) *J. Biol. Chem.* **265**, 2413-2416.

Corvera, S., Jaspers, S. & Pasceri, M. (1991) *J. Biol. Chem.* **266**, 9271-9275.

Cuppoletti, J., Jung, C. Y. & Green, F. A. (1981) *J. Biol. Chem.* **256**, 1305-1306.

Cushman, S. W. & Wardzala, L. J. (1980) *J. Biol. Chem.* **255**, 4758-4762.

Davies, A., Meeran, K., Cairns, M. T. & Baldwin, S. A. (1987) *J. Biol. Chem.* **262**, 9347-9352.

Davies, A., Ciardelli, T. L., Lienhard, G. E., Boyle, J. M., Whetton, A. D. & Baldwin, S. A. (1990) *Biochem. J.* **266**, 799-808.

Davies, A. F., Cairns, M. T., Davies, A., Preston, R. A. J., Clark, A., Holman, G. & Baldwin, S. A. (1992) Molecular Mechanisms of Transport. (E. Qagliariello, F. Palmieri, eds. Elsevier Science Publications). 125-131.

Del Vecchio, R. L. & Pilch, P. F. (1991) *J. Biol. Chem.* **266**, 13278-13283.

Ellis, L., Clauser, E., Morgan, D. O., Edeng, M., Roth, R. A. & Rutter, W. J. (1986) *Cell* **45**, 721-732.

Ellman, G. E. (1958) *Arch. Biochem. Biophys.* **74**, 443-450.

Feugeas, J.-P., Neel, D., Pavia, A. A., Laham, A., Goussault, Y. & Derappe, C. (1990) *Biochim. Biophys. Acta* **1030**, 60-64.

Forsayeth, J. R., Caro, J. F., Sinha, M. K., Maddux, B. A. & Goldfine, I. D. (1987) *Proc. Natl. Acad. Sci. USA* **84**, 3448-3451.

Frost, S. C. & Lane, M. D. (1985) *J. Biol. Chem.* **260**, 2646-2652.

Fukumoto, H., Seino, S., Imura, H., Seino, Y., Eddy, R. L., Fukushima, Y., Byers, M. G., Shows, T. B. & Bell. G. I. (1988) *Proc. Natl. Acad. Sci. USA* **85**, 5434-5438.

Garcia, J. C., Strube, M., Leingang, K., Keller, K. & Mueckler, M. M. (1992) *J. Biol. Chem.* **267**, 7770-7776.

Gibbs, A. F., Chapman, D. & Baldwin, S. A. (1988) *Biochem. J.* **256**, 421-427.

Gorga, F. R., Baldwin, S. A. & Lienhard, G. E. (1979) *Biochem. Biophys. Res. Commun.* **91**, 955-961.

Gorga, F. R. & Lienhard, G. E. (1981) *Biochemistry* **20**, 5108-5113.

Gould, G. W. & Lienhard, G. E. (1989) *Biochemistry* **28**, 9447-9452.

Gould, G. W., Thomas, H. M., Jess, T. J. & Bell, G. I. (1991) *Biochemistry* **30**, 5139-5145.

Gould, G. W. & Holman, G. D. (1993) *Biochem. J.* **295**, 329-341.

Hara, K., Yonezawa, K., Sakaue, H., Ando, A., Kotani, K., Kitamura, T., Ido, Y., Ueda, H., Stephens, L., Jackson, T. R., Hawkins, P. T., Dhand, R., Clark, A. E., Holman, G. D., Waterfield, M. D. & Kasuga, M. (1993) Manuscript submitted.

Haring, H. U., Kemmler, W., Renner, R. & Hepp, K. D. (1978) *FEBS Lett.* **95**, 177-180.

Harrison, S. A., Buxton, J. M., Helgerson, A. L., MacDonald, R. G., Chlapowski, F. J., Carruthers, A. & Czech, M. P. (1990) *J. Biol. Chem.* **265**, 5793-5801.

Harrison, S. A., Buxton, J. M., Clancy, B. M. & Czech, M. P. (1991) *J. Biol. Chem.* **266**, 19438-19449.

Hasegawa, K., Anraku, Y., Kasahara, M., Akamatsu, Y. & Nishijima, M. (1990) *Biochim. Biophys. Acta* **1051**, 221-229.

Hashimoto, F., Horigome, T., Kanbayashi, M., Yoshida, K. & Sugano, H. (1983) *Analytical Biochemistry* **129**, 192-199.

Hashiramoto, M., Kadowaki, T., Clark, A. E., Muraoka, A., Momomura, K., Sakura, H., Tobe, K., Akanuma, Y., Yazaki, Y., Holman, G. D. & Kasuga, M. (1992) *J. Biol. Chem.* **267**, 17502-17507.

Hebert, D. N. & Carruthers, A. (1992) *J. Biol. Chem.* **267**, 23829-23838.

Helgerson, A. L. & Carruthers, A. (1987) *J. Biol. Chem.* **262**, 5464-5475.

Hellwig, B. & Joost, H. G. (1991) *Molecular Pharmacology* **40**, 383-389.

Hellwig, B., Brown, F. M., Schurmann, A., Shanahan, M. F. & Joost, H. G. (1992) *Biochim. Biophys. Acta* **1111**, 178-184.

Herman, P. K., Stack, J. H. & Emr, S. D. (1992) *Trends in Cell Biol.* **2**, 363-368.

Holman, G. D., Pierce, E. J. & Rees, W. D. (1981) *Biochim. Biophys. Acta* **646**, 382-388.

Holman, G. D., Parkar, B. A. & Midgley, P. J. W. (1986) *Biochim. Biophys. Acta* **855**, 115-126.

Holman, G. D. & Rees, W. D. (1987) *Biochim. Biophys. Acta* **897**, 395-405.

Holman, G. D., Karim, A. R. & Karim, B. (1988) *Biochim. Biophys. Acta* **946**, 75-84.

Holman, G. D., Kozka, I. J., Clark, A. E., Flower, C. J., Saltis, J., Habberfield, A. D., Simpson, I. A. & Cushman, S. W. (1990) *J. Biol. Chem.* **265**, 18172-18179.

Ishihara, H., Asano, T., Katagiri, H., Lin, J.-L., Tsukuda, K., Shibasaki, Y. & Oka, Y. (1991) *Biochem. Biophys. Res. Commun.* **176**, 922-930.

Ishizuka, T., Cooper, D. R., Arnold, T., Hernandez, H. & Farese, R. V. (1991) *Diabetes* **40**, 1274-1281.

Jacobs, D. B., Berenski, C. J., Spangler, R. A. & Jung, C. Y. (1987) *J. Biol. Chem.* **262**, 8084-8087.

James, D. E., Brown, R., Navarro, J. & Pilch, P. F. (1988) *Nature* **333**, 183-185.

James, D. E., Strube, M. & Mueckler, M. (1989) *Nature* **338**, 83-87.

Jarvis, S. M., Ellory, J. C. & Young, J. D. (1986) *Biochim. Biophys. Acta* **855**, 312-315.

Jhun, B. H., Rampal, A. L., Liu, H. Z., La Chaal, M. & Jung, C. Y. (1992) *J Biol. Chem.* **267**, 17710-17715.

Jo, I., Hah, J. S., Rampal, A. L., Chakrabarti, R., Paterson, A. R. P., Craik, J. D., Cass, C. E., Zobel, C. R. & Jung, C. Y. (1992) *Biochim. Biophys. Acta* **1106**, 45-55.

Jordan, N. J. & Holman, G. D. (1992) *Biochem. J.* **286**, 649-656.

Kahn, C. R. & White, M. F. (1988) *J. Clin. Invest.* **82**, 1151-1156.

Karim, A. R., Rees, W. D. & Holman, G. D. (1987) *Biochim. Biophys. Acta* **902**, 402-405.

Karnieli, E., Zarnowski, M. J., Hissin, P. J., Simpson, I. A., Salans, L. B. & Cushman, S. W. (1981) *J. Biol. Chem.* **256**, 4772-4777.

Katagiri, H., Asano, T., Shibasaki, Y., Lin, J.-L., Tsukuda, K., Ishihara, H., Akanuma, Y., Takaku, F. & Oka, Y. (1991) *J. Biol. Chem.* **266**, 7769-7773.

Katagiri, H., Asano, T., Ishihara, H., Tsukuda, K., Lin, J.-L., Inukai, K., Kikuchi, M Yazaki, Y. & Oka, Y. (1992) *J. Biol. Chem.* **267**, 22550-22555.

Kayano, T., Fukumoto, H., Eddy, R. L., Fan, Y.-S., Byers, M. G., Shows, T. B. & Bell, G. I. (1988) *J. Biol. Chem.* **263**, 15245-15248.

Kayano, T., Burant, C. F., Fukumoto, H., Gould, G. W., Fan, Y.-S., Eddy, R. L., Byers, M. G., Shows, T. B., Seino, S. & Bell, G. I. (1990) *J. Biol. Chem.* **265**, 13276-13282.

Keen, J. H. (1990) *Annu. Rev. Biochem.* **59**, 415-438.

Kelly, K. L., Ruderman, N. B. & Chen, K. S. (1992) *J. Biol. Chem.* **267**, 3423-3428.

Kim, S. S. & Jung, C. Y. (1992) *Diabetes* **41**, suppl. 1, no. 538.

King, A. P. J., Ku Tai, P.-K. & Carter-Su, C. (1991) *Biochemistry* **30**, 11546-11553.

Klip, A., Ramlal, T., Young, D. A. & Holloszy, J. O. (1987) *FEBS Lett.* **224**, 224-230.

Kono, T., Suzuki, K., Dansey, L. E., Robinson, F. W. & Blevins, T. L. (1981) *J. Biol. Chem.* **256**, 6400-6407.

Kozka, I. J., Clark, A. E. & Holman, G. D. (1991) *J. Biol. Chem.* **266**, 11726-11731.

Kuroda, M., Honnor, R. C., Cushman, S. W., Londos, C. & Simpson, I. A. (1987) *J. Biol. Chem.* **262**, 245-253.

Laemmli, U. K. (1970) *Nature* **227**, 680-685.

Lawrence Jr., J. C., Hiken, J. F. & James, D. E. (1990a) *J. Biol. Chem.* **265**, 2324-2332.

Lawrence Jr., J. C., Hiken, J. F. & James, D. E. (1990b) *J. Biol. Chem.* **265**, 19768-19776.

Lin, J.-L., Asano, T., Katagiri, H., Tsukuda, K., Ishihara, H., Inukai, K., Yazaki, Y. & Oka, Y. (1992) *Biochem. Biophys. Res. Commun.* **184**, 865-870.

Lowe, A. G. & Walmsley, A. R. (1986) *Biochim. Biophys. Acta* **857**, 146-154.

Maiden, M. C. J., Davis, E. O., Baldwin, S. A., Moore, D. C. M. & Henderson, P. J. F. (1987) *Nature* **325**, 641-643.

Marshall-Carlson, L., Celenza, J. L., Laurent, B. C. & Carlson, M. (1990) *Mol. Cell. Biol.* **10**, 1105-1115.

May J. M. (1989) *J. Membr. Biol.* **108**, 227-233.

Midgley, P. J. W., Parkar, B. A., Holman, G. D., Thieme, R. & Lehmann, J. (1985a) *Biochim. Biophys. Acta* **812**, 27-32.

Midgley, P. J. W., Parkar, B. A. & Holman, G. D. (1985b) *Biochim. Biophys. Acta* **812**, 33-41.

Mueckler, M., Caruso, C., Baldwin, S. A., Panico, M., Blench, I., Morris, H. R., Allard, W. J., Lienhard, G. E., & Lodish, H. F. (1985) *Science* **229**, 941-945.

Nishimura, H., Saltis, J., Habberfield, A. D., Garty, N. B., Greenberg, A. S., Cushman, S. W., Londos, C. & Simpson, I. A. (1991) *Proc. Natl. Acad. Sci. USA* **88**, 11500-11504.

Nishimura, H., Kuzuya, H., Kosaki, A., Okamoto, M., Okamoto, M., Kono, S., Inoue, G., Maeda, I. & Imura, H. (1992) *Biochem. J.* **281**, 103-106.

Nishimura, H., Pallardo, F. V., Seidner, G. A., Vannucci, S., Simpson, I. A. & Birnbaum, M. J. (1993) *J. Biol. Chem.* **268**, 8514-8520.

Oka, Y., Asano, T., Shibasaki, Y., Kasuga, M., Kanazawa, Y. & Takaku, F. (1988) *J. Biol. Chem.* **263**, 13432-13439.

Oka, Y., Asano, T., Shibasaki, Y., Lin, J.-L., Tsukuda, K., Katagiri, H., Akanuma, Y. & Takaku, F. (1990) *Nature* **345**, 550-553.

Palfreyman, R. W., Clark, A. E., Denton, R. M., Holman, G. D. & Kozka, I. J. (1992) *Biochem. J.* **284**, 275-281.

Panayotou, G. & Waterfield, M. D. (1992) *Trends in Cell Biol.* **2**, 358-360.

Pawagi, A. B. & Deber, C. M. (1990) *Biochemistry* **29**, 950-955.

Pearse, B. M. F. & Robinson, M. S. (1990) *Annu. Rev. Cell Biol.* **6**, 151-171.

Pessino, A., Hebert, D. N., Woon, C. W., Harrison, S. A., Clancy, B. M., Carruthers, A. & Czech, M. P. (1991) *J. Biol. Chem.* **266**, 20213-20217.

Piper, R. C., Hess, L. J. & James, D. E. (1991) *Am. J. Physiol.* **260**, C570-C580.

Piper, R. C., Tai, C., Slot, J. W., Hahn, C. S., Rice, C. M., Huang, H. & James, D. E. (1992) *J. Cell Biol.* **117**, 729-743.

Piper, R. C., Tai, C., Kulesza, P., Pang, S., Warnock, D., Baenziger, J., Slot, J. W., Geuze, H. J., Puri, C. & James, D. E. (1993) *J. Cell Biol.* **121**, 1221-1232.

Poku, J., Chakrabarti, R., Joly, M. & Corvera, S. (1992) *Diabetes* **41**, suppl. 1, no. 535.

Quiocho, F. A. (1986) *Ann. Rev. Biochem.* **55**, 287-315.

Rampal, A. L. & Jung, C. Y. (1987) *Biochim. Biophys. Acta* **896**, 287-294.

Robinson, L. J., Pang, S., Harris, D. S., Heuser, J. & James, D. E. (1992) *J. Cell Biol.* **117**, 1181-1196.

Satoh, S., Nishimura, H., Clark, A. E., Kozka, I. J., Vannucci, S. J., Simpson, I. A., Quon, M. J., Cushman, S. W. & Holman, G. D. (1993) *J. Biol. Chem.* **268**, 17820-17829.

Shibasaki, Y., Asano, T., Lin, J.-L., Tsukuda, K., Katagiri, H., Ishihara, H., Yazaki, Y. & Oka, Y. (1992) *Biochem. J.* **281**, 829-834.

Saltis, J., Habberfield, A. D., Egan, J. J., Londos, C., Simpson, I. A. & Cushman, S. W. (1991) *J. Biol. Chem.* **266**, 261-267.

Saperstein, R., Vicario, P. P., Strout, H. V., Brady, E., Slater, E. E., Greenlee, W. J., Ondeyka, D. L., Patchett, A. A. & Angauer, D. G. (1989) *Biochemistry* **28**,

5694-5701.

Schagger, H. & Von Jagow, G. (1987) *Anal. Biochem.* **166**, 368-379.

Schürmann, A., Rosenthal, W., Schultz, G. & Joost, H. G. (1992a) *Biochem. J.* **283**, 795-801.

Schürmann, A., Mieskes, G. & Joost, H. G. (1992b) *Biochem. J.* **285**, 223-228.

Shanahan, M. F. (1982) *J. Biol. Chem.* **257**, 7290-7293.

Shanahan, M. F., Morris, D. P. & Edwards, B. M. (1987) *J. Biol. Chem.* **262**, 5978-5984.

Slot, J. W., Geuze, H. J., Gigengach, S., Lienhard, G. E. & James, D. E. (1991a) *J. Cell Biol.* **113**, 123-135.

Slot, J. W., Geuze, H. J., Gigengach, S., James, D. E. & Lienhard, G. E. (1991b) *Proc. Natl. Acad. Sci. USA* **88**, 7815-7819.

Smith, R. M., Charron, M. J., Shah, N., Lodish, H. F. & Jarett, L. (1991) *Proc. Natl. Acad. Sci. USA* **88**, 6893-6897.

Sollner, T., Whiteheart, S. W., Brunner, M., Erdjument-Bromage, H., Geromanos, S., Tempst, P. & Rothman, J. E. (1993) *Nature* **362**, 318-324.

Suzuki, K. & Kono, T. (1980) *Proc. Natl. Acad. Sci. USA* **77**, 2542-2545.

Tanner, L. I. & Lienhard, G. E. (1989) *J. Cell Biol.* **108**, 1537-1545.

Tanti, J.-F., Gautier, N., Cormont, M., Baron, V., Van Obberghen, E. & Le Marchand-Brustel, Y. (1992) *Endocrinology* **131**, 2319-2324.

Taylor, L. P. & Holman, G. D. (1981) *Biochim. Biophys. Acta* **642**, 325-335.

Thoidis, G., Kotliar, N. & Pilch, P. F. (1993) *J. Biol. Chem.* **268**, 11691-11696.

Thomas, H. M., Takeda, J. & Gould, G. W. (1993) *Biochem J.* **290**, 707-715.

Thorens, B., Sarkar, H. K., Kaback, H. R. & Lodish, H. F. (1988) *Cell* **55**, 281-290.

Tordjman, K. M., Liengang, K. A. & Mueckler, M. (1990) *Biochem. J.* **271**, 201-207.

Van Der Sluijs, P., Hull, M., Zahraoui, A., Tavitian, A., Goud, B. & Mellman, I. (1991) *Proc. Natl. Acad. Sci. USA* **88**, 6313-6317.

Vannucci, S. J., Nishimura, H., Satoh, S., Cushman, S. W., Holman, G. D. & Simpson, I. A. (1992) *Biochem. J.* **288**, 325-330.

Waddell, I. D., Zomerschoe, A. G., Voice, M. W. & Burchell, A. (1992) *Biochem. J.* **286**, 173-177.

Wadzinski, B. E., Shanahan, M. F., Seamon, K. B. & Ruoho, A. E. (1990) *Biochem J.* **272**, 151-158.

Wardzala, L. J. & Jeanrenaud, B. (1981) *J. Biol. Chem.* **256**, 7090-7093.

Warren, G. (1993) *Nature* **362**, 297-298.

Weber, T. M., Joost, H. G., Simpson, I. A. & Cushman, S. W. (1988) Insulin Receptors, Part B: Clinical Assessment, Biological Responses, and Comparison to the IGF-1 Receptor, 171-187.

Wellner, M., Monden, I. & Keller, K. (1992) *FEBS Lett.* **309**, 293-296.

Wheeler, T. J. & Hinkle, P. C. (1981) *J. Biol. Chem.* **256**, 8907-8914.

Wheeler, T. J. (1988) *J. Biol. Chem.* **263**, 19447-19454.

White, M. F., Maron, R. & Kahn, C. R. (1985) *Nature* **318**, 183-186.

Whitesell, R. R. & Gliemann, J. (1979) *J. Biol. Chem.* **254**, 5276-5283.

Widdas, W. F. (1952) *J. Physiol.* **118**, 23-39.

Williams, K. A. & Deber, C. M. (1991) *Biochemistry* **30**, 8919-8923.

Xiao, J. S., Rothenberg, P., Kahn, C. R., Backer, J. M., Araki, E., Wilden, P. A., Cahill, D. A., Goldstein, B. J. & White, M. F. (1991) *Nature* **352**, 73-77.

Yamamoto, T., Seino, Y., Fukumoto, H., Koh, G., Yano, H., Inagaki, N., Yamada, Y., Inoue, K., Manabe, T. & Imura, H. (1990) *Biochem. Biophys. Res. Commun.* **170**, 223-230.

Yang, J., Clark, A. E., Harrison, R., Kozka, I. J. & Holman, G. D. (1992a) *Biochem. J.* **281**, 809-817.

Yang, J., Clark, A. E., Kozka, I. J., Cushman, S. W. & Holman, G. D. (1992b) *J. Biol. Chem.* **267**, 10393-10399.

Yang, J. & Holman, G. D. (1993) *J. Biol. Chem.* **268**, 4600-4603.

Yano, Y. & May, J. M. (1993) *Biochem. J.* **295**, 183-188.

Zorzano, A., Wilkinson, W., Kotliar, N., Thoidis, G., Wadzinkski, B. E., Ruoho, A. E. & Pilch, P. F. (1989) *J. Biol. Chem.* **264**, 12358-12363.